

**Functional divergence of Midkine growth factors:
Non-redundant roles during neural crest induction,
brain patterning and somitogenesis**

Dissertation zur Erlangung des
naturwissenschaftlichen Doktorgrades
der Bayerischen Julius-Maximilians-Universität Würzburg

vorgelegt von

Daniel Liedtke

aus

Fulda

Würzburg, 2007

Eingereicht am:

Mitglieder der Promotionskommission:

Vorsitzender:

Gutachter: Prof. Dr. Christoph Winkler

Gutachter: PD Dr. med. Ute Felber

Tag des Promotionskolloquiums:

Doktorurkunde ausgehändigt am:

Darin besteht das Wesen der Wissenschaft.
Zuerst denkt man an etwas, das wahr sein könnte
– und dann sieht man nach, ob es der Fall ist, und im Allgemeinen ist es nicht der Fall.

Bertrand Russell

Index

Index **1**

Summary **5**

Zusammenfassung **6**

1. Introduction **7**

1.1. Differentiation of the vertebrate brain and spinal cord 7

1.1.1. Structure of the vertebrate brain 7

1.1.2. Induction of neural tissues 8

1.1.3. Patterning of the brain 9

1.1.4. Patterning of the vertebrate spinal cord 10

1.2. Development and functions of neural crest cells 12

1.2.1. Induction of neural crest cells 12

1.2.2. Molecular networks involved in ncc differentiation 14

1.2.3. Development of the neural crest in zebrafish 15

1.2.4. Development of sensory neurons in zebrafish 17

1.2.5. Open questions in ncc and sensory neuron development 18

1.3. Gradients and clockworks in somitogenesis 19

1.4. The zebrafish as a model system 21

1.5. Gene duplication in zebrafish 22

1.6. Midkine and Pleiotrophin 23

1.6.1. Midkine and pleiotrophin genes in vertebrates 23

1.6.2. *Midkine* and *pleiotrophin* genes in zebrafish 25

1.7. Aim of the PhD thesis 26

2. Material **29**

2.1. Fish maintenance and breeding 29

2.2. Bacterial strains 29

2.3. Morpholinos 29

2.4. Antibodies 31

2.5. Oligonucleotides 31

2.6. Kits 31

2.7. Enzymes 32

2.8. Chemicals 32

2.9. Technical devices 32

3. Methods	34
3.1. Microbiological methods	34
3.1.1. Sterilization	34
3.1.2. Growth media	34
3.1.3. Bacteria cultivation and long time storage	34
3.1.4. Chemically competent bacteria	35
3.1.5. Bacterial transformation	35
3.2. Molecular biological methods	35
3.2.1. Plasmid DNA amplification and isolation	35
3.2.2. DNA purification	36
3.2.3. DNA and RNA precipitation	36
3.2.4. Determination of nucleic acid concentrations	36
3.2.5. Agarose gel electrophoresis	36
3.2.6. Gel extraction of DNA fragments	37
3.2.7. DNA sequencing	37
3.2.8. RNA extraction	38
3.2.9. Reverse transcription	38
3.2.10. Polymerase chain reaction (PCR)	39
3.2.11. Enzymatic DNA digestion	40
3.2.12. Capped RNA synthesis	40
3.2.13. Riboprobe synthesis	40
3.2.14. Whole-mount RNA in situ hybridization	41
3.2.15. Immunostaining	44
3.2.16. Cartilage staining	44
3.3. Chemical treatments of zebrafish embryos	45
3.3.1. DEAB treatment	45
3.3.2. SU5402 treatment	45
3.3.3. LiCl treatment	46
3.4. Microinjection into zebrafish embryos	46
3.4.1. Collection of embryos	46
3.4.2. Microinjection	46
3.4.3. Cultivation of injected embryos	47
4. Results	49
4.1. Analysis of <i>mdkb</i> expression during stages of ncc induction	49
4.2. Regulation of <i>mdkb</i> expression by neural crest inducing signals	51
4.2.1. Loss of retinoic acid signaling represses <i>mdkb</i> expression	52
4.2.2. <i>mdkb</i> expression requires FGF signaling	53
4.2.3. FGF but not RA inhibition alters neural plate size	54
4.2.4. Altered Wnt signaling has diverse effects on <i>mdkb</i> expression	55
4.2.5. Delta-Notch signaling does not interfere with <i>mdkb</i> expression	56
4.3. <i>mdkb</i> regulates ncc specification	57
4.3.1. Design and activity of the <i>mdkb</i> splice Morpholinos	57

4.3.2.	Mdkb regulates earliest steps of ncc induction during gastrulation _____	60
4.3.3.	Misexpression of <i>mdkb</i> alters expression of prominent ncc specifiers _____	61
4.3.4.	Rescue of ncc defects in <i>mdkb</i> morphants by RNA co-injection _____	63
4.3.5.	Loss of ncc in <i>mdkb</i> morphants is not a consequence of increased apoptosis_	65
4.3.6.	Analysis of ncc recovery in late embryonic stages of <i>mdkb</i> morphants _____	66
4.4.	Mdkb regulates sensory neuron specification _____	69
4.4.1.	Mdkb influences primary sensory neuron induction _____	69
4.4.2.	Absence of sensory neuron recovery in <i>mdkb</i> morphants _____	70
4.5.	Non-overlapping activities of Midkine growth factors during mid- and hindbrain formation _____	73
4.5.1.	Mostly non-overlapping expression patterns of <i>mdka</i> , <i>mdkb</i> and <i>ptn</i> during zebrafish brain development _____	73
4.5.2.	Overexpression of <i>midkine</i> genes affects different aspects of brain patterning	77
4.5.3.	Double and triple knockdown of Midkine factors: Design and activity of <i>mdka</i> and <i>ptn</i> splice Morpholinos _____	81
4.5.4.	Single knockdown of <i>midkine</i> genes reveals non-overlapping functions during brain patterning _____	82
4.5.5.	Combined knockdown reveals an exclusive role of <i>mdka</i> during MHB establishment _____	84
4.5.6.	Knockdown of <i>ptn</i> function results in hindbrain patterning defects _____	85
4.6.	Somitogenesis is regulated by <i>ptn</i> _____	87
4.6.1.	Combined knockdown of <i>mdka</i> , <i>mdkb</i> and <i>ptn</i> results in somite fusion _____	87
4.6.2.	Expression of <i>midkine</i> genes during somitogenesis in the paraxial and presomitic mesoderm (PSM) _____	88
4.6.3.	Knockdown of <i>ptn</i> inhibits somite formation _____	89
5.	Discussion _____	93
5.1.	Functions of Mdkb in neural crest and sensory neuron induction _____	93
5.1.1.	Spatiotemporal expression of <i>mdkb</i> is consistent with a role during ncc and sensory neuron induction at the neural plate border _____	93
5.1.2.	<i>mdkb</i> expression is regulated by known ncc-inducing signals, but not by Delta-Notch signaling _____	94
5.1.3.	Mdkb regulates neural crest and sensory neuron induction at the neural plate border _____	98
5.1.4.	Model of Mdkb action on cell induction at the neural plate border _____	100
5.2.	Restricted expression patterns of <i>midkine</i> genes during early brain development	102
5.2.1.	Comparison of <i>mdka</i> , <i>mdkb</i> and <i>ptn</i> expression during early brain development _____	102
5.2.2.	Different aspects of zebrafish brain patterning are regulated by Midkine growth factors _____	104
5.3.	<i>Ptn</i> is essential for somite boundary formation _____	108
5.3.1.	Combined knockdown of midkine and pleiotrophin function interferes with somitogenesis _____	109
5.3.2.	Triple knockdown of <i>mdka</i> , <i>mdkb</i> and <i>ptn</i> does not interfere with initiation of the somitogenesis clock but affects somitomere maturation _____	109

5.3.3.	Knockdown of Ptn function is responsible for somite ablation in triple morphants _____	110
5.3.4.	Enhanced numbers of <i>foxd3</i> positive cells in the tail bud suggest possible cell fate changes in <i>ptn</i> morphants _____	111
5.3.5.	The efficiency of the <i>ptn</i> MO is increased by a second binding site in the intron of the pre-mRNA target _____	112
6.	Future perspectives _____	113
7.	References _____	114
8.	Appendix _____	122
8.1.	Characterization of <i>ptn</i> MO _____	122
8.1.1.	<i>ptn</i> ATG and splice Morpholinos show different potencies _____	122
8.1.2.	Combinatorial knockdown reveals no synergistic effects of midkines and pleiotrophin on somite formation _____	124
8.2.	Table of used primers _____	125
8.3.	Abriviations _____	126
8.4.	Lebenslauf / Curriculum vitae _____	128
8.5.	Schriftenverzeichnis / Own puplications _____	128
8.6.	Teilnahme an Wissenschaftliche Tagungen _____	130
8.7.	Eidesstattliche Erklärung _____	131
8.8.	Danksagung _____	132

Summary

Neural crest cells and sensory neurons are two prominent cell populations which are induced at the border between neural and non-neural ectoderm during early vertebrate development. The neural crest cells are multipotent and highly migratory precursors that give rise to face cartilage, peripheral neurons, glia cells, pigment cells and many other cell types unique to vertebrates. Sensory neurons are located dorsally in the neural tube and are essential for sensing and converting environmental stimuli into electrical motor reflexes. In my PhD thesis, I obtained novel insights into the complex processes of cell induction at the neural plate border by investigating the regulation and function of *mdkb* in zebrafish. First, it was possible to demonstrate that *mdkb* expression is spatiotemporally correlated with the induction of neural crest cells and primary sensory neurons at the neural plate border. Second, it became evident that the expression of *mdkb* is activated by known neural crest cell inducing signals, like Wnts, FGFs and RA, but that it is independent of Delta-Notch signals essential for lateral inhibition. Knockdown experiments showed that *mdkb* function is necessary for induction of neural crest cells and sensory neurons at the neural plate border, probably through determination of a common pool of progenitor cells during gastrulation.

The present study also used the advantages of the zebrafish model system to investigate the *in vivo* function of all *midkine* gene family members during early brain development. In contrast to the situation in mouse, all three zebrafish genes show distinct expression patterns throughout CNS development. *mdka*, *mdkb* and *ptn* expression is detected in mostly non-overlapping patterns during embryonic brain development in the telencephalon, the mid-hindbrain boundary and the rhombencephalon. The possibility of simultaneously knocking down two or even three mRNAs by injection of morpholino mixtures allowed the investigation of functional redundancy of midkine factors during brain formation. Knockdown of Midkine proteins revealed characteristic defects in brain patterning indicating their association with the establishment of prominent signaling centers such as the mid-hindbrain boundary and rhombomere 4.

Interestingly, combined knockdown of *mdka*, *mdkb* and *ptn* or single knockdown of *ptn* alone prevented correct formation of somites, either by interfering with the shifting of the somite maturation front or interference with cell adhesion in the PSM. Thus, Ptn was identified as a novel secreted regulator of segmentation in zebrafish.

Zusammenfassung

Neuralleistenzellen und sensorische Neuronen werden während der frühen Wirbeltierentwicklung an der Grenze zwischen dem neuralen und epidermalen Ektoderm gebildet. Neuralleistenzellen sind multipotente Vorläufer von verschiedenen Geweben, wie der Knorpelanteile des Kopfskeletts, peripherer Neurone, Gliazellen, Pigmentzellen und vieler weiterer Derivate. Sensorische Neurone befinden sich im dorsalen Rückenmark und sind wichtig für die Wahrnehmung von Hautreizen. Durch Untersuchung der Regulation und Funktion von *mdkb* im Zebrafisch konnte ich in meiner Doktorarbeit neue Einsichten in den komplexen Prozess der Zellinduzierung an der Grenze der Neuralplatte erlangen. Es zeigte sich, dass die Expression von *mdkb* zeitlich und räumlich mit der Induktion von Neuralleistenzellen und primären Neuronen an der Neuralplattengrenze korreliert. Weiterhin konnte ich nachweisen, dass die *mdkb* Expression durch Signalwege reguliert wird, die für die Induktion von Neuralleistenzellen wichtig sind, wie Wnt, FGF und Retinolsäure. Signale der Delta-Notch Familie, welche essentiell für laterale Inhibition sind, werden dagegen nicht für die *mdkb* Expression benötigt. Weitere knockdown Experimente zur Reduktion der *mdkb*-Funktion bewiesen, dass *mdkb* notwendig für die Induktion von Neuralleistenzellen und der sensorischen Neuronen an der Neuralplattengrenze ist.

Des Weiteren konnten im Verlauf dieser Doktorarbeit die *in vivo* Funktionen aller Mitglieder der *midkine* Genfamilie während der frühen Gehirnentwicklung untersucht werden. Im Unterschied zu höheren Vertebraten, wie z. B. der Maus, wiesen alle drei *midkine* Gene des Zebrafisches unterschiedliche Expressionsmuster während der Entwicklung auf. *mdka*, *mdkb* und *ptn* zeigten in Regionen hoher Zellproliferation, wie dem Telencephalon, der Mittel-Nachhirngrenze und dem Nachhirn in der Regel keine Überlappung während der embryonalen Gehirnentwicklung. Die Möglichkeit der simultanen Reduktion zweier oder dreier Proteine durch Injektion von Morpholinogemischen erlaubte die Untersuchung einer eventuellen funktionellen Redundanz während der Gehirnentwicklung. Die Reduktion der Midkine Proteine resultierte in charakteristischen Defekten während der Regionalisierung des Gehirns, was auf eine Rolle während der Bildung essentieller Signalzentren im Gehirn hindeutet. Auffallend waren auch Defekte in der Somitenbildung, die nach gleichzeitiger Reduktion von *mdka*, *mdkb* und *ptn* auftraten. Diese Defekte beruhen entweder auf einer Positionsveränderung der Somiten-Reifungszone oder auf einer Störung der Zelladhäsion im präsomitischen Mesoderm durch Ptn. Somit zeigen die Daten eine neue Funktion von Ptn als sekretiertem Regulator der Somitogenese im Zebrafisch.

1. Introduction

1.1. Differentiation of the vertebrate brain and spinal cord

The central nervous system (CNS) of vertebrates, the most prominent part of the nervous system, is composed of the brain and the spinal cord. Together with the peripheral nervous system (PNS), it is responsible for the ability of an animal to carry out its behavioral repertoire. Fundamental for its functionality is an extensive number of highly diverse neuron and glia cells. The correct quantity of these cells has to be formed at the right time and at the correct position during embryonic development.

1.1.1. Structure of the vertebrate brain

The embryonic vertebrate brain is morphologically and functionally subdivided into three sections (for zebrafish see Fig.1): the prosencephalon (forebrain), the mesencephalon (midbrain) and the rhombencephalon (hindbrain).

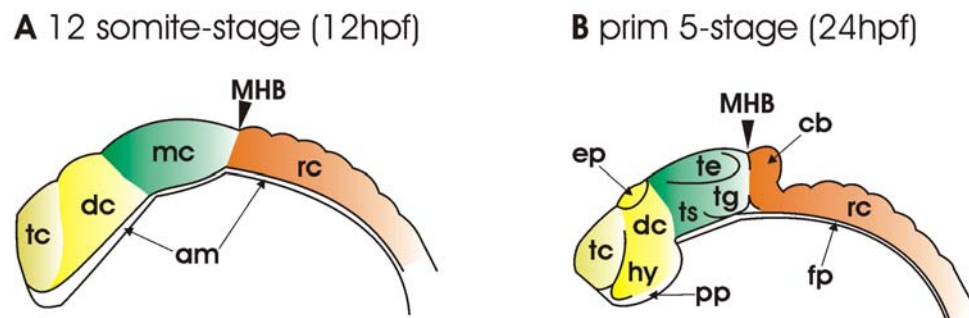


Fig. 1: Structure of the embryonic zebrafish brain

A Lateral view of the brain of a zebrafish embryo at the 12-somite-stage (12 hours post fertilization (hpf)). Anteriormost lies the prosencephalon (yellow region), consisting of the telencephalon (tc) and the diencephalon (dc). More posteriorly the mesencephalon (mc; green) and the rhombencephalon (rc; orange) are formed. Between mid- and hindbrain the Mid-Hindbrain boundary (MHB) is formed. The axial mesoderm underlies the CNS primordium ventrally.

B Lateral view depicting the brain of a zebrafish embryo at the prime 5-stage (24hpf). The prosencephalic regions of the telencephalon (tc), the diencephalon (dc), the hypothalamus (hy) and the epiphysis (ep) are now clearly visible. The midbrain structures of the dorsal tectum (te), the torus semicircularis (ts) and the tegmentum (tg) are distinguishable. Further hindbrain structures of the cerebellum (cb) and the rhombencephalon (rc) are formed. The prechordal plate (pp) lies ventral to the prosencephalon, while the floor plate (fp) lies ventral to the mesen- and rhombencephalon.

The prosencephalon is subdivided into two regions. First the anterior telencephalon which in humans is the brain structure accountable for language, communication, movement, olfaction and memory. Second, the more caudal diencephalon which comprises structures like the pretectum, the thalamus and the hypothalamus. Therefore, the diencephalon is essential for regulation of visceral activities and the control of homeostasis. The mesencephalon is the brain region of highest dopamine production. Among others, it is essential for eye movement

and iris muscle innervation. Furthermore, it inherits fiber tracts between the anterior and the posterior brain. It is composed of the dorsal tectum and the ventral torus semicircularis and tegmentum.

The posteriormost part of the brain, the rhombencephalon, is subdivided into seven smaller compartments called rhombomeres, which are periodic segments along the embryonic anterior-posterior (AP) axis. A functional partition into the anterior metencephalon, comprising the cerebellum and the pons, and the posterior myelencephalon, including the medulla oblongata, is evident. Functions of the rhombencephalon are for example the coordination of movements and balance (Gilbert, 2000; Purves et al., 2001).

The molecular networks underlying the formation of such a complex structure as the brain are highly sophisticated and are far from being understood completely. Nevertheless, essential genes and signaling cascades are known today that regulate correct establishment of brain patterns during earliest embryonic development and result in correct brain regionalization. The mechanisms responsible early patterning seem to be evolutionary well conserved throughout the chordate phylum, in contrast to the highly diverse functional and morphological differentiation found in individual species during later development (Schilling and Knight, 2001; Meinhardt, 2006).

1.1.2. Induction of neural tissues

The first steps in CNS development are the induction of the neural plate (neural induction) and the formation of distinct regions (early neural patterning) along its AP axis. These processes have been of great interest to scientists for many years and are still a field of intensive research.

Neural induction is defined as the process by which ectodermal cells are affected to acquire a neural fate rather than giving rise to epidermis (Stern, 2006). Several models for neural induction have been proposed, e.g. Nieuwkoop's activation/transformation hypothesis (Nieuwkoop, 1973), and are under constant revision and discussion (Stern, 2001; Wilson and Edlund, 2001; De Robertis and Kuroda, 2004). Initial neural ectoderm induction and determination of cells to a neuron specific cell fate occurs during gastrulation, before neurulation, and shortly after the separation of the neural plate (dorsal ectoderm, neural ectoderm) from the non-neural ectoderm (epidermal ectoderm). This process is thought to be initiated by a primary organizer, the Spemann-Mangold organizer, by secretion of molecules that antagonize BMP and Wnt signaling from the non-neural ectoderm, like Chordin, Noggin, Dickkopf or Cerberus (Spemann, 1924; Stern, 2005; De Robertis, 2006). The initially induced

neural cells only have anterior cell fate properties and are expressing genes characteristic for fore- or midbrain tissues (Sive et al., 1989). To adopt posterior neuronal identity further posteriorizing signals are necessary, including Wnt and Nodal signals (Niehrs, 2004).

1.1.3. Patterning of the brain

After the induction of the neural ectoderm further patterning of the neural plate is required for separation of the different subdomains of the CNS. This process is thought to be regulated by local, secondary organizers along the AP axis. These act as signaling centers and secrete morphogens to induce tissue specific gene expression in surrounding cells (Rhinn et al., 2006).

Pattern formation in the forebrain is achieved by two secondary organizers. The anteriormost one is the anterior neural ridge (ANR). This structure is established with appearance of the first prosencephalic cells of the telencephalon at the margin of the neural plate (Woo and Fraser, 1995; Wilson and Rubenstein, 2000). Ablation of the ANR organizer during gastrulation leads to cell death and disruption of correct gene expression in the anterior forebrain (Houart et al., 1998). Further experiments clarified that through the action of secreted Nodal and Wnt factors the anterior neural plate is posteriorized and therefore forebrain fates are induced (Wilson and Rubenstein, 2000). Subsequent to forebrain induction, FGF molecules secreted from the ANR organizer, induce gene expression in eye field precursor cells, the hypothalamus and the diencephalon (Houart et al., 1998; Rubenstein et al., 1998; Walshe and Mason, 2003). A second, more posteriorly situated organizer that acts on forebrain patterning is the zona limitans intrathalamica (ZLI). This organizer is characterized by secretion of Hedgehog factors and is responsible for correct establishment of diencephalic subdivisions like the thalamus (Scholpp et al., 2006). The ZLI is situated in between the prethalamus and the functionally distinct thalamus (Scholpp et al., 2006).

In contrast to the situation in the forebrain, only one local signaling center is found in the mesencephalon, the isthmic organizer. The isthmic organizer resides at the border between the mesen- and the rhombencephalon (mid-hindbrain boundary, MHB; Wurst and Bally-Cuif, 2001). The establishment of the correct position of the MHB organizer starts during late gastrulation by expression of *otx2* in the anterior and *gbx2* in the posterior region of the mesencephalon. The overlapping territory of both expression patterns demarcates the future position of the MHB (Simeone et al., 1992; Muller et al., 1996). Shortly after correct positioning of the MHB, expression of *pax2.1*, *wnt1*, *pou2* and *fgf8* is induced and MHB formation continues (Krauss et al., 1991; Muller et al., 1996; Reifers et al., 1998; Belting et

al., 2001). These genes are responsible for the maintenance and activation of gene expression in the organizer, morphogenesis and lineage restriction around the MHB. In zebrafish, *pax2.1* initiates the expression of the transcription factors *eng2* and *eng3* in the MHB and hence is essential for the correct positioning of the boundary (Brand et al., 1996; Lun and Brand, 1998). In addition, Wnt1/Wnt10 are essential factors for MHB-self maintenance (Lekven et al., 2003) and the secreted signaling factor Fgf8 is crucial for patterning the adjacent anterior hindbrain primordium (Reifers et al., 1998).

Besides the secreted signals from the MHB, another secondary organizer for the hindbrain is presumably localized in rhombomere 4 (r4). The combined expression of *fgf3* and *fgf8* in r4 of zebrafish is required for development of cell identity in the posteriorly situated r5 and r6 (Maves et al., 2002; Walshe et al., 2002). These two rhombomeres have been characterized in detail by utilizing the zebrafish *valentino* mutant and the *Kreisler* mouse mutant, both lacking *mafB* function (Cordes and Barsh, 1994; Moens et al., 1996; Prince et al., 1998). *mafB* is a bZIP transcription factor directly regulating *hox* gene expression and therefore influencing correct segmental patterning (Prince et al., 1998; Manzanares et al., 1999). Establishment of a correct *hox* gene expression pattern in the hindbrain is essential for induction of anterior-posterior cell identity (Schilling et al., 2001) and determines rhombomere identity by transcriptional activation of downstream specifiers (Krumlauf et al., 1993). Beside the MHB- and the r4-organizer, RA builds up an anterior-posterior morphogen gradient in the hindbrain responsible for correct rhombencephalic patterning by activation of *hox* genes (Marshall et al., 1992; Gavalas and Krumlauf, 2000; Moens and Prince, 2002). The peak of the RA morphogen gradient occurs at the spinal cord/hindbrain boundary with gradually decreasing levels to the anterior direction. The loss of the RA gradient results in disturbed hindbrain patterning and cranial neuron development as shown in the zebrafish *raldh2* mutant *neckless* (Begemann et al., 2001; Begemann et al., 2004).

1.1.4. Patterning of the vertebrate spinal cord

The second, posterior part of the vertebrate CNS is the spinal cord. Neurons in the spinal cord are essential for sensing external impulses, interpretation of the sensory inputs and the initiation of muscular responses. For each of these purposes different neuronal subclasses need to be specified in the spinal cord. These subclasses are located in a typical dorso-ventral (DV) pattern in the neural tube (Fig. 2). The dorsalmost neuronal subclass is represented by the group of cutaneous sensory neurons. In amniotes and zebrafish, these are called Rohon-Beard sensory neurons (RBs; Bernhardt et al., 1990). Ventral to those, cell populations of

different interneuron classes are positioned that build axonal circuits between the dorsal sensory neurons and the ventrally located motor neurons. Ventralmost in the spinal cord, motor neurons are formed, which are responsible for myotome and axial muscle innervations.

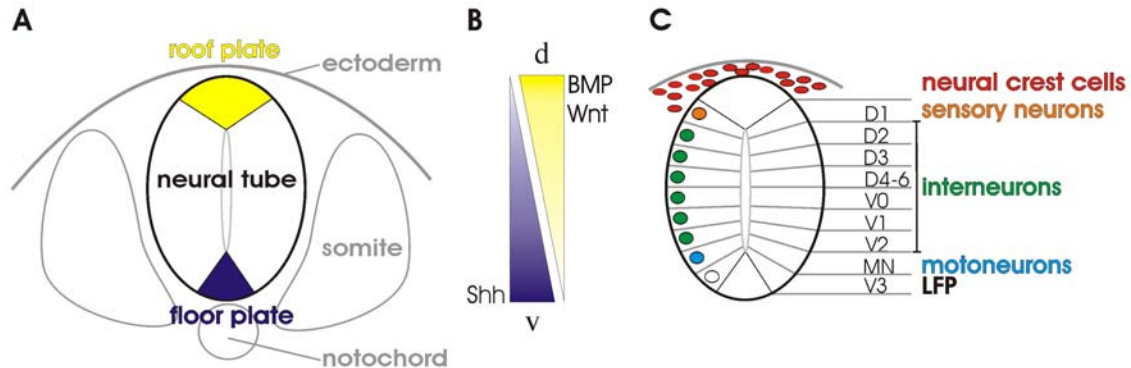


Fig. 2: Dorso-ventral patterning of the neural tube

A Two signaling centers are found in the neural tube, the dorsal roof plate and the ventral floor plate. **B** BMPs and Wnts are secreted factors from the roof plate, while the floor plate and the notochord secrete Shh. These factors act as morphogens and build up opposing gradients throughout the neural tube. **C** Different neuronal progenitor cell domains are formed according to different threshold concentrations of these factors along the DV axis. LFP=lateral floor plate

The establishment of this highly organized pattern of different neurons along the DV axis is accomplished by two signaling centers in the neural tube, the dorsal roof plate and the ventral floor plate. Both centers are non-neural cell populations which secrete characteristic signaling molecules (Fig. 2).

The floor plate in zebrafish consists of two zones, the lateral and the medial floor plate (Odenthal et al., 2000). The medial floor plate is induced at early gastrulation before the notochord has formed and is induced by Nodal-factors like *cyclops* (Hatta et al., 1991), *one-eyed pinhead* (Schier et al., 1997; Zhang et al., 1998) and *schmalspur* (Sirotkin et al., 2000). The lateral floor plate is induced by Sonic hedgehog (Shh) signals from the underlying notochord (Strahle et al., 2004). After floor plate formation the secretion of Shh is initiated and together with Shh secreted from the notochord these floor plate signals build up a DV morphogen gradient in the neural tube. Due to this Shh gradient, pattern formation of distinct ventral neuronal progenitor cells of motoneurons and V0 to V3 interneurons is initiated (Briscoe and Ericson, 1999). Cells along the DV axis sense the different concentrations of Shh and respond by repressing (class I) or activating (class II) the transcription of homeodomain transcription factors (Jessell, 2000). These transcription factors initiate selective repressive interactions between complementary pairs of class I and class II homeodomain proteins and thereby define distinct progenitor domains (Briscoe et al., 2000; Jessell, 2000). Additional signals of the BMP, TGF- β , RA and Fgf pathways and *gli* genes

have recently been found to be essential for cell specification or signal integration in the ventral neural tube and are currently being integrated into this model (Persson et al., 2002; Stamatakis et al., 2005; Lupo et al., 2006).

On the dorsal side of the neural tube the roof plate is located. It secretes factors like BMPs and Wnts to build up a second DV gradient in the neural tube (Barth et al., 1999; Wilson and Maden, 2005). This opposing gradient acts antagonistically to the Shh gradient and has its highest protein levels in the dorsal neural tube (Fig. 2B). This second gradient is essential for patterning the dorsal neural tube into D1 to D6 interneuron domains, by activating the expression of bHLH and LIM homeobox proteins and thereby regulating cell differentiation, growth control and cell specification (Helms and Johnson, 2003; Chizhikov and Millen, 2005). In close proximity to the roof plate a vertebrate specific and highly migratory cell population is found, the neural crest cells (Fig. 2C).

1.2. Development and functions of neural crest cells

Neural crest cells (ncc) are exclusively observed in vertebrates and are a distinctive hallmark of vertebrate evolution (Shimeld and Holland, 2000). They give rise to a large variety of peripheral structures in the developing embryo. These include face cartilage, connective tissue, pigment cells, neurons and glia of the peripheral nervous system and many other derived tissues (Le Douarin and Kalcheim, 1999). It is assumed that all ncc derivatives arise from multipotent ncc stem cells which are able to differentiate and self-renew (Stemple and Anderson, 1992; LaBonne and Bronner-Fraser, 1998a; Le Douarin and Dupin, 2003).

1.2.1. Induction of neural crest cells

Ncc are induced at the border between the neural plate, the progenitor structure to the CNS, and the non-neural ectoderm during gastrulation. In recent years, significant progress has been made in determining the molecular mechanisms underlying the induction of these cells during gastrulation by identification of essential signaling molecules (Knecht and Bronner-Fraser, 2002). These include members of the BMP, Wnt, FGF and retinoic acid (RA) signal pathway families that interact in a highly coordinated and spatiotemporal fashion (Aybar and Mayor, 2002; Knecht and Bronner-Fraser, 2002; Barembaum and Bronner-Fraser, 2005).

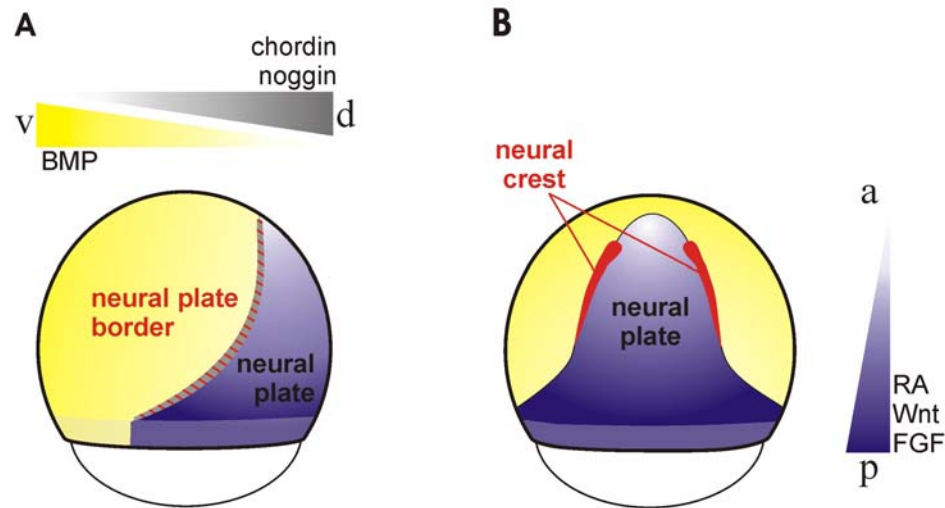


Fig. 3: Two-step model of neural crest induction during gastrulation in zebrafish

A The neural plate border is specified by intermediate levels of BMP from the ventral non-neural ectoderm (v, yellow) and BMP-antagonists secreted by the dorsal organizer (d). **B** Neural crest cells are induced at the neural plate border by posterior (p) Fgf, Wnt and RA signals. a = anterior

A first step in ncc induction is the divergence of neural plate and non-neural ectoderm (Fig. 3A). Experiments on *Xenopus* suggested a neural default state model of ectodermal cells induced during gastrulation (Hawley et al., 1995; Wilson and Hemmati-Brivanlou, 1997). This model proposes that ectodermal cells have a default neural fate, which they adopt if they receive no signals from neighboring cells. During gastrulation, BMPs inhibit this fate and specify epidermis on the ventral side of the embryo (Wilson and Hemmati-Brivanlou, 1997). According to this model an intermediate BMP level established by secreted ectodermal BMPs and organizer derived BMP antagonists interact to configure the neural plate border (Tribulo et al., 2003).

In a second step, Wnt, Fgf and RA signals are necessary for the transformation of the posterior neural plate border to establish distinct ncc domains (Fig. 3B; Aybar and Mayor, 2002; Villanueva et al., 2002). Studies in *Xenopus* ectodermal explants showed that loss of Wnt function by utilizing a dominant-negative form GSK-3 (Saint-Jeannet et al., 1997) and gain of function by overexpression of *Xwnt7b* (Chang and Hemmati-Brivanlou, 1998) result in a change of ncc induction. Furthermore, Wnts have been implicated to act as a ncc inducing signal also in many other species (LaBonne, 2002; Yanfeng et al., 2003). A second pathway regulating ncc induction is activated by FGFs (LaBonne and Bronner-Fraser, 1998b; Villanueva et al., 2002). In *Xenopus*, FGF8 secreted from the paraxial mesoderm can induce ncc at the neural plate border (Monsoro-Burq et al., 2003). Further studies showed that FGF signals act in parallel to Wnts on *msx* genes, which are essential neural plate specifiers (see

chapter 1.2.2; Monsoro-Burq et al., 2005). The role of RA signaling on ncc induction has been analyzed in *Xenopus* in more detail by showing that RA or an constitutive active RA receptor is sufficient to transform the anterior neural plate border into ncc (Villanueva et al., 2002). In summary, a two step activation by BMP, Wnt, Fgf and RA pathways during gastrulation results in the induction of ncc at the neural plate border.

1.2.2. Molecular networks involved in ncc differentiation

Following ncc induction at the neural plate border, several factors coordinate further ncc specification, maintenance, migration and final differentiation of the multipotent cells into their highly diverse derivatives. Observations of ncc development in several species, like chicken, *Xenopus*, mouse and zebrafish, led to the establishment of a complex molecular network for ncc development (simplified in Fig. 4; Meulemans and Bronner-Fraser, 2004; Barembaum and Bronner-Fraser, 2005; Steventon et al., 2005).

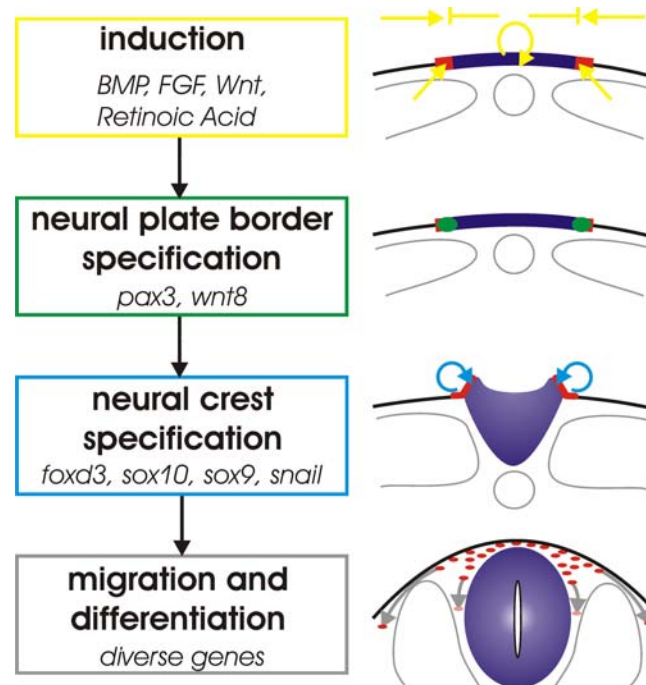


Fig. 4: Different steps of ncc development

Several processes can be distinguished in ncc development. Initial induction of the neural plate border is achieved by activation through several signals. This process leads to the expression of neural plate border specifying genes and subsequently to expression of ncc specific genes. The final step of ncc migration and differentiation is orchestrated by diverse genes.

red squares/dots = neural plate border or neural crest cells; blue structures = neural plate/neural tube; black line = non-neural ectoderm/epidermis; grey structures = notochord and somites

According to this model, the initial establishment of a field of competence at the neural plate border (described in 1.2.1) is followed by the initiation of neural plate border specifying gene transcription. The induced group of genes encodes transcription factors downstream of BMP, Fgf or Wnt signaling, e.g. *pax3/7*, *dlx5*, *msx1/3* and *zic1* (Woda et al., 2003; Monsoro-Burq et al., 2005; Sato et al., 2005). The timing of their expression at the neural plate border and the capacity of these genes to regulate the expression of ncc specific targets distinguish them from slightly later activated ncc specifier genes. The group of ncc specifier genes consists of *slug/snail*, *tfap2*, *foxd3*, *sox10*, *sox9* and *c-myc*. They are expressed in early non-migratory and in some cases in late migratory ncc. This set of genes is autoregulatory, essential for ncc maintenance, ncc survival and the induction of ncc effector genes (Heeg-Truesdell and LaBonne, 2004; Steventon et al., 2005). The group of ncc effector genes comprises a huge variety of downstream mediators responsible for ncc migration, epithelial-to-mesenchymal transition (EMT) and differentiation. Examples for essential migration genes of this class are *cadherins*, which are able to change cell shape and adhesion of ncc progenitors (Pla et al., 2001) and *sox* genes, which are differentiation factors able to induce cartilage, glia or melanocytes (Ng et al., 1997; Mollaaghababa and Pavan, 2003). Signals for ncc induction of the Wnt or BMP families are re-used in these latest steps of ncc differentiation (Raible and Ragland, 2005).

1.2.3. Development of the neural crest in zebrafish

Zebrafish ncc form the same range of derivatives like in other vertebrates, for example sensory neurons, jaw tissue and pigment cells. Moreover many aspects of ncc development are similar in zebrafish. Initial neural ectoderm formation and subsequent ncc induction are highly reminiscent of that of other vertebrates.

Planar signals by the BMP, FGF and Wnt family are essential for correct ncc induction in zebrafish by regulating neural plate establishment and posterization of neural tissues (reviewed in Solnica-Krezel, 2002). One prominent example of disturbed ncc induction is the zebrafish *swirl* mutant, which lacks a functional *bmp2b* gene and shows gain of neural plate tissue with concomitant ncc reduction (Nguyen et al., 1998). In contrast to *Xenopus* the significance of RA for zebrafish ncc formation remains to be elucidated. Zebrafish *neckless* mutants lacking Raldh2 function display disrupted RA synthesis and have defects in patterning of the posterior cranial mesoderm. However, no defects in ncc induction are observed (Begemann et al., 2001).

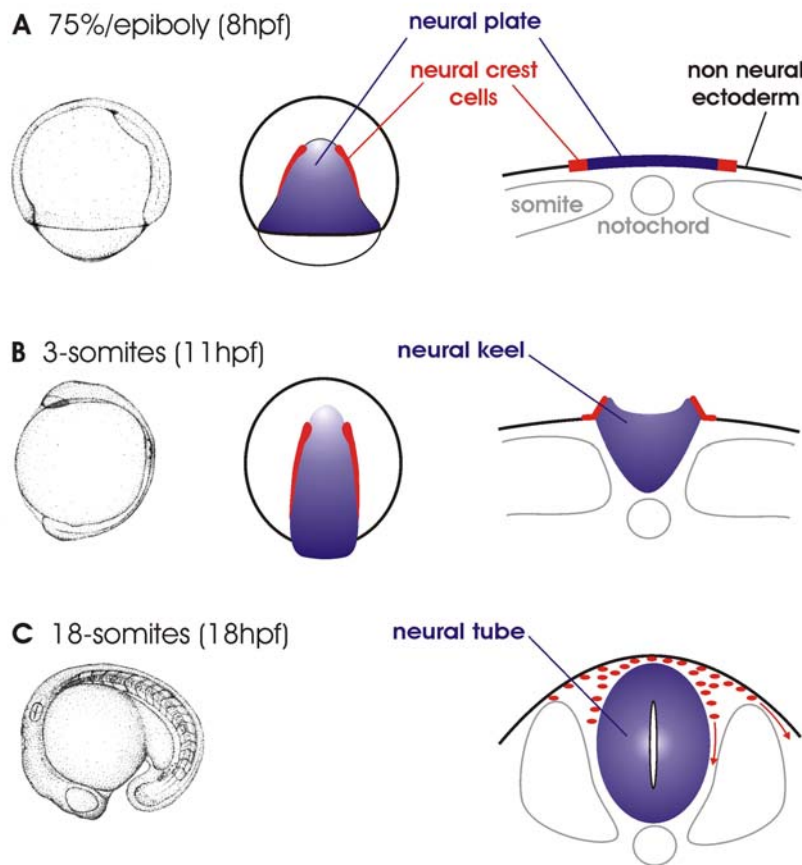


Fig.5: Neural crest development during zebrafish neurulation

On the left lateral views of zebrafish embryos of the corresponding developing stage are shown (taken from Kimmel et al., 1995); the mid-panel depicts dorsal views of the neural plate and the ncc domains; on the right, sections represent the dorso-ventral positioning of the ncc.

A At 8hpf, premigratory ncc can be observed at two positions at the border between the non-neural ectoderm and the neural ectoderm during late gastrulation at 75% epiboly. **B** Upon segmentation at the 1-3 somite stage (11hpf) ncc are found at the dorsal lips of the neural keel. **C** After closure of the neural tube (18hpf) the two ncc domains are joined and ncc migration is initiated.

In zebrafish, the process of ncc induction starts during mid-gastrulation (6-8 hours post fertilization, hpf; Fig. 5A). Initially, the establishment of morphogen gradients across the embryo leads to the expression of *wnt8b* and *pax3*, typical neural plate border defining genes, at the anterior neural plate border between the neural and non-neural ectoderm (Seo et al., 1998; Lewis et al., 2004). Zebrafish *wnt8b* expression is found around the margin at 80% epiboly, but a second expression domain is also present at the dorsal neural plate overlapping with *pax3* expression at the presumptive ncc domain. Knockdown of *wnt8b*, but not of *wnt8a*, results in loss of ncc markers like *sox10* or *foxd3* at the 3-somite stage (Lewis et al., 2004). Interestingly, regain of ncc derivatives at later developmental stages in these morphants suggested a short timeframe of Wnt8b activity during ncc induction.

After the neural plate border is established, zebrafish homologues of neural plate border specifiers are expressed and act on cell specification of ncc and sensory neurons, e.g. the *msx* genes or *dlx* genes (Kaji and Artinger, 2004; Phillips et al., 2006). In case of the *dlx* genes, which code for homeodomain transcription factors, combined knockdown of *dlx3b* and *dlx4b* resulted in loss of RBs, trigeminal placodes and *fhx6* expressing ncc (Kaji and Artinger, 2004). Additionally, Kaji and Artinger (2004) showed an influence of *dlx3b/dlx4b* on *bmp2b* expression at the neural plate border during gastrulation in these morphants. Therefore, knockdown of *dlx* function indicates changes in the BMP gradient with subsequently altered neural ectoderm boundary formation.

The expression of neural crest specifiers like *foxd3*, *sox9b*, *snail1b* and *sox10* starts at 11hpf (3-somite stage) along the border of the neural keel, which forms after convergence of the neural plate (Fig. 5B; Thisse et al., 1995; Odenthal and Nusslein-Volhard, 1998; Dutton et al., 2001; Li et al., 2002). The neural keel is a fish specific structure that forms after convergence of the neural plate. Mutant analysis revealed prominent functions during ncc differentiation and maintenance in zebrafish for most of these genes, but none of them interferes with ncc induction (*foxd3*: Dutton et al., 2001; Montero-Balaguer et al., 2006; *sox9*: Yan et al., 2005; *sox10*: Dutton et al., 2001; Carney et al., 2006).

The neural tube in zebrafish is formed at about 18hpf and trunk ncc start to undergo EMT (Fig.5C). Ncc begin to migrate along one of two routes through the embryonic body to reach their final destination. These migration routes either lie between the somites and the epidermis, referred to as the lateral pathway, or between the somites and the neural tube, defined as the medial pathway (Raible et al., 1992). Many novel factors for EMT initiation, cell adhesion and cell guidance have been experimentally investigated by Morpholino (MO) knockdown or mutant analysis in zebrafish (reviewed in Halloran and Berndt, 2003).

1.2.4. Development of sensory neurons in zebrafish

Similar to ncc, the first sensory neurons are specified at the neural plate border during zebrafish gastrulation (3-somite stage; Fig. 6A). Several transcription factors have recently been implicated to play a role in the progression of cell fate decisions at the neural plate border of the zebrafish including *prdm1/blimp-1* (Roy and Ng, 2004; Hernandez-Lagunas et al., 2005) and *olig3* (Filippi et al., 2005). *prdm1/blimp-1* is not only able to interfere with ncc induction but also represses induction of neuronal cells specified at the neural plate border, e.g. RB-neurons and placodes (Roy and Ng, 2004). A similar result has been observed after simultaneous knockdown of *tfap2a* and *tfap2c* (Li and Cornell, 2007) or *dlx* genes (Kaji and

Artinger, 2004). These observations indicate a common precursor population of ncc and RB-neurons or a common zone of specification at the neural plate border. The cell fate decision leading from these common precursors to either ncc or RB neurons is regulated by lateral inhibition via the Delta-Notch pathway and *ngn1* during neurogenesis (Cornell and Eisen, 2000, 2002). The novel transcription factor *olig3* mediates Delta-Notch signals in this context by inducing neural cell fates at the expense of ncc. Knockdown of *olig3* results in ablation of RBs but simultaneously gain of ncc (Filippi et al., 2005).

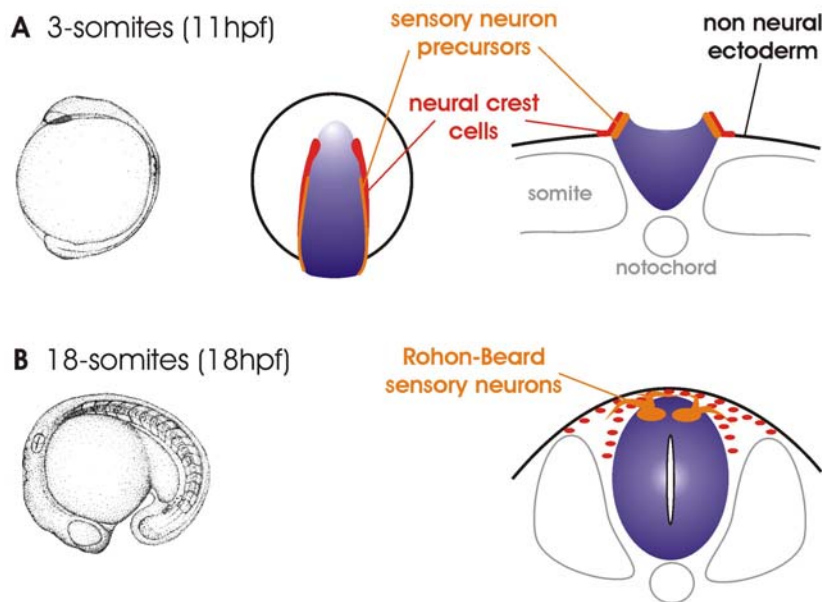


Fig. 6: Rohon-Beard sensory neuron development in zebrafish

A First sensory neuron precursors are formed at 11 hpf (1-3 somite stage) at the border of the neural plate and the non-neural ectoderm in close proximity to ncc. **B** After closure of the neural tube at 18 hpf, Rohon-Beard sensory neurons differentiate in the dorsal neural tube and initiate axonal growth towards the dermis.

After closure of the neural tube the induced RB sensory neurons represent the dorsalmost neuron population in the neural tube and form a continuous double column at the dorsal surface (Fig. 6B).

1.2.5. Open questions in ncc and sensory neuron development

There is a great number of open questions concerning the basic process of ncc and sensory neuron induction at the neural plate border. It is assumed that the establishment of the BMP morphogen gradient across the embryo specifies the neural plate border. This assumption is challenged by recent findings showing that the Bmp antagonists Noggin, Follistatin and Chordin are not essential for ncc induction in zebrafish (Ragland and Raible, 2004).

Furthermore, this study demonstrates that signals from the underlying mesoderm (vertical signals) are dispensable for ncc induction. Instead, factors derived from the ectoderm (planar signals) are required and essential for ncc induction and signal integration (Ragland and Raible, 2004). Therefore, new models and species specific differences are discussed for the mechanisms of ncc induction (Raible, 2006).

After setting up the neural plate border, subsequent signaling by Wnts and FGFs is essential for induction of ncc specific transcriptional factors, e.g. *pax3*, *sox10*. These factors activate a complex molecular network for further specification and survival of ncc (chapter 1.2.2; Meulemans and Bronner-Fraser, 2004). Nevertheless, it remains unclear how the initial signals are resolved and integrated into specific activation of downstream transcriptional factors at the correct place and time. Of special interest in this context is the identification of secreted factors derived from the neural plate, which act to establish the neural plate border or to induce ncc fates. Only very few of these factors are known today, like *wnt8a* in zebrafish (Lewis et al., 2004).

Another open question is whether ncc and sensory neurons are arising from a common progenitor population of multipotent cells at the neural plate border. It was shown that sensory neurons derive from the same neural plate domain as neural crest (Cornell and Eisen, 2000). Several studies in zebrafish showed that interference with Delta-Notch signals resulted in supernumerary sensory neurons at the expense of trunk neural crest (Cornell and Eisen, 2000, 2002). Additionally, several transcription factors expressed in the non-neural ectoderm or the neural plate border have been identified to be essential for this cell fate decision (Kaji and Artinger, 2004; Roy and Ng, 2004; Hernandez-Lagunas et al., 2005; Li and Cornell, 2007). Nevertheless, to date no secreted factor from the neural plate is known to influence the induction of both cell populations at the neural plate border.

One candidate factor that might solve these open questions is *Mdkb*, which is characterized in detail in this thesis. Initial experiments had shown that *mdkb* is expressed in the early neural plate and that interference with *Mdkb* function results in a reduction of ncc (Winkler and Moon, 2001).

1.3. Gradients and clockworks in somitogenesis

Ncc migration and derivate patterning depends on growth factors secreted from somites that flank the neural tube on both sides. In chicken ncc are guided through the ventral pathway and patterned by signals from the somites to form dorsal root ganglia (Lallier and Bronner-Fraser, 1988). In addition, the somites secrete signals to pattern the surrounding tissues like the neural

tube. For example, RA derived from the somites inhibits FGF activity in the neuroepithelium and the paraxial mesoderm of chicken and thereby regulates patterning and differentiation in the neural tube (Diez del Corral et al., 2003). Vice versa, factors secreted from the neural tube also influence development of somite derivatives. Shh secreted from the floor plate and the notochord is required for the formation of myoblast cell fates and for axial cartilage development (Dockter, 2000; Ingham and Kim, 2005). Wnt1 and Wnt3a secreted from the roof plate regulate the formation of the medial compartment of the dermamyotome in mouse (Ikeya and Takada, 1998; Brent and Tabin, 2002).

Somites are bilateral cell aggregates in the paraxial mesoderm of the vertebrate body. They contain precursors of the axial muscles, dermis, tendons and the skeleton. Somitic segments form repeatedly along the AP axis in a highly synchronized process called somitogenesis. Somitogenesis is subdivided into three steps. First, stem cells of the tailbud leave their undetermined stage while the tail elongates caudally and become prepatterned. Second, when reaching the anterior presomitic mesoderm (PSM) border these cells form aggregates, called somitomes, and establish AP polarity. Finally, the somitomes epithelialize and bud off from the PSM to form a somite. During the segmentation period, this process occurs constantly in the presomitic mesoderm (PSM) of the embryonic tailbud and results in the elongation of the AP axis (Pourquie, 2001; Dubrulle and Pourquie, 2004a; Holley, 2007).

Several models have been proposed to explain somitogenesis and have been confirmed or rejected by experimental observations (Dale and Pourquie, 2000; Baker et al., 2006). Today, the “clock and wavefront” model is the most favored and accepted concept to explain the spatiotemporal appearance of somites (Cooke and Zeeman, 1976; Dubrulle and Pourquie, 2002; Baker et al., 2006). This model consists of two essential components, an intrinsic cellular oscillator and an activity gradient along the AP axis of the PSM. The cellular oscillator, also referred to as the segmentation clock, acts in the cells of the PSM and sets up a periodic temporal signal for boundary formation. It is associated with periodic activation of the Notch and the Wnt pathway. This results in a wave-like, periodic expression of different target genes in the PSM (Aulehla and Herrmann, 2004; Giudicelli and Lewis, 2004). Examples for targets of the segmentation clock are the mouse *hey2* gene (Leimeister et al., 2000) or members of the *her* gene family in zebrafish (Holley et al., 2000).

The AP-position where somite differentiation is started and intersomitic boundaries are formed is propagated by the determination front which is formed by a dynamic gradient in the PSM. At this position of the PSM, PSM become independent from the segmentation clock and somite epithelialization can occur. The position of the determination front is defined by a

threshold activity of FGF signaling mediated by Fgf8 expression and activated MAP-kinase (Dubrulle et al., 2001; Sawada et al., 2001; Dubrulle and Pourquie, 2004b).

Two other gradients in the PSM are essential for correct somite formation. One is the Wnt gradient, which has been identified in the PSM and is thought to be responsible for linking the segmental clock to the wavefront through Wnt3a and Axin2 (Aulehla et al., 2003; Aulehla and Herrmann, 2004). An anterior-posterior RA gradient in the segmented region antagonizes the determination front by counteracting the FGF8 gradient in the neural tube and the PSM (Diez del Corral and Storey, 2004; Moreno and Kintner, 2004). In addition, RA is an essential determinant of correct left-right patterning of somites (Brent, 2005; Kawakami et al., 2005; Vermot et al., 2005; Vermot and Pourquie, 2005).

Although essential components of the somitogenesis clock and the wavefront are known, several unanswered questions still remain. For example, it is still unclear whether there are additional signals that are essential to stabilize the maturation front at the right position. Furthermore, differences between anterior and posterior trunk segmentation in zebrafish somitogenesis mutants are detected and are not yet fully understood (Holley, 2006). Noteworthy, it has been described that gain of *Mdka* function influences formation of both anterior and posterior somite boundaries (Winkler et al., 2003). In addition, overexpression of *mdka* resulted in a loss of *myod* expression in all somites and adaxial mesoderm (Winkler et al., 2003) but did not interfere with the onset of the somitogenesis clock (personal communication with C. Winkler). Remarkably, *mdka* is expressed in the paraxial mesoderm in a dynamic AP-wave that progresses caudally with its edge overlapping with the somite determination front (Schaefer et al., 2005). These observations led to the assumption that *Mdka*, secreted from paraxial cells, might act as an anterior signal determining the position of somite maturation. Nevertheless, detailed studies supporting this hypothesis are still missing.

1.4. The zebrafish as a model system

The zebrafish (*Danio rerio*) is a small tropical fish of 3 to 4 cm in adult size, which is often found as an ornamental fish in home aquaria. It originates from rivers in India, Pakistan, Nepal and Myanmar. In recent years, it has become a well accepted model for scientists as an oviparous animal system that is easy and inexpensive to maintain in the laboratory and can be efficiently used to study different aspects of vertebrate development. Some reasons for the popularity of zebrafish are its rapid external embryonic development, the transparency of embryos and larvae, the short generation time of three months, a completed genome

sequencing project and up-to-date embryological and genetic methods (Kimmel et al., 1995; Westerfield, 1995; www.zfin.org; www.sanger.ac.uk/Projects/D_rerio).

During the last 20 years, numerous methods have been developed to perform forward genetics like ENU screens (Driever et al., 1996; Haffter and Nusslein-Volhard, 1996), large-scale insertional mutagenesis (Amsterdam et al., 2004; Amsterdam and Hopkins, 2006) or gene trap experiments (Ellingsen et al., 2005) resulting in a huge variety of available mutant lines. Reverse genetic methods allow specific targeting of single genomic loci by TILLING (Wienholds et al., 2003). In addition, generation of stable transgenic lines is possible by simple DNA injection (Culp et al., 1991). Furthermore, an easy method to repress gene function can be achieved by Morpholino injection (Nasevicius and Ekker, 2000). New methods are constantly being developed to use the zebrafish for compound and small molecule screening (Peterson et al., 2000; Burns et al., 2005), drug development (Zon and Peterson, 2005) or as a human disease model (Dooley and Zon, 2000; Lieschke and Currie, 2007). Nowadays, fast evolving optical methods make it possible to use zebrafish to monitor cell behavior in an living *in vivo* system (Beis and Stainier, 2006). Taken together, the zebrafish has become a well established model system, which is frequently used for investigations of vertebrate development, evolution and genetics.

1.5. Gene duplication in zebrafish

One striking finding in zebrafish genomics was that gene duplication can be frequently observed in many gene families. This phenomenon seems to be common in the genomes of many teleost species when compared to mammalian genomes (Wittbrodt et al., 1998). Reasons for gene duplication may be single gene or whole genome duplications (Meyer and Schartl, 1999). A prominent example for the duplication of an entire gene cluster, supporting the idea of a whole genome duplication are the seven *hox* clusters in the zebrafish genome (Amores et al., 1998; Meyer and Malaga-Trillo, 1999).

It is now generally accepted that a fish-specific whole genome duplication happened after the divergence of the ray-finned fish (Actinopterygii) and the lobe-finned fish (Sarcopterygii) about 320 million years ago. At the same time, teleost radiation resulted in about 22.000 species of ray-finned fish (Taylor et al., 2003; Vandepoele et al., 2004). The evolutionary driving force behind this huge radiation event was the gain of a complete second set of genes with the possibility to change protein functions and gene expression in the duplicates (Taylor and Raes, 2004). In principle, several evolutionary fates of a duplicated gene are possible. First, a degradation of one gene copy by accumulation of non- or missense mutations will lead

to the formation of a non-functional pseudogene. Second, sub-functionalization (subfunction partitioning) could occur where common gene functions are split up into discrete functions in each duplicate. This process may also be accompanied by changes in the expression of both genes into two new non-overlapping patterns. Third, mutations in the duplicate may lead to novel functions or expression domains different from functions and expression pattern of the ancestral gene. This process is called neo-functionalization. Furthermore, combinations of these three possible fates or unchanged gene functions in duplicates (functional redundancy) are likely outcomes of a gene duplication event (Force et al., 1999; Volf and Schartl, 2003). The zebrafish model offers the advantage to analyze evolutionary hypotheses with developmental and genetic methods. Accordingly, several gene duplication events with subsequent sub-functionalization and changes of expression have been intensively investigated in zebrafish. One example is the zebrafish *sox9* gene (Chiang et al., 2001; Yan et al., 2005). Sox9 is a transcriptional regulator required for testis and cartilage development which is duplicated in zebrafish. Both co-orthologues have obtained distinct spatiotemporal expression patterns during zebrafish development (Chiang et al., 2001). Different functions of both orthologues during ncc, bone and cartilage development have been determined by mutant analysis and MO knockdown (Yan et al., 2005). Knockdown of both genes resulted in pronounced defects in facial skeleton formation similar to those observed in higher vertebrates (Yan et al., 2005). Therefore, studying duplicated co-orthologs in teleost models facilitates the analysis of conserved gene functions in humans (Yan et al., 2005).

1.6. Midkine and Pleiotrophin

1.6.1. Midkine and pleiotrophin genes in vertebrates

Another example for a gene duplication event in zebrafish has been described for members of the *midkine* gene family (Winkler et al., 2003). This family consists of only two genes in higher vertebrates: *midkine* (*MDK*, also called *NEGF2*) and *pleiotrophin* (*PTN*, also called *HB-GAM*, *NEGF1*, *HARP*). Both encoded proteins show approximately 50% identity in amino acid sequences and share common protein motives as well as an identical domain organization (Iwasaki et al., 1997; Kilpelainen et al., 2000; Muramatsu, 2002). Both factors are secreted growth factors of low molecular weight with heparin-binding abilities (Kadomatsu and Muramatsu, 2004). *Mdk* was initially identified in a differentiation screen for retinoic-acid responsive genes in embryonic carcinoma cells (Kadomatsu et al., 1988), while *PTN* was first discovered due to its ability to promote neurite outgrowth and its mitogenic

activities in fibroblasts (Milner et al., 1989; Rauvala, 1989). In cell culture assays, both factors share a variety of biological activities in neurogenesis, apoptosis, angiogenesis and vasculogenesis (Kadomatsu and Muramatsu, 2004). The activities of both factors are mediated through several putative receptors. Binding assays in several cell lines demonstrated that Mdk and Ptn are able to interact with heparan sulfate proteoglycans (Kojima et al., 1996), anaplastic lymphoma kinase (ALK; Stoica et al., 2001; Stoica et al., 2002) and different members of the receptor-type protein tyrosine phosphatase family (Rptp; Maeda et al., 1999; Sakaguchi et al., 2003). Affinity chromatography studies suggested the LDL receptor-related protein (LRP) to be a component of the receptor complex of Mdk (Muramatsu et al., 2000). Different isoforms of Ptn can be generated by C-terminal cleavage of the full length protein. These isoforms are able to selectively bind to only one receptor and hence promote glioblastoma proliferation via ALK-binding, respectively cell migration via Rptp-binding (Lu et al., 2005). In addition, dimer formation through transglutaminase-mediated cross-linking has been reported to be an important step for Mdk activity and receptor binding (Kojima et al., 1997).

A role for *mdk* and *ptn* in human diseases, especially in cancer, has long been assumed due to their expression profiles and their *in vitro* abilities to act as mitogenic, anti-apoptotic and transforming factors. Clinical studies revealed increased serum levels of Ptn in tumor patients (Souttou et al., 1998). To gain deeper insight into their *in vivo* functions and to establish an animal model for cancer research, mouse knockout lines were established for both genes. *mdk* knockout mice showed no severe abnormalities during development, but displayed prolonged expression of *calretinn* in the dentate gyrus granule cell layer of the hippocampus of infant mice (Nakamura et al., 1998). Additionally, *mdk* *-/-* mice revealed memory deficiencies and increased anxiety in behavioral tests. In *ptn* knockout mice, no gross anatomical abnormalities, but a lowered threshold of long-term potentiation were observed (Amet et al., 2001). To analyze compensatory effects of both genes, double knockout mice were generated. *ptn/mdk* *-/-* mice showed increased early embryonic lethality, slower growth rates and female infertility in homozygous littermates (Muramatsu et al., 2006). Deficiencies in expression of *β -tectorin*, a crucial factor in the reception of acoustic input in the cochlea were also observed in double-knockout mice (Zou et al., 2006). Hence, there is only limited use of *mdk/ptn* double-knockout or single gene knockout mice to investigate the embryonic functions of *midkine* genes *in vivo*.

1.6.2. *midkine* and *pleiotrophin* genes in zebrafish

In addition to investigations in cell culture studies and in mice, *mdk* and *ptn* were also identified and functionally characterized in zebrafish. Initially, a *mdk* orthologue in zebrafish, *mdkb*, was identified in an expression cloning screen for neural-inducing factors (Winkler and Moon, 2001). *mdkb* is expressed during zebrafish gastrulation in the neural plate and later in distinct CNS tissues like the telencephalon, the rhombencephalon and the roof plate. Expression of *mdkb* is strongly down-regulated by increased levels of RA and BMP. Initial overexpression and injection of a dominant-negative version of Mdkb interfered with posterior neural induction, hindbrain patterning and *ncc* development (Winkler and Moon, 2001). These results point to *mdkb* as an important planar determinant of dorsal cell fates in the neural plate, e.g. neural crest or roof plate cells.

Subsequently, a second co-ortholog, *mdka*, was identified in the zebrafish genome. The expression pattern of *mdka* differs significantly from that of *mdkb*. *Mdka* can be detected in the fore- and hindbrain, in the medial neural tube and in the paraxial mesoderm, where expression propagates in a wave like fashion from anterior to posterior (Winkler et al., 2003). Gain of *Mdka* function resulted in a strong expansion of the medial floor plate without alteration of dorsal cell fates in the neural tube (Winkler et al., 2003). A gene knockdown for *mdka* by Morpholino injection reduced the floor plate size with a simultaneous increase in notochord cell number (Schafer et al., 2005). This effect on floor plate and notochord is independent of factors which specify midline precursor cells during gastrulation in the tailbud, e.g. *cyclops* (Tian et al., 2003). *Mdka* rather affects specification of medial floor plate versus notochord cells in the trunk region after gastrulation (Schafer et al., 2005).

Both zebrafish *mdk* genes evolved by an ancient fish-specific chromosomal block duplication event from a common ancestor (Winkler et al., 2003). After this event, the duplicates gained highly restricted non-overlapping expression patterns during zebrafish development, in contrast to the ubiquitous expression of *mdk* in mice during midgestation and adult kidney (Fan et al., 2000). It was proposed that a process of sub-functionalization and/or possibly neo-functionalization was responsible for the different functions of the zebrafish gene duplicates (Winkler et al., 2003).

There is a single *ptn* ortholog in zebrafish. Its expression was previously described during zebrafish development by RT-PCR. Transcripts were identified from fertilization onwards at low levels until 2 dpf. In contrast to this, hatched (72hpf) and adult fish showed high expression levels in the brain and intestine (Chang et al., 2004). Moreover, enhancement of neurite outgrowth was detected after PC12 cells were transfected with a full-length zebrafish

ptn cDNA. Additional coinjection of DNA constructs for HA-tagged *ptn* along with a HuC driven GFP construct into zebrafish embryos resulted in enhanced neural outgrowth along the body axis (Chang et al., 2004). Further investigations of *ptn* functions in zebrafish have not been conducted.

Despite several *in vitro* studies in mammalian systems, receptors for Midkine and Pleiotrophin remain unidentified in zebrafish. It is unknown, whether both Mdk co-orthologues and Ptn have different affinities to a same receptor or completely distinct receptors for their divergent biological functions. It furthermore is likely that Mdka and Mdkb are able to form heterodimers, which could additionally modulate receptor specificities. Therefore, it is of great interest to investigate the level of functional redundancy in regions of overlapping expression of *mdka*, *mdkb* and *ptn* in zebrafish, most notably in the developing brain.

1.7. Aim of the PhD thesis

Aim of this thesis was to characterize the role of Midkine growth factors during three important developmental processes, i.e. neural crest cell (ncc) formation, brain patterning and somitogenesis.

A complex network of different signaling cascades regulates the induction of ncc at the neural plate border. However, little is known about the interactions of these signaling pathways. In particular, it remains unclear, how several opposing gradients are integrated at the molecular level to establish a restricted zone of competence at the neural plate border where ncc and RB neurons are formed. Recently, it was suggested that factors from the neural plate (planar signals) are essential to fulfill this task (Lewis et al., 2004). Mdkb is a putative candidate for such a planar signal in zebrafish. First, *mdkb* expression is found at the neural plate border during the time of ncc and sensory neuron induction. Second, *mdkb* has the ability to influence posterior ncc and neuron formation (Winkler and Moon, 2001). Third, *mdkb* encodes a secreted heparin-binding growth factor with a small diffusion radius. Therefore, one aim of my PhD thesis was to elucidate the control of *mdkb* expression by known ncc inducing pathways. Furthermore, I wanted to investigate the function of *mdkb* during cell induction at the neural plate border in detail.

In mice, expression of *ptn* and *mdk* is ubiquitous during midgestation and disappears during adulthood (Fan et al., 2000). Furthermore, the lack of any obvious defect in knockout mice indicated functional redundancy of both growth factors (Amet et al., 2001). In contrast to mice, all three zebrafish orthologues are expressed in restricted and mostly non-overlapping

patterns during early brain development in zebrafish. This is consistent with specific and non-redundant functions of these genes during establishment of brain patterning. Expression of *ptn* in the hindbrain rhombomeres r5 and r6 directly adjacent to the organizer r4 is of special interest in this context, because it suggests a possible function of *ptn* during hindbrain segmentation. Hence, a second aim of my PhD thesis was to investigate the roles of *mdka*, *mdkb* and *ptn* during zebrafish brain pattern formation. A special focus in this project was to study aspects of functional redundancy and to assess possible overlapping activities by combined knockdown of two or three genes.

Previously, distinct effects of overexpressed *mdka* and *mdkb* were described on somite formation (Winkler et al., 2003). Endogenous *mdka* is expressed in the paraxial mesoderm at a position where the first somites are formed and progresses in a rostral to caudal wavelike fashion. In addition, overexpression of *mdka*, but not of *mdkb* resulted in loss of all somite boundaries and ablated expression of *myod*. These observations suggest an important function of *mdka* for early steps of somite formation. Consequently, aim of the third project of my PhD thesis was to explore effects of single or combined gene knockdown of *midkine* genes on somite formation. These experiments are expected to give additional information about redundant, respectively non-overlapping activities of Midkine growth factors.

2. Material

2.1. Fish maintenance and breeding

The zebrafish (*Danio rerio*) is a tropical fish belonging to the minnow family of Cyprinidae and is named for the five uniformly pigmented, horizontal blue stripes on the side of the body. Adult fish are about 4 cm in body size and are able to produce 100 -300 eggs per spawning. Males are thin, torpedo-shaped and have golden stripes between the blue stripes, while female fish are larger than males, have bigger bellies and are more silver in coloration. The generation time under optimal conditions is between 2.5 and 3 month. Embryonic development is fast and takes 2 to 3 days at 28°C until hatching of swimming larvae.

Zebrafish were maintained and staged as described (Kimmel et al., 1995; Westerfield, 1995). The developmental stages indicated in figures refer to hours post fertilization (hpf) at 28 °C or somite number. Wildtype fish used were of the AB/TU strain (ZFIN ID: ZDB-GENO-010924-10) that has been kept as closed colony stock in our laboratory for many generations. The *mindbomb* (*mib^{ta52b}*) mutants were originally described in (Kelsh et al., 1996).

2.2. Bacterial strains

For plasmid-vector amplification usually chemically competent bacteria of the DH5 α or XL1-Blue strains were used for vector transformation.

DH5 α *supE44* Δ *lacU169* (ϕ 80*laxZ* Δ M15) *hsdR17* *recA1* *endA1* *gyrA96* *thi-1* *relA1*

XL1-Blue *recA1*, *lac-*, *endA1*, *gyrA96*, *thi*, *hsdR17* (*rk-*, *mk+*), *supE44*, *relA1*, λ -,
[F',*proAB*, *lacIqZ*, Δ M15, Tn10 (*tetr*)]

2.3. Morpholinos

For gene knockdown experiments in zebrafish embryos, Morpholino anti-sense oligonucleotides (MO; Gene Tools, Philomath, OR) were designed to specifically block mRNA translation (ATG MO) or to inhibit correct pre-mRNA splicing (splice MO). Both approaches generally lead to a reduction of protein production by interference with translation and therefore result in a knock down of endogenous gene function.

Working solutions with different concentrations were made from Morpholino stock solutions (25 ng/nl in deionized water). These working solutions were heat treated (10 min, 65°C) before microinjection into one or two cell-stage zebrafish embryos. For splice MO injection,

MOs directed against a splice donor and a splice acceptor site of one intron were injected as a 1:1 mixture. The efficiency of splice MOs was controlled by RT-PCR utilizing gene specific DNA primers amplifying the stabilized intron (sequences of used oligonucleotide primers are listed in the appendix chapter 8.2). Effective blocking of splicing by MO injection leads to the appearance of a larger band corresponding to the size of the stabilized intron. For cDNA synthesis, 30 embryos either non-injected or injected with the splice MOs were collected and used for RNA extraction and subsequent cDNA synthesis.

The following Morpholinos were used:

mdkb splice MO: directed against the boundaries of intron 3 (78bp) of the genomic *mdkb* sequence:

mdkbspliceUP (splice donor junction exon3-intron3; e3i3)

5'-GCATAACTGCTTACCGCCAAAGTCC-3'

mdkbspliceDOWN (splice receptor junction i3e4)

5'-GTACTIONGTCAGTCGGCTACAAATAAG-3'

for RT-PCR analysis, primers mk003 and mk004 were used

mdka splice MO: directed against the boundaries of intron 3 (199bp) of the genomic *mdka* sequence:

mdkasspliceUP (splice donor junction e3i3)

5'-CAGTTTAACTCACCTCCAAATTCTT-3'

mdkasspliceDOWN (splice receptor junction e3i4)

5'-ACTTGCAGTCAGCTGCAGGAAATGA-3'

for RT-PCR analysis, primers mkESTup and mk3-2 were used

ptn splice MO: directed against the boundaries of intron 2 (2037bp) of the genomic *ptn* sequence:

ptn MO up (splice donor junction e1i2; zfptnspliceUP)

5'-AATGTTCCGATACCTTGTTTTTCTG-3'

ptn MO down (splice receptor junction i2e2; zfptnspliceDO)

5'-GCTCTTCTTACCTGTCAAGAGTCG-3'

for RT-PCR analysis, primers tfptnfl01 and tfptnfl02 or ptnMO01 and ptnMO02 were used

ptn ATG MO: directed against the translation start site of the *ptn* mRNA:
5'-ATGCTGTAGTCTGAGGAATAGTTT-3'

control MO: standard control MO:
5'-CCTCTTACCTCAGTTACAATTTATA-3'

2.4. Antibodies

For in situ hybridization and immunostaining the following antibodies and Fab-fragments were used:

Anti-Digoxigenin:	Fab-fragments from sheep directed against Digoxigenin coupled to alkaline phosphatase (Roche, Basel); dilution 1:2000 in PBST
Anti-Fluorescein:	Fab-fragments from sheep directed against Fluorescein coupled to alkaline phosphatase (Roche, Basel); dilution 1:2000 in PBST
Anti-c-Myc:	monoclonal antibody derived from mouse; clone 9E10; dilution 1:1500 in PBST (Santa-Cruz Biotechnology, Santa-Cruz, CA)
Anti-acetylated tubulin:	monoclonal antibody derived from mouse; clone 6-11B-1; dilution 1:2500 in PBST (Sigma-Aldrich, Taufkirchen)
Anti-Mouse IgG-HRP:	peroxidase coupled; dilution 1:1000 (Santa-Cruz Biotechnology, Santa-Cruz, CA)
Anti-Mouse IgG-biotin:	Biotinylated; from Vectastain Elite ABC kit (Vector Lab., Burlingame, CA); dilution 1:1000

2.5. Oligonucleotides

Oligonucleotides were synthesized and purchased from Biomers (Ulm) and Sigma-Aldrich (Taufkirchen) in HPLC quality. A list of used primers and their sequences is found in the appendix (chapter 8.2).

Actin Primers directed against zebrafish *acta1* were used for PCR control.

2.6. Kits

The following kits were used:

Plasmid-DNA extraction:	QIAGEN Plasmid Midi Kit, Qiagen (Hilden) peqGOLD Plasmid Miniprep Kit II, Peqlab (Erlangen)
Gel-extraction:	Concert Gel Extraction System, Invitrogen (Karlsruhe) Min Elute Gel Extraktion Kit, Qiagen (Hilden)
cDNA synthesis:	RevertAid™ First Strand cDNA Synthesis, Fermentas (St.Leon-Rot)
Capped RNA synthesis:	mMESSAGE mMACHINE kit, Ambion (Austin, TX)

RNA-purification:	RNeasy Mini Kit, Qiagen (Hilden)
Immunostaining:	Vectastain Elite ABC Kit, Vector Lab (Burlingame, CA)
Apoptosis detection:	ApopTaq Kit; Intergen Company (Gaithersburg, MD)

2.7. Enzymes

RQ 1 DNase:	Boehringer Mannheim (Mannheim)
ProteinaseK:	Sigma-Aldrich (Taufkirchen)
Restriction endonucleases:	Invitrogen (Karlsruhe), NEB (Ipswich, MA), Fermentas (St.Leon-Rot)
RNA polymerases:	Ambion (Austin, TX), Roche (Basel), Promega (Madison, WI)
RNasin:	Boehringer Mannheim (Mannheim)
Taq DNA Polymerase:	Invitrogen (Karlsruhe) Eppendorf (Hamburg)
Lysozym:	Boehringer Mannheim (Mannheim)

2.8. Chemicals

Basic chemicals of highest purity were purchased from MERCK (Darmstadt), Pharmacia (Heidelberg), Carl Roth GmbH&CO (Karlsruhe), Sigma-Aldrich (Taufkirchen) and Biozym (Hameln). All solutions were prepared using deionized water of Millipore quality.

Substances used for preparation of bacteria growth media were supplied by Carl Roth GmbH&CO (Karlsruhe) and Invitrogen (Karlsruhe).

2.9. Technical devices

Microinjection

Microinjector:	FemtoJet and Microinjector 5242, Eppendorf (Hamburg)
Micromanipulator:	Leitz (Wetzlar)
Stereo microscope:	Stemi SV6 and SV11, Zeiss (Oberkochen)
Capillary puller:	Kopf vertical pipette puller model 720, Bachhofer (Reutlingen)
Glass capillaries:	GC100F-10; Harvard Apparatus (Harvard, UK)

Documentation

- Microscope: Axiophot POL, Zeiss (Oberkochen) with attached digital camera Fujix hc-2000, Fujifilm (Düsseldorf)
- Stereo microscope: SMZ1000, Nikon (Düsseldorf) with attached digital camera CC-12 FW Soft imaging system, Olympus (Münster)

PCR and Gel electrophoresis

- Gel chambers: Department's workshop
- Power supply: EPS 301, Amersham-Pharmacia biotech (Buckinghamshire, UK)
- Thermocycler: TGradient, Biometra (Goettingen) and DNA Engine Dyad thermal cycler, Biorad (Hercules, CA)

Centrifuges

- Tabletop: Centrifuge 5415D and Centrifuge 5415R with rotor F45-24-11, Eppendorf (Hamburg)
- High-speed: Sorvall RC-5B with rotor GSA and SLA-1500 rotor, DuPont (Bad Homburg) and MinifugeRF, Heraeus (Hanau)

Lab equipment

- Incubator: B5050E, Heraeus (Hanau)
- Water bath: Model 1083, GFL (Burgwedel)
- pH meter: pH523, WTW (Weilheim)
- Balance: BP, Kern & Sohn (Albstadt)
- Shaker: Reax3, Heidolph (Schwabach)
- Spectrophotometer: BioPhotometer, Eppendorf (Hamburg)
- Thermal block: Thermomixer compact, Eppendorf (Hamburg)
- UV-sterilizer: GS GeneLinker, Biorad (Hercules, CA)
- Vortex mixer: Vortex genie, Scientific industries INC. (New York, NY)
- Pipettes: Pipetman, Gilson (Middleton, WI)

Hardware

- PC- und Macintosh-systems

Software

- Word-processing: Microsoft Word 2002 (Microsoft)
Ultraedit-32 (IDM Computer Solutions)
Endnote 9.0 (Thomson ISI ResearchSoft)
- Graphics: Photoshop 7.0 (Adobe)
CorelDRAW Graphics Suite 12 (Corel)
ImageJ (NCBI)
- Statistics: Microsoft Excel 2002 (Microsoft)
- Vector database: Vector NTI advance 10 (Invitrogen)

3. Methods

3.1. Microbiological methods

3.1.1. Sterilization

Solutions, media and buffers were sterilized by autoclaving at 120°C and 1.1 bar. Solutions containing heat-sensitive compounds were sterilized by filtration using sterile 0.2 µm filters (Millipore, Billerica, MA).

3.1.2. Growth media

Bacteria growth media and agarose plates were produced as described in Sambrook et al., 1989 and www.cshprotocols.org and subsequently autoclaved. Antibiotics were added in the following concentrations to the media: Ampicillin (50 µg/ml); Kanamycin (30 µg/ml); Streptomycin (200 µg/ml).

Luria-Bertani-medium:
(LB) 10 g/l tryptone
 5 g/l yeast extract
 10 g/l sodium chloride
 adjusted to pH 7.4 and autoclaved

LB-agar plates: supplement LB-medium with 15 g/l agar,
 autoclave and cool down to 40°C,
 add antibiotic(s) at appropriate concentrations,
 pour liquid LB-agar into Petri dishes (diameter 6 cm) and
 cool down to RT to polymerize

3.1.3. Bacteria cultivation and long time storage

For bacteria cultivation, growth medium was used containing appropriate concentrations of antibiotics for colony selection according to vector requirements (for stock solutions see table A6 in Sambrook et al., 1989). Cultivation was performed over night at 37°C with permanent shaking.

For blue-white selection, bacteria were plated on LB-agar plates with 40 µl of 40 mg/ml IPTG (Isopropyl-β-D-thiogalactopyranosid; Carl Roth GmbH&CO, Karlsruhe) and 40µl of 40 mg/ml X-Gal-solution (5-Brom-4-chlor-3-indoxyl-β-D-galactosid; Carl Roth GmbH&CO, Karlsruhe).

For long term storage of bacteria, 800 µl of a freshly prepared bacteria suspension were mixed with 200 µl sterile glycerol in a safe lock vial, frozen in liquid nitrogen and stored at -80°C.

3.2.2. DNA purification

For purification and cleaning of DNA from solutions containing proteins, enzymes, ions and other impurities, phenol-chloroform extractions were performed. The DNA solution was mixed with 100 μ l TE-buffer saturated Roti-phenol and 100 μ l chloroform:isoamyl alcohol (24:1) and vortexed for 1 min. For phase separation, the solution was centrifuged for 2 min at 13000 rpm at room temperature. The upper phase containing the DNA was transferred into a new reaction tube. For additional purification, a second volume of 100 μ l chloroform:isoamyl alcohol (24:1) was added to the solution and vortexed for 1 min. After another centrifugation for 2 min at 13000 rpm at room temperature, the upper phase was recovered and the DNA was precipitated.

3.2.3. DNA and RNA precipitation

DNA and RNA precipitation was performed using a sodium acetate/ethanol protocol (Sambrook et al., 1989). For DNA, 1/10 volume 3M sodium acetate was added, while for RNA 1/10 volume of 2M sodium acetate was added to the solutions. After mixing, 2 to 3 volumes pure ethanol were added, the solution was mixed and incubated at -80°C for 30 min. After centrifugation at 13000 rpm and 4°C for 15 min, the supernatant was removed and the pellet was washed with 80% ethanol. After complete removal of all ethanol the pellet was dissolved in water or TE-buffer.

3.2.4. Determination of nucleic acid concentrations

The concentration of nucleic acids was determined by measuring the absorption of an aqueous solution at a wavelength of 260 nm using a spectrophotometer. For this purpose, DNA or RNA was diluted 1:80 in deionized water and the absorption spectrum was measured at the range of 240 to 320 nm after having calibrated the photometer with pure water. The concentration (c) of the original solution was calculated by the following formula:

$$\text{DNA } c = 50 \times A_{260\text{nm}} \times \text{dilution factor } [\mu\text{g/ml}]$$

$$\text{RNA } c = 40 \times A_{260\text{nm}} \times \text{dilution factor } [\mu\text{g/ml}]$$

3.2.5. Agarose gel electrophoresis

Electrophoretic separation of RNA and DNA was performed in 0.5% up to 2% (w/v) agarose gels. DNA containing samples were mixed with 10 x DNA sample buffer and loaded onto the

gel. The gel run was carried out at 10 to 200 V in an electrophoresis chamber containing 1x TAE-buffer. RNA samples were mixed with “Gel Loading Buffer II” (Ambion, Austin, TX) containing formamide and SDS and denatured at 70°C for 10 min. DNA and RNA fragments were visualized by 15 min EtBr staining of the gel after separation had finished and subsequent inspection on an UV-transilluminator at a wavelength of 254 nm.

50x TAE-buffer: 242 g Tris base
 57.1 ml acetic acid
 100 ml 0.5M EDTA
 Add ddH₂O to 1 liter and adjust pH to 8.5

10x DNA-loading buffer: 25 mg bromophenol blue
 25 mg xylene-cyanol
 3 ml glycerol
 2 ml 0.5 M EDTA
 1 ml 10% SDS
 Add ddH₂O to 10ml

DNA-standards: 100 µl “1 kb-DNA-Ladder” (Invitrogen, Karlsruhe)
 or 100 µl “100bp-DNA-Ladder” (Invitrogen, Karlsruhe)
 100 µl 10x DNA-loading-buffer
 Add ddH₂O to 1ml

3.2.6. Gel extraction of DNA fragments

To purify DNA fragments separated by gel electrophoresis, the desired band was cut out of the gel and extracted with the „Concert Rapid Gel Extraction System“ (Qiagen, Hilden). Faint bands with low DNA content were purified via the „Min Elute Gel Extraktion Kit“ (Qiagen, Hilden) to obtain samples with higher concentrations. The purified DNA was dissolved in 10 to 50 µl deionized water or TE-buffer at pH 7.4.

3.2.7. DNA sequencing

DNA sequencing was carried out using the “CEQ-DTCS Quick Start Kit” (Beckman-Coulter, Fullerton, CA) for sample preparation and sequence reaction. The automated sequencing protocol, based on the chain-terminating method according to Sanger, was carried out on a CEQ 8000 sequencer (Beckman-Coulter, Fullerton, CA). The sequencing results were analyzed with the CEQ 8000 computer program v9.0 (Beckman-Coulter, Fullerton, CA).

3.2.8. RNA extraction

30 to 50 zebrafish embryos of the desired stage were transferred to a 1.5 ml reaction tube. Remaining liquid was withdrawn and the embryos were homogenized with a micropistil. 200 μ l solutionD were added drop-wise for cell lysis. After addition of 20 μ l 2 M sodium acetate (pH 4.0), the solution was mixed. Afterwards, 200 μ l water-saturated Roti-phenol and 100 μ l chloroform:isoamyl alcohol (24:1) were added and the solution was vortexed for 30 sec. After incubation for 20 min on ice, the solution was centrifuged at room temperature (10 min 13000 rpm). The upper phase was transferred into a new reaction tube, without taking over parts of the interphase. For further purification and removal of phenol, the upper phase was mixed with 200 μ l chloroform:isoamyl alcohol (24:1) and separated again by centrifugation at room temperature (10 min 13000 rpm). The upper phase was transferred to a new reaction tube and mixed with 2 volumes of RNase-free, pure ethanol. This solution was incubated at -80°C for at least 30 min. The precipitated RNA was pelleted by centrifugation for 1h at 4°C and maximum speed and the supernatant was discarded. The resulting pellet was washed with RNase-free 80% ethanol at room temperature. After removal of all remaining ethanol, the pellet was dissolved in 100 μ l DNase Master-Mix. The remaining DNA was digested by 30 min incubation at 37°C on a heat block. The RNA solution was cleaned and extracted by a second phenol/chloroform:isoamyl alcohol (24:1) extraction. After a further ethanol precipitation, the purified RNA pellet was dissolved in 35 μ l RNase free water and stored at -80°C .

SolutionD: 23.4 g guanidine thiocyanate
 1.67 ml 750 mM sodium citrate
 2.5 ml 10% sarkosyl
 27.8 ml ddH₂O
 add 7.2 μ l/ml Beta-mercaptoethanol just prior to use

DNase Master-Mix: 5 μ l restriction buffer 2 (NEB, Ipswich, MA)
 1 μ l RQ1 DNase (1 U/ μ l)
 0.5 μ l RNAsin
 0.5 μ l 100 mM DTT
 add ddH₂O to 100 μ l

3.2.9. Reverse transcription

Using 0.5 μ g to 2 μ g of total RNA as template, single-stranded cDNA was synthesized by reverse transcriptase (MMLV, from Moloney Murine Leukemia Virus) and oligo-dT primers. All compounds needed for reverse transcription were taken from the “RevertAid™ First

Strand cDNA Synthesis” kit (Fermentas. St.Leon-Rot). For negative control, a second reaction with the same compounds and RNA concentration but lacking the reverse transcriptase was set up (-RT control). The generated cDNA could be used directly in polymerase chain reactions or stored at -20°C.

3.2.10. Polymerase chain reaction (PCR)

PCR was used for amplification of DNA fragments from cDNA, plasmid or genomic DNA templates. In a PCR reaction, double stranded DNA is first denatured, and then short DNA primers are allowed to bind to their target sequences. The last step is the elongation starting from the primers by a Taq DNA-polymerase to synthesize a complementary strand.

A standard PCR reaction mix consisted of:

2.5 µl 10x PCR buffer (Invitrogen, Karlsruhe)
 1.0 µl magnesium chloride (50 mM)
 1.0 µl dNTP-Mix (each nucleotide at 2.5 mM)
 0.5 µl Taq-polymerase (5 U/µl; Invitrogen, Karlsruhe)
 1.0 µl Primer 1 (10 pmol/µl)
 1.0 µl Primer 2 (10 pmol/µl)
 1.0 µl cDNA
 add ddH₂O to 25 µl

A standard program for the PCR thermo-cycler was:

reaction step	temperature	time
pre-heating	95°C	pause
denaturation	95°C	5 min
separation	95°C	30 sec
primer annealing	depending on primer pair	30 sec
elongation	72°C	1 min per 1kb
final elongation	72°C	5 min
end of reaction	4°C	pause

} 35x

For special templates or primer combinations, the reaction mix or the program was modified with respect to altered magnesium concentrations, addition of DMSO, longer elongation times and variable annealing temperatures. The optimal annealing temperature (T_D) was calculated according to the formula:

$$T_D = [(C_n + G_n) \times 4 + (A_n + T_n) \times 2]^\circ\text{C}$$

The duration of the elongation phase is depending on the fragment length and the used DNA-polymerase.

For nested PCR application two subsequent PCR reactions were performed with 2 sets of primers. The second set of primers is intended to amplify a secondary target within the first run product and thereby enhance PCR sensitivity. 1 μ l of the first run reaction was added instead of cDNA in the second PCR reaction.

3.2.11. Enzymatic DNA digestion

For enzymatic digestion of DNA fragments, restriction enzymes from different companies were used together with the corresponding buffers, reaction temperatures and inactivation procedures. Generally, 2 to 5 U of enzyme were used for 1 μ g DNA at an incubation of 1 to 6 h. Double digestions were performed according to manufacturer's standards.

3.2.12. Capped RNA synthesis

For capped RNA synthesis, pCS2p+ plasmids containing full-length cDNAs were used. The plasmids were linearized by enzymatic digestion and subsequently transcribed *in vitro* into RNA using Sp6 RNA polymerase and the "mMessage mMachine" kit from Ambion (Austin, TX). Different amounts of capped RNA were injected into one or two cell-stage zebrafish embryos.

Full length capped RNAs were synthesized from the following genes:

Zebrafish *mdka* (Winkler et al., 2003), *mdkb* (Winkler et al., 2003), *ptn* (Cordula Neuner, unpublished), and Medaka *fgf8* (plasmid was a generous gift from Matthias Carl, London; translated ORF shows 77% identity to zebrafish FGF8).

3.2.13. Riboprobe synthesis

Synthesis of labeled RNA probes for whole-mount in situ hybridizations (riboprobes) was performed under RNase-free conditions. For preparation of one probe, 5 to 10 μ g plasmid DNA containing the target gene fragment was digested for 12 h with the corresponding restriction enzyme. The reaction was stopped by enzyme denaturation at 65°C for 20 min. After a phenol-chloroform extraction and subsequent DNA precipitation the pellet was

dissolved in 20 μ l deionized water. Complete digestion was controlled by agarose gel electrophoresis with 1 μ l of the purified DNA template.

After complete plasmid restriction, *in vitro* transcription of digoxigenin-UTP (DIG) or fluorescein-UTP (FLU) labeled riboprobes was performed utilizing the Sp6- and T7-RNA-polymerases from the „*in vitro* Transkription” kit (Promega, Madison, WI). A typical reaction mixture consisted of:

- 2.0 μ l DNA template (0.5 to 1 μ g DNA)
- 2.0 μ l DTT (100 mM; Promega, Madison, WI)
- 2.0 μ l DIG- or FLU-RNA labeling-mix (Roche, Basel)
- 0.5 μ l RNase-inhibitor (Promega, Madison, WI)
- 4.0 μ l 5x transcription buffer (Promega, Madison, WI)
- 1.0 μ l Sp6- or T7-RNA polymerase (Promega, Madison, WI)
- add ddH₂O to 20 μ l

This mixture was incubated for 2 h at 37°C. The template DNA was removed by addition of 1 μ l RQ 1 DNase (1U, Boehringer Mannheim, Mannheim) and incubation at 37°C for 30 min. After addition of 80 μ l deionized water, the synthesized riboprobes were purified using the “RNeasy” kit (Qiagen, Hilden), precipitated and resolved in 25 μ l deionized water. 1 μ l of the riboprobe solution was used for RNA gel electrophoresis to control RNA quality. The remaining 24 μ l were mixed with 76 μ l HybMix solution (see “Whole-mount RNA in situ hybridization” protocol) and stored at -20°C.

3.2.14. Whole-mount RNA in situ hybridization

One and two color RNA in situ hybridizations were performed as described (Hauptmann and Gerster, 1994) with RNA probes labeled with digoxigenin-UTP (DIG-UTP) or fluorescein-UTP (FLU-UTP) to visualize gene expression in the complete embryo.

Production of preabsorbed Fab-AP fragments

50 to 100 zebrafish wildtype embryos were fixed at different developmental stages and stored in MeOH. They were rehydrated in 50% methanol/PBST and pure PBST. After transfer into a 1.5 ml Eppendorf tube, embryos were homogenized in 1 ml PBST using a micropistill. After addition of 10 μ l Anti-DIG Fab fragments coupled to alkaline phosphatase (Fab-AP; Roche, Basel) or Anti-FLU Fab-AP fragments (Roche, Basel), the solution was mixed and incubated for at least over night at 4°C. After centrifugation (5 min, 13000 rpm), the supernatant was sterile filtered (0.22 μ m filter) and diluted with 9 ml PBST. The remaining pellet was resuspended with 1 ml PBST again. After a second centrifugation and sterile filtration of the

supernatant this solution was diluted with 9 ml PBST. Both aliquots were mixed together, resulting in a 1:2000 dilution of the Fab-AP fragments, and stored at 4°C.

Rehydration

To rehydrate embryos stored in methanol, they were incubated in solutions with decreasing methanol content (75% methanol/PBST, 50% methanol/PBST, 25% methanol/PBST; each incubation for 5 min) on a shaker. For complete rehydration the embryos were incubated two times in 100% PBST for 5 min.

Permeabilization

To permeabilize embryos for riboprobe application, embryos older than 12hpf were treated with proteinaseK (10 µg/ml in PBST) for different time periods (3 min for 12 to 24hpf embryos, 5 min for 24 to 48hpf embryos). To stop proteinaseK digestion, the embryos were rinsed with glycine solution twice. Subsequent fixation of the embryos with 4% PFA for 20 min and five washing steps in PBST followed the permeabilization.

Hybridization

For prehybridization, embryos were incubated in Hyb-mix for at least 1 h at 65°C. During this period, diluted riboprobes (standard riboprobe dilution was 1:100 in Hyb-mix; final concentration of RNA probe 0.5 to 5 ng/µl) were incubated at 80°C for 10 min to denature secondary RNA structures. Directly after prehybridization, the Hyb-mix was removed and embryos were incubated in 300 µl of the heated riboprobe solution over night at 65°C. The next day, the riboprobe solution was removed and stored at -20°C for re-use. To increase stringency and signal specificity the embryos were incubated two times for 30 min in FA/SSCT, followed by one incubation for 30 min in 2x SSCT and two incubations for 30 min in 0.2x SSCT at 65°C. For salt removal, the embryos were subsequently rinsed in PBST.

Antibody binding and detection

To reduce unspecific binding of the Dig- and Flu-Fab-AP fragments the embryos were incubated for 1 h in blocking solution. Afterwards, preabsorbed Fab-AP fragments were added and the embryos were incubated over night at 4°C or for 2 h at room temperature. Afterwards, the embryos were washed six times in PBST for 20 min each prior to staining. For two-color staining, first red staining was performed by incubating the embryos in Tris-Cl/0.1% Tween (pH8.2) for two times and 5 min each. Embryos were then stained with “Fast-

red” (Roche, Basel; 1 tablet in 2 ml Tris-Cl/0.1% Tween) and coloration was developed in the dark, visually controlled utilizing a stereomicroscope and stopped by three subsequent PBST washes. To remove the Fab-AP fragments from this first staining, the embryos were incubated in 0.1 M glycine-Cl/0.1% Tween (pH 2.2) for two times 10 min each and subsequently washed four times for 10 min in PBST. The embryos were then incubated with the second Fab-AP fragment over night at 4°C or for 2 h at room temperature. After six 20 min washing steps with PBST, the second color reaction was performed. For blue color processing the embryos were incubated two times in staining buffer for 5 min and stained with NBT/BCIP staining solution. To stop the reaction the embryos were washed three times with PBST. For single color applications the first coloration and the Fab-AP fragment removal was skipped.

20x SSC:	176 g/l sodium chloride 88.2 g/l sodium citrate
1x SSCT:	10 ml 20x SSC 190 ml ddH ₂ O 0.1% (w/v) Tween20
Hyb-Mix:	50% (w/v) formamide 5% (w/v) 1xSSC 0.1% (w/v) Tween20 5 mg/ml Heparin (Sigma-Aldrich, Taufkirchen) 150 µg/ml Torula-RNA (Sigma-Aldrich, Taufkirchen)
FA/SSCT:	50% (v/v) formamide 50% (v/v) 4x SSCT
Glycine solution:	1 M glycine in PBST
Blocking solution:	1:20 dilution of sheep serum (Sigma-Aldrich, Taufkirchen) in PBST
Staining buffer:	1.0 ml 5 M sodium chloride 2.5 ml 1 M magnesium chloride 5.0 ml 1 M Tris-Cl (pH 9.5) 0.1% (w/v) Tween20 add ddH ₂ O to 50 ml
Staining solution:	1 tablet NBT/BCIP (Roche, Basel) 200 µl 5 M sodium chloride 0.1% (w/v) Tween20 add ddH ₂ O to 10 ml

3.2.15. Immunostaining

Neurons were visualized in fixed whole-mount zebrafish embryos using immunostaining with an antibody directed against acetylated tubulin (diluted 1:2500; Sigma-Aldrich, Taufkirchen) according to standard protocols (Winkler and Moon, 2001). The same protocol utilizing the anti-c-myc antibody (diluted 1:1500, Santa-Cruz Biotechnology, Santa-Cruz, CA) was used for detection of myc-tagged recombinant proteins. For enhanced signal detection, the Vectastain Elite ABC-Kit (Vector Lab., Burlingame, CA) and DAB (3,3'-Diaminobenzidine; Sigma-Aldrich, Taufkirchen) as substrate for the horseradish peroxidase were used.

Apoptosis in fixed embryos was detected by utilizing the ApopTaq Kit (Intergen Company; Gaithersburg, MD). For this protocol fixed or in situ colored embryos were used. Rehydration or in situ was followed by three 15 min washes in PBST. Endogenous peroxidase activity was blocked by incubation in 1ml 3% hydrogen peroxide in PBST over night at 4°C. After 2x washing in PBST for 1min, the embryos were transferred into 1.5ml Eppendorf tubes. Immediately after removal of the liquid, 100-150 µl Equilibration Buffer was added and embryos were incubated for 20 to 30 min at room temp. After removing the Equilibration Buffer, 50 µl TdT enzyme solution was added and incubated for 1 h at 37°C. Enzyme solution of TdT enzyme was freshly made prior to application by adding 30 µl TdT enzyme to 70 µl reaction buffer. After removal of the enzyme solution 250 µl Stop/Wash Buffer solution (10 µl Stop/Wash buffer from kit + 430 µl dH₂O) were added and incubated for up to 10 minutes at RT. Afterwards, the embryos were washed three times with 1 ml PBST for 1 min. After removal of the liquid, 100 µl Anti-Digoxigenin-Peroxidase were applied for 30 min at RT or overnight at 4°C. Subsequently, the embryos were washed four times in 1ml PBST for 2 min and transferred to 8ml glass vials for peroxidase staining with the substrate DAB. For this, the embryos were first incubated in 500 µl DAB/dH₂O-solution for 30 min (1 DAB tablet in 1ml H₂O) RT on a tumbler. After removal of the liquid, 500 µl DAB/urea/H₂O₂ (1 DAB tablet and 1 DAB/urea/H₂O₂ tablet in 1 ml H₂O) were added and the staining was developed for approximately 2 min. Staining was controlled with a stereomicroscope and stopped by washing with PBST for at least three times and 5 min each.

3.2.16. Cartilage staining

Cartilage in zebrafish embryos was stained by Alcian blue (Schilling et al., 1996). Larvae were fixed in 4% paraformaldehyde in PBST at 4°C overnight, and then transferred into a 0.1% solution of Alcian blue dissolved in 80% ethanol/20% glacial acetic acid. After staining

in this solution overnight, embryos were rinsed in ethanol and rehydrated gradually with PBS. Tissues were cleared in 0.05% trypsin dissolved in a saturated solution of sodium tetraborate for 1-3 hours. Pigmentation was then removed by bleaching in 3% hydrogen peroxide/PBS for several hours.

3.3. Chemical treatments of zebrafish embryos

3.3.1. DEAB treatment

The retinoid signaling inhibitor DEAB (4-diethylaminobenzaldehyde; Sigma-Aldrich, Taufkirchen/Fluka) was dissolved to 1 mM in DMSO and stored at 4°C in the dark. Working dilutions of 10, 25 and 50 µM in 0.3x Danieau's medium were prepared directly before use. Embryos were manually dechorionated and incubated in DEAB at 28°C in darkness starting at shield stage for 3 h until 80% epiboly was reached. After incubation, embryos were fixed in 4% paraformaldehyde. Dechorionated control embryos were incubated in equivalent dilutions of DMSO in 0.3x Danieau's medium.

0.3x Danieau's medium: 17.4 mM sodium chloride
 0.21 mM potassium chloride
 0.12 mM magnesium sulfate
 0.18 mM calcium nitrate
 1.5 mM HEPES
 pH 7.2

3.3.2. SU5402 treatment

The FGF receptor inhibitor SU5402 (Sigma-Aldrich, Taufkirchen; (Mohammadi et al., 1997; Griffin and Kimelman, 2003) was dissolved in DMSO to a final concentration of 10 mM. Working dilutions of 25, 50 and 100 µM were prepared in 0.3x Danieau's medium as described above. Dechorionated embryos were incubated for 3 h from shield stage to 80% epiboly at 28°C in the dark. After this, embryos were fixed in 4% paraformaldehyde and prepared for in situ hybridization. The efficiency of SU5402 treatment was monitored by altered *erm1* expression (Raible and Brand, 2001). Dechorionated control embryos were incubated in equivalent concentrations of DMSO in 0.3x Danieau's medium.

3.3.3. LiCl treatment

LiCl treatment on dechorionated embryos was used to inhibit GSK3 activity, which induces the Wnt pathway (Stachel et al., 1993; Amacher et al., 2002). Embryos at different stages of development were treated for 15 min at 28°C with a 0.3 M solution of LiCl in 0.3x Danieau's medium. After complete removal of the LiCl solution the embryos were rinsed 5 times in 0.3x Danieau's medium and incubated at 28°C until the 14 somite stage.

3.4. Microinjection into zebrafish embryos

3.4.1. Collection of embryos

The evening before an injection experiment was scheduled, two male and three female zebrafish were put together in a spawning tank with plastic insert and sieve bottom (Aquarienbau Schwarz, Göttingen). Shortly after start of the light-phase on the injection day, the water in the spawning tank was replaced by fresh aquarium water to get rid of over night excrements. 30 to 45 min after beginning of the light cycle, spawning started and egg production continued for maximal 1 h. The freshly laid eggs were transferred into a Petri dish with fresh 0.3x Danieau's medium. The developmental stage of embryos was controlled with a stereomicroscope prior to injection start.

3.4.2. Microinjection

The used microinjection method has been previously described in detail (Stuart et al., 1988; Winkler et al., 1991; Westerfield, 1995). Other than in the described method, no phenol red was added to the injection solution and the depression slide was exchanged with an angular injection dish (Fig. 7). The injection dish was freshly made with 2% agarose in 0.3x Danieau's medium or manufactured with transparent synthetic resin for long-term usage. Before injection started, eggs were aligned along the groove and the remaining liquid was almost completely removed with a 1ml plastic pipette. The remaining liquid established enough surface tension to hold back the embryos in the groove after injection.

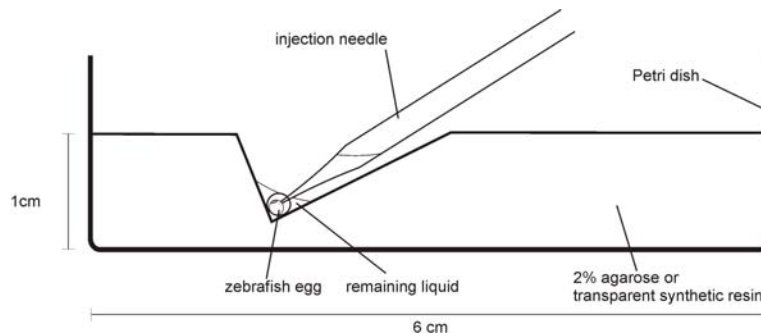


Fig. 7: Schematic drawing of an injection dish for microinjection of zebrafish eggs.

The concentration of injected RNA solutions was determined by photometric measurements prior to injection. MO solutions were pretreated for 10 min at 60°C to resolve secondary structures. Solutions were backloaded into injection needles (1 mm outer diameter and 0.58 mm inner diameter, Harvard apparatus) using Eppendorf microloaders. The needles were fixed in a micromanipulator (Leitz) and constant air pressure was supplied by a microinjector (Eppendorf, Hamburg). The needle tip was carefully opened with the blunt end of a pair of tweezers to result in a needle opening with a diameter of approximately 2 to 3 μm . In a single injection about 500 μl of liquid solution was injected into the cytoplasm of a one- or two-cell stage zebrafish embryo by appliance of a constant injection pressure. The injected volume was visually controlled by observation of the injection procedure with a stereomicroscope (Zeiss). Applied injection pressure and time were adjusted to the size of the needle opening.

3.4.3. Cultivation of injected embryos

After injection, the embryos were washed out of the injection plate groove with 0.3x Danieau's medium and transferred to a new Petri dish (diameter 6 cm) containing fresh 0.3x Danieau's medium. Embryos were cultivated in an incubator at 28°C until the desired stage of development (Kimmel et al., 1995). Visual control for dead embryos and developmental malformations was conducted every day. Fixation with 4% paraformaldehyde in PBST over night was performed to stop development. The chorion surrounding the embryo was removed with tweezers after fixation, when embryos were younger than 18hpf. Older embryos were dechorionized prior to fixation. For long time storage and dehydration after fixation, the embryos were transferred to glass vials, washed three times 5 min each with PBST, and then incubated in pure methanol and stored at -20°C.

10x PBS: (Phosphate Buffered Saline)	100 mM sodium chloride 19.5 mM potassium chloride 11 mM potassium dihydrogen phosphate 59 mM disodium hydrogen phosphate
PBST:	100 ml 10x PBS 900 ml ddH ₂ O 0.1% (w/v) Tween20 (Polysorbat-20; polyethylen- glycolsorbitanmonolaurat)
4% paraformaldehyde: (PFA)	2 g paraformaldehyde 5 ml 10x PBS add ddH ₂ O to 45 ml Dissolve by addition of 4 µl 1 M sodiumhydroxid and constant mixing at 70°C for 2 h; after cooling to room temperature neutralize to pH 8.0 by addition of hydrochloric acid.

4. Results

4.1. Analysis of *mdkb* expression during stages of ncc induction

Ncc are multipotent migratory cells unique to vertebrates, with a strong potential to differentiate into a huge number of different cell types. It is still unclear, how different morphogen gradients in the early embryo are integrated to result in the induction of ncc at the neural plate border. Planar signals derived from the neural ectoderm are proposed to play an important role in this process (Meulemans and Bronner-Fraser, 2004). Earlier studies have indicated that *Mdkb* might act as such a planar signal in zebrafish (Winkler and Moon, 2001). Aim of this thesis was to analyze, whether *mdkb* is regulated by known ncc inducers and whether it acts as a planar signal during ncc and sensory neuron induction.

Using whole mount RNA in situ hybridization, I first analyzed *mdkb* expression during the period of ncc and sensory neuron induction. Comparison with the expression of specific ncc and sensory neuron markers was performed to determine the spatiotemporal regulation of *mdkb* expression with respect to the induction of these cell types at the neural plate border.

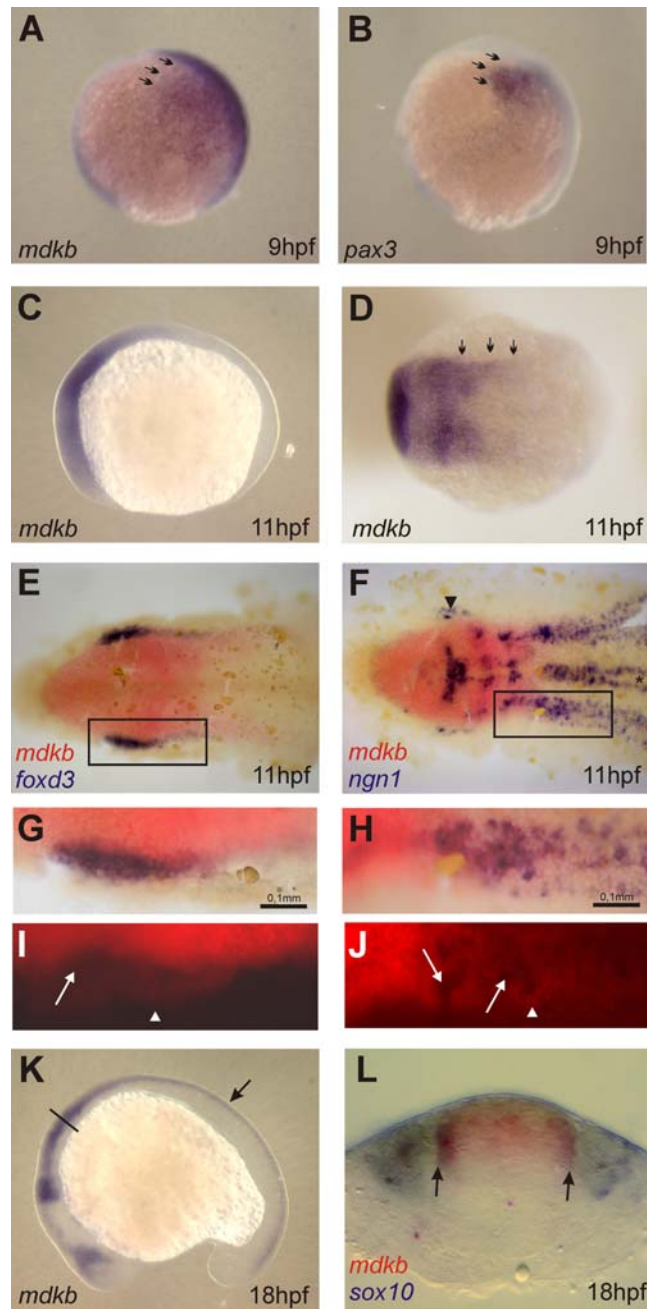


Fig. 8: Expression of *mdkb* during early zebrafish development.

A Lateral view of an embryo at 80% epiboly showing *mdkb* expression in blue as analyzed by whole-mount in situ hybridization. **B** Expression of *pax3* in the lateral neural plate containing ncc precursors at the same embryonic stage. Arrows indicate area of overlapping expression of *mdkb* and *pax3* in the presumptive ncc domain. **C,D** Expression of *mdkb* at the 3-somite stage (11hpf) in a lateral (**C**) and dorsal (**D**) view. Arrows indicate expression at the edge of the neural plate at hindbrain level. **E,G,I** Expression of *mdkb* and *foxd3* in the head/trunk region of the converging neural plate at the 3-somite stage (dorsal view with anterior to the left). Note co-expression of *foxd3* and *mdkb* in premigratory ncc precursors at the lateral neural plate border (**G**, higher magnification view of area boxed in **E**, bright field; **I**, dark field; arrow indicates *foxd3* positive cells in the *mdkb* domain, arrowhead marks lateral edge of the *mdkb* domain). **F,H,J** Co-localization of *mdkb* and *ngn1* expression in an area of forming sensory precursors (**H**, higher magnification bright field view of boxed area; **J**, dark field). **K** Expression of *mdkb* in a 18-somite stage embryo (18hpf). Arrow indicates expression in the dorsal neural tube. **L** Transverse section of an embryo at the level indicated in **K**, showing expression of *mdkb* in the dorsal neural tube and *sox10* in ncc. Note overlapping expression at the border of the neural tube (marked by arrows).

mdkb expression is first detected in the epiblast of gastrulating zebrafish embryos at 60% epiboly (6.5hpf; Winkler and Moon, 2001). Shortly later at 80% epiboly, *mdkb* transcripts are found throughout the complete presumptive neural plate with increased levels of expression at the emerging neural plate border (Fig. 8A). I next compared its expression to that of *pax3*, which is expressed in the neural plate including its lateral borders (Bang et al., 1997). There, it precedes expression of known early neural crest markers like *foxd3* (Lewis et al., 2004). *mdkb* expression is completely overlapping with the domain of early *pax3* expression in the anterior regions of the neural plate border at 80% epiboly (arrows in Fig. 8A,B), indicating that it is expressed at the correct time and place to be involved in neural crest induction. After 90% epiboly, *mdkb* expression becomes regionally restricted with increased levels directly posterior to the emerging mid-hindbrain boundary (MHB) and caudally in two bilateral stripes at the border of the converging neural plate (Winkler and Moon, 2001). At the 3-somite stage, *mdkb* expression was exclusively found in the developing head and at the neural plate border (Fig. 8D). Two color in situ hybridization of *mdkb* and *foxd3*, one of the earliest markers exclusively expressed in the presumptive neural crest (Nguyen et al., 1998) showed that the lateral edge of *mdkb* expression completely overlaps with the *foxd3* domain (Figs. 8E,G,I). Double-staining for *mdkb* and *ngn1*, an essential factor for RB sensory neuron induction (Cornell and Eisen, 2002), revealed that expression of both genes co-localizes within the field of sensory neuron precursors at the edges of the neural plate (Fig. 8F,H,J). No overlap in expression was observed in ventral motor neuron precursors (asterisk in Fig. 8F) and the trigeminal ganglia (arrowhead in Fig. 8F). Expression of *mdkb* at 18hpf is restricted to dorsal regions of the dien- and mesencephalon, the rhombencephalon posterior to the MHB and the neural tube (Fig. 8K; also see Winkler and Moon, 2001). Sections at the hindbrain level revealed that *mdkb* expression in the neural tube is directly adjacent to the expression of *sox10* in migrating ncc (arrows in Fig. 8L). Co-localization of *mdkb* with neural crest markers was also found in the diencephalon, as well as in more posterior regions of the neural tube (data not shown). Thus, colocalization of *mdkb* expression with markers expressed in trunk ncc precursors was observed before ncc start to delaminate from the neural tube. Taken together, *mdkb* is expressed in the ectoderm within the ncc and sensory neuron precursor domain during early steps of induction and adjacent to migratory ncc during later stages.

4.2. Regulation of *mdkb* expression by neural crest inducing signals

As restricted *mdkb* expression is found at the neural plate border colocalizing with ncc and sensory neuron precursors from earliest stages onwards, *mdkb* expression could be regulated

by known factors involved in the induction of these cell types. To test this, I investigated the regulation of *mdkb* by BMP, RA, FGF, Wnt pathways for *ncc* (Aybar and Mayor, 2002) and Delta-Notch signaling for Rohon-Beard sensory neurons (RB neurons; Cornell and Eisen, 2000). For this, chemical inhibitors, RNA overexpression and analysis in zebrafish mutants was used.

Earlier investigations in zebrafish mutants with defects in BMP signaling had revealed that *mdkb* expression is negatively regulated by BMP during gastrulation (Winkler and Moon, 2001). Reduced BMP signaling in *snailhouse* and *swirl* mutants, with mutations in *bmp7* and *bmp2b* respectively, resulted in ventrally expanded *mdkb* expression. Loss of the BMP antagonist *chordin*, on the other hand, resulted in reduced *mdkb* expression.

4.2.1. Loss of retinoic acid signaling represses *mdkb* expression

Winkler and Moon (2001) also showed that the level of *mdkb* transcription is gradually regulated by different doses of exogenously applied RA. Low levels of ectopic RA ($<10^{-8}$ M) enhanced *mdkb* expression, while high levels of ectopic RA ($>10^{-7}$ M) inhibited its transcription.

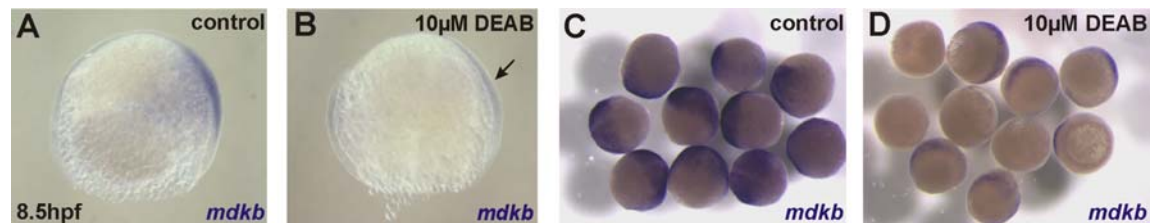


Fig. 9: Effect of RA signaling inhibition on *mdkb* expression by DEAB.

A,B Lateral views of *mdkb* expression in a DMSO treated control embryo at 8.5hpf (A) and of an embryo treated with 10 μM DEAB (B). **C,D** Group of DMSO treated control embryos showing regular *mdkb* expression (C). Embryos treated with 10 μM DEAB showing reduced *mdkb* expression (D). Arrow indicates area of reduced *mdkb* expression.

To investigate whether *mdkb* expression also requires endogenous RA, I incubated embryos in DEAB (diethyl aminobenzaldehyde), a competitive, reversible inhibitor of retinaldehyde dehydrogenases (Begemann et al., 2004). Embryos were incubated in 10 μM DEAB from shield stage, shortly before endogenous *mdkb* expression is initiated, until 80% epiboly. This resulted in a dramatic reduction of *mdkb* expression in 67% of the analyzed embryos (n=42; Fig. 9A-D). Low levels of remaining *mdkb* expression were observed on the dorsal side of the embryo. For more efficient inhibition of endogenous RA synthesis, higher concentrations of DEAB were used. This resulted in a repression of *mdkb* expression in 85% of the embryos

(n=14 for 30 μ M DEAB; n=20 for 50 μ M). However, a complete loss of *mdkb* expression was observed only in less than 5% of all analyzed embryos suggesting incomplete repression of RA synthesis even at 50 μ M DEAB (for comparison see Begemann et al., 2004). A weak reduction of *mdkb* expression was detected in 15% (n=81) of control embryos treated with DMSO alone. This observation suggests the dependence of *mdkb* expression *in vivo* on RA signaling.

4.2.2. *mdkb* expression requires FGF signaling

FGF signaling from the paraxial mesoderm is crucial for neural crest induction (Monsoro-Burq et al., 2003). To test whether early *mdkb* expression is modulated by FGF signaling, I treated embryos with SU5402, an inhibitor of FGF receptor activity (Griffin and Kimelman, 2003).

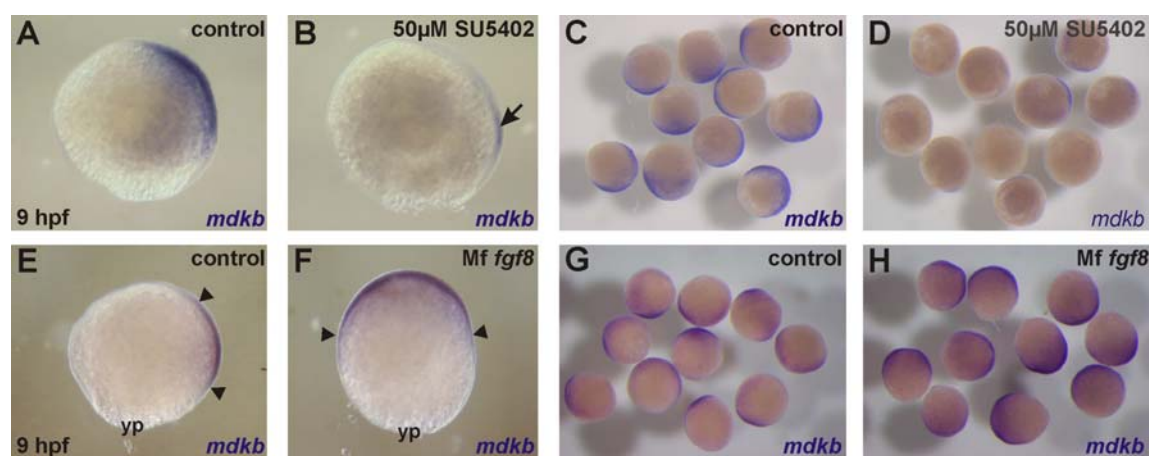


Fig. 10: Effect of FGF inhibition and FGF8 overexpression on *mdkb* expression.

A,B Lateral views of a control embryo at 9hpf (A) and an embryo treated with 50 μ M SU5402 (B). Arrow indicates area with remaining *mdkb* expression. **C,D** Groups of control embryos (C) and SU5402 treated embryos (D) showing *mdkb* expression. **E,F** Lateral views of embryos showing expression of *mdkb* in non-injected control embryo (E) and embryo injected with 30 pg Medaka *fgf8* mRNA (F) at 9hpf. **G,H** Groups of control embryos and Medaka *fgf8* RNA injected embryos showing enhanced *mdkb* expression. yp=yolk plug.

The efficiency of SU5402 treatment was monitored by analyzing the reduction of *erm* expression at 80% epiboly after 3 h treatment with 50 μ M SU5402 (in 100% of treated embryos, n=15; Raible and Brand, 2001). While only 15% of DMSO treated control embryos showed a mild reduction of *mdkb* expression, incubating embryos with 50 μ M SU5402 strongly reduced *mdkb* expression in 69% of treated embryos (n = 172; Fig. 10A-D). In 9.3% of these embryos, *mdkb* expression was completely absent. In the other embryos, remaining expression was detected on the dorsal side in the shield. Incubation of embryos at lower (25

μM) or higher (100 μM) doses resulted in reduced *mdkb* expression in 47% (n=49), respectively 84% (n=45). This suggests a dose-dependent activation of *mdkb* transcription by FGF signaling.

To further investigate the regulation of *mdkb* by FGF signaling, I injected 30 pg Medaka *fgf8* RNA into early zebrafish embryos. The injected embryos showed characteristic developmental defects, including the loss of ventral and posterior structures, similar to what has been described for ectopic expression of zebrafish *fgf8* (data not shown; Furthauer et al., 1997). In *fgf8* injected embryos, expression of *mdkb* was not restricted to the dorsal side at 90% epiboly, but instead was expanded into ventral domains in 95% of injected embryos (n=20; Fig. 10E-H). This suggests that *mdkb* transcription is regulated by and dependent on FGF signaling during gastrulation. At present, however, I can not exclude that this effect is indirectly caused by an altered neural plate size, as treatment of embryos with 50 μM SU5402 resulted in considerable reduction of the neural plate (see chapter 4.2.3). These results point to a positive regulation of *mdkb* expression by FGF signals.

4.2.3. FGF but not RA inhibition alters neural plate size

To determine whether the reduction of *mdkb* expression in DEAB and SU5402 treated embryos is a direct consequence of diminished RA or FGF signaling, or indirectly caused by a size reduction of the neural plate, I analyzed inhibitor treated embryos for repression of *mdkb* expression and simultaneous alterations of *tfap2*. Expression of *tfap2* is found in the non-neural, i.e. epidermal ectoderm (Li and Cornell, 2007).

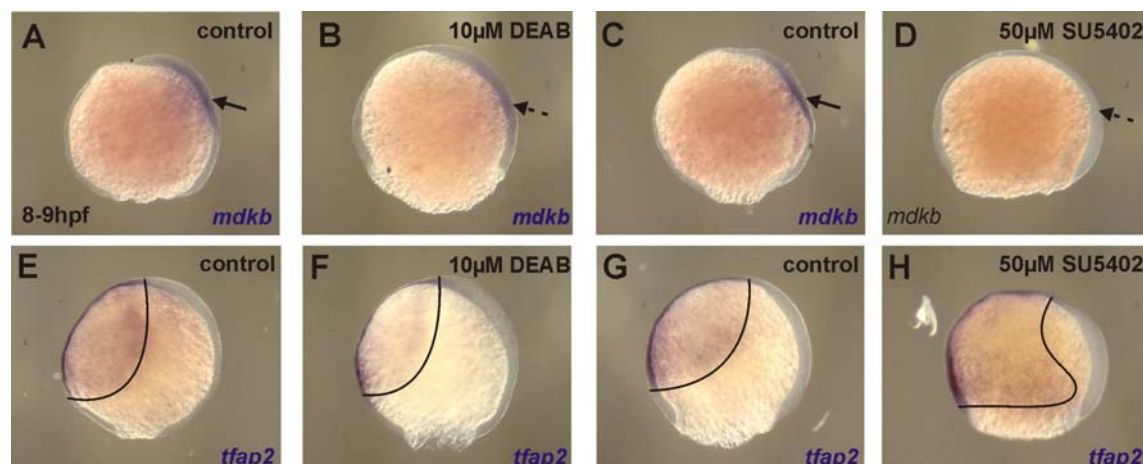


Fig. 11: Effect of DEAB and SU5402 treatment on neural plate size.

A,B Incubation of embryos in 10 μM DEAB results in reduction of *mdkb* expression (A, DMSO incubated control embryo,) at 70-90% epiboly. **E,F** Expression of *tfap2* in non-neural ectoderm and thus neural plate size is not affected. **C,D,G,H**

Incubation of embryos with 50 μ M SU5402 results in a reduction of both, *mdkb* expression and neural plate size as indicated by an expanded *tfap2* expression domain. The border of *tfap2* expression is indicated by a black line.

DEAB treatment resulted in a significant reduction of *mdkb* expression in all analyzed embryos (n=10; Fig. 11B), while the size of the non-neural ectoderm was normal in 92% of the analyzed embryos (n=13; Fig. 11F). This suggests that the inhibitory effect on *mdkb* expression is directly caused by reduced retinoid signaling rather than a secondary consequence of a reduced neural plate size.

Embryos treated with the FGF inhibitor SU5402 showed strongly reduced *mdkb* expression in all embryos (n=11; Fig. 11D). However, the great majority of embryos (85%) also showed a broader expression of *tfap2* (n=20; Fig. 11H) indicating that FGF inhibition leads to a larger non-neural ectoderm domain. The effects of the FGF inhibitor on *mdkb* expression might therefore be indirectly caused by the reduction of the neural plate.

4.2.4. Altered Wnt signaling has diverse effects on *mdkb* expression

It has been shown that reiterative Wnt signaling is crucial for posterior neural development and neural crest induction (Lewis et al., 2004). To test whether *mdkb* expression is modulated by Wnt activity, embryos were treated with LiCl to inhibit GSK3 activity and ectopically activate the Wnt pathway (Klein and Melton, 1996).

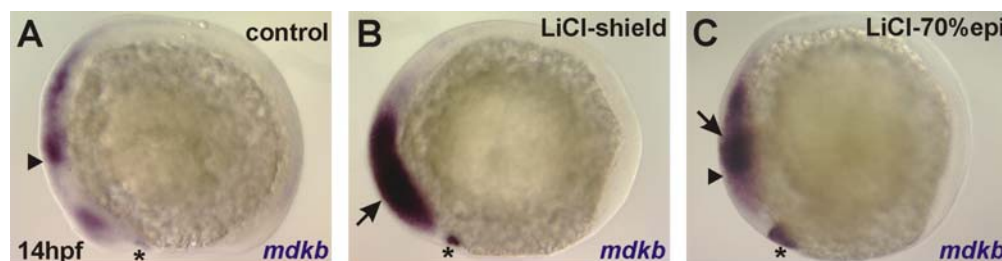


Fig. 12: Effect of ectopic Wnt signaling on *mdkb* expression.

Expression of *mdkb* is shown in embryos incubated with 0.3 M LiCl. **A** Control embryo incubated with DMSO. **B,C** *mdkb* expression is increased in embryos treated with LiCl for 15 min at shield stage (**B**) and at 70% epiboly (**C**). Arrowheads mark the MHB and asterisks mark the anteriormost *mdkb* expression domain.

15 min treatment with a 0.3 M solution of LiCl in 0.3x Danieau's medium at the shield stage resulted in a loss of the anteriormost brain structures, as previously described (Kim et al., 2002). In these embryos, I observed a strong enhancement of *mdkb* transcription throughout the head region at 14hpf in 66% of the treated embryos (n=12; Fig. 12B). No regionally restricted expression domains were detectable in the anterior head and the sharp edge of *mdkb* expression usually observed posterior to the MHB was absent. LiCl treatment at 70% epiboly

resulted in a less pronounced, but still significant change of *mdkb* expression (100%; n=28; Fig. 12C). *mdkb* was enhanced in the rhombencephalon posterior to the MHB (arrowhead in Fig. 12C). In both treatments, expression of *mdkb* in the prechordal plate appeared enhanced (asterisk in Fig. 12A-C). This indicates that *mdkb* transcription is under positive control of canonical Wnt signaling.

4.2.5. Delta-Notch signaling does not interfere with *mdkb* expression

Delta-Notch signaling via the bHLH transcription factor Olig3 is crucial for establishing the cell fate decision between ncc versus the sensory neuron lineage at the neural plate border (Filippi et al., 2005). To investigate whether *mdkb* expression is influenced by Delta-Notch signaling, I analyzed its expression in zebrafish *mindbomb* (*mib^{ta52b}*) mutants. These mutants lack a functional ubiquitin ligase required for Delta-Notch signaling and show an excess of primary motor and sensory neurons at the expense of ncc (Itoh et al., 2003).

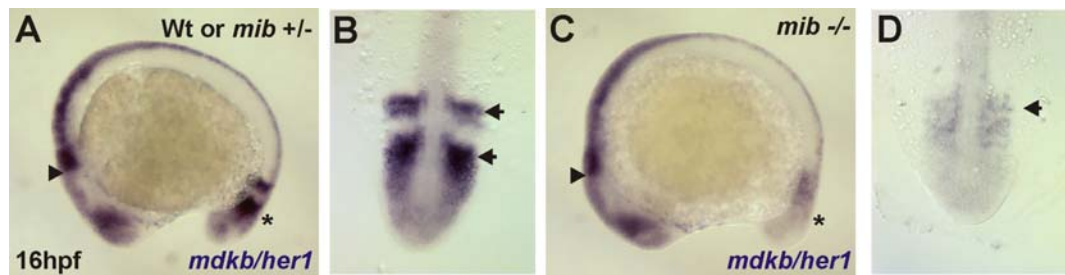


Fig. 13: *mdkb* expression is not regulated by Delta-Notch signaling.

A-D Expression of *mdkb* and *her1* in wildtype or heterozygous (A,B) and homozygous (C,D) *mindbomb* mutant embryos (*mib^{ta52b}*). **B,D** show dorsal views of tail bud regions as in A and C. Note unaltered *mdkb*, but reduced *her1* expression in the tail bud of homozygous *mib* mutants (marked by asterisk in C; D).

In homozygous *mib* embryos, identified by impaired expression of *her1* in the tail bud at 16hpf (Oates and Ho, 2002), I found no apparent alteration of *mdkb* expression in the brain or dorsal neural tube at the 14-somite stage (n=13; Fig. 13C,D). This strongly suggests that Mdkb acts upstream of or independently from Delta-Notch mediated proneural cell fate decisions.

In summary, the analysis of *mdkb* expression in inhibitor treated or mutant embryos suggests a tight regulation by known ncc inducing pathways like BMP, RA and Wnt. Modulation of FGF signaling also affects *mdkb* expression, however this also strongly affects neural plate formation and therefore could influence *mdkb* expression indirectly. Finally, Delta-Notch signaling essential for sensory neuron formation is not needed for correct *mdkb* expression.

4.3. *mdkb* regulates ncc specification

It was earlier shown that overexpression of *mdkb* leads to a posteriorization of injected embryos with strongly enhanced *foxd3* expression in premigratory ncc (Winkler and Moon, 2001). Furthermore, injection of a dominant-negative variant of *mdkb* led to a reduction of *foxd3* positive ncc and reduced *krox20* expression in r3 and r5. To analyze the role of Mdkb during induction, differentiation and maintenance of ncc precursors in more detail, I used two different approaches. First, gain of *mdkb* function was achieved by injection of *in vitro* synthesized mRNA into zebrafish embryos. Second, loss of *mdkb* function was studied in an antisense approach using injection of splice site Morpholino oligos (MOs). These functional studies should reveal specific roles of *mdkb* for ncc development. In addition, they should also show whether sensory neurons, induced at the neural plate border, are also affected by deregulation of Mdkb activity.

4.3.1. Design and activity of the *mdkb* splice Morpholinos

Initially, *mdkb* specific splice MOs were designed to block either the splice acceptor or donor site of intron 3 in the *mdkb* pre-mRNA, respectively (Fig. 14). RT-PCR analysis of uninjected embryos revealed a fragment of 480 nt corresponding to a correctly spliced product (Fig. 14B, lane 2; used primers mk-003 and mk-004). Injection of either one of the splice site MOs resulted in two fragments representing the correctly spliced product in addition to a 75 nt larger, unspliced variant still containing intron 3 (single MO concentrations 18.5 ng/nl each; Fig. 14B, lanes 3,4). This suggests that a partial repression of *mdkb* splicing and presumably Mdkb activity was obtained in these embryos. On the other hand, simultaneous injection of a solution of both splice site MOs in a 1:1 ratio resulted in a complete inhibition of intron 3 splicing (overall MO concentration 18.5 ng/nl; Fig. 14B, lane 5).

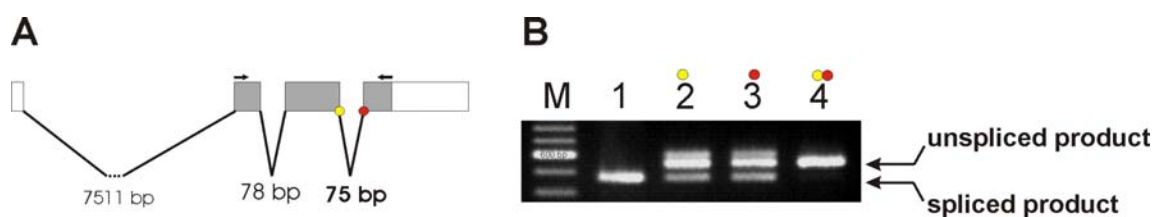


Fig. 14: Design and efficiency of *mdkb* splice MOs.

A Schematic drawing showing the organization of the *mdkb* pre-mRNA (red and yellow dots indicate blocked splice sites), intron sizes and regions of primer binding. **B** *mdkb* splice-site Morpholinos block normal processing of endogenous *mdkb* pre-mRNA. RT-PCR analysis of *mdkb* transcription in uninjected embryos (lane 1), embryos injected with one MO (Up, lane 2; Down, lane 3) and embryos coinjected with both MOs at the 3 somite stage (lane 4). Lane M represents a 100 bp DNA size ladder.

To test the efficiency and the stability of the *mdkb* splice MOs at different stages of zebrafish development, *mdkb* specific RT-PCR was performed (used primers mk-003 and mk-004). For this purpose, cDNAs from uninjected control embryos and embryos injected with a solution of *mdkb* splice MOs (1:1 ratio with a final concentration of 12.5 mg/ml) from 4 different stages were used (Fig. 15; investigated stages: 90% epiboly, 9hpf; 3-somite stage, 11hpf; 14-somite stage, 16hpf; prim-16, 32hpf). Amplification of *actin* was used as loading control and showed similar cDNA levels in all reactions (lower panel in Fig. 15; used primers RTacta1UP and RTacta1DO). Uninjected embryos of all developmental stages showed only one correctly spliced *mdkb* product (upper panel in Fig. 15). On the other hand, in all embryo groups injected with the *mdkb* splice MOs one or two larger, unspliced/incorrectly spliced product bands were detectable in all developmental stages (larger bands in the upper panel in Fig. 15). Appearance of correctly spliced products in the RT-PCR after MO injection may be due to improper injection of single embryos and subsequent amplification of the smaller correctly spliced band. Any decay of the *mdkb* splice MO ability to interfere with *mdkb* splicing was not evident, as unspliced *mdkb* products could be amplified even 32h after injection (last lane in the upper panel of Fig. 15).

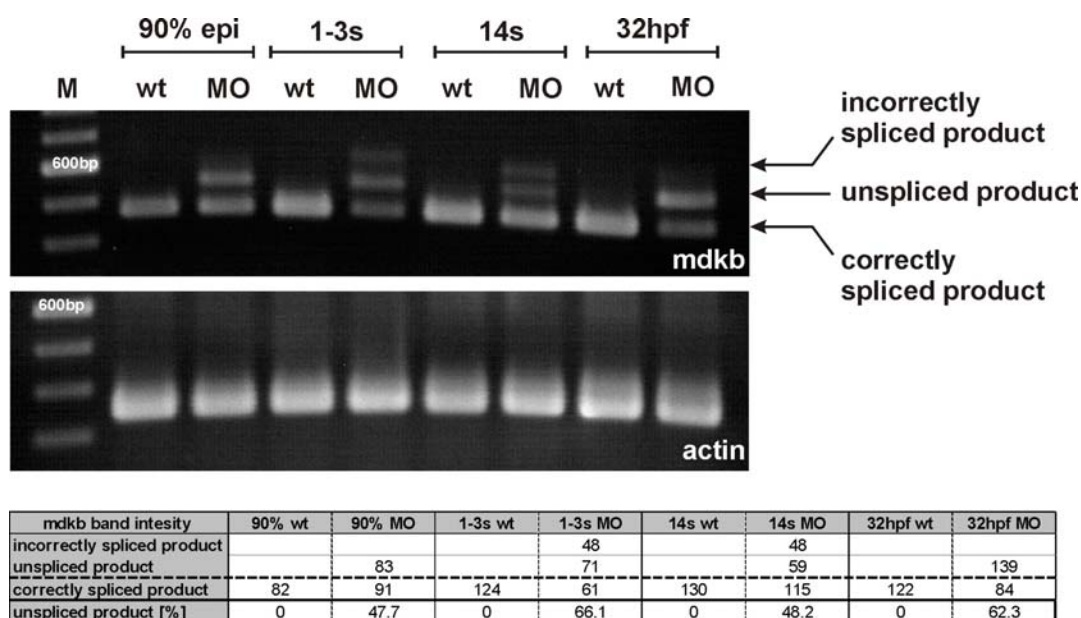


Fig. 15: Efficiency and stability of the used *mdkb* splice MOs.

RT-PCR analysis of *mdkb* transcripts in uninjected embryos (wt bands) and embryos injected with *mdkb* splice MO (MO bands) at different developmental stages. The upper panel shows correctly spliced *mdkb* products (bands at 490 bp) and MO induced unspliced products (bands at 550 and 600 bp). The middle panel shows corresponding *actin* products for loading control. Bottom: The percentage of unspliced PCR products was determined with ImageJ by measuring the mean band intensity and comparison of unspliced products in relation to correctly spliced products. M=100bp DNA ladder; wt= cDNA from wildtype embryos; MO= cDNA from embryos injected with *mdkb* splice MO.

To semi-quantitatively determine the level of reduction of correctly spliced *mdkb* mRNA transcripts, relative measurements of the intensities of unspliced and correctly spliced *mdkb* bands were made using the ImageJ software (band intensities of the different product values are noted in Table in Fig. 15). Calculations of the percentage of unspliced products were performed by comparison of the intensity value of the unspliced and incorrectly spliced band(s) and the intensity value of the correctly spliced band (unspliced product [%] = (intensity unspliced band + intensity incorrectly spliced band) x 100/(intensity unspliced band + incorrectly spliced band + intensity correctly spliced band); Table in Fig. 15). This shows that the unspliced and incorrectly spliced products in all *mdkb* MO injected embryos represent at least 47% of the present transcripts. These observations suggest that injection of *mdkb* splice MO results in a significant reduction of *mdkb* transcripts up to pharyngula stages. Utilizing the splice MOs, I next determined the effect of reduced Mdkb activity on mesodermal derivatives, extension of the neural plate and patterning of the hindbrain.

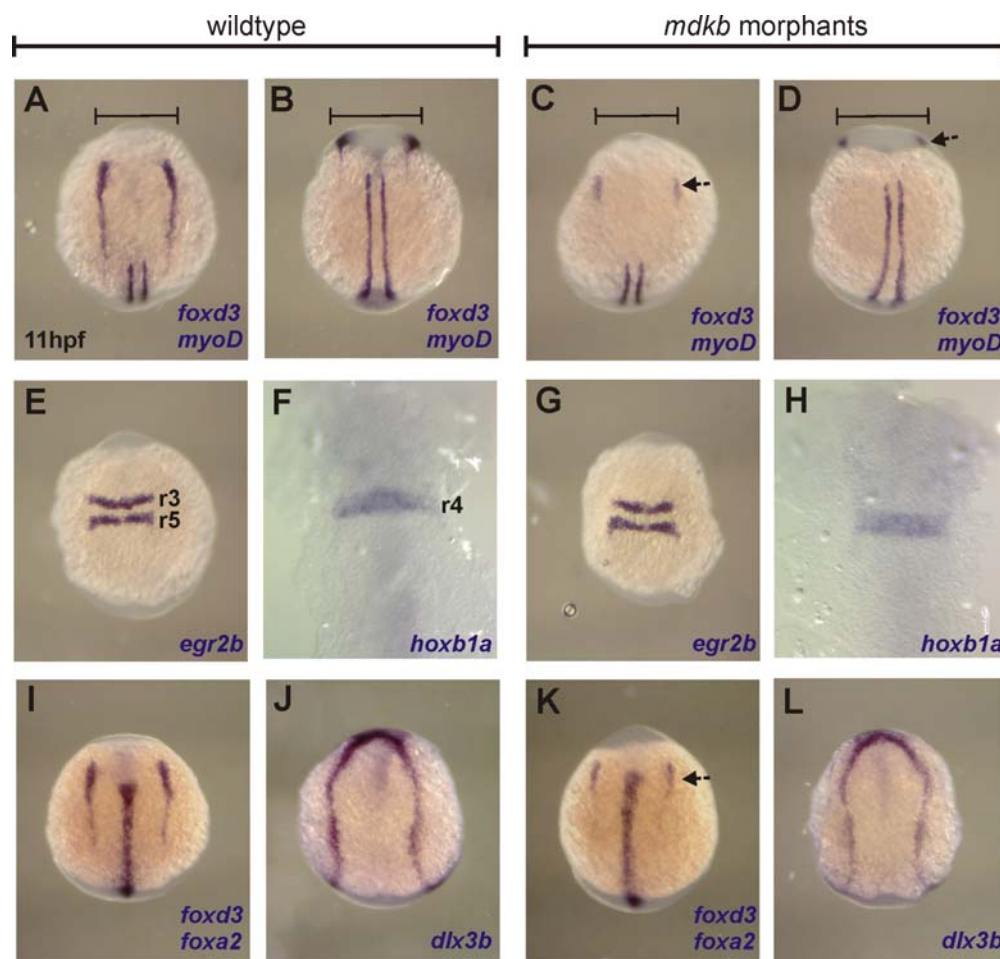


Fig. 16: *mdkb* splice MOs specifically reduce *ncc*.

A-D No effect of reduced Mdkb activity on *myoD* expression in the adaxial mesoderm, while *foxd3* expression is reduced in

premitigratory ncc. (A and C) Dorsal views of anterior trunk regions, (B and E) dorsal views of posterior trunk regions. **E-H** Normal hindbrain patterning in *mdkb* morphants, as evident by regular *egr2b* expression in rhombomeres r3 and r5, and *hoxb1a* expression in r4. **I-L** No effect of reduced Mdkb activity on *foxa2* expression in the axial mesoderm and on *dlx3b* expression, indicating regular convergence and size of the neural plate.

In situ hybridization analysis of *myoD*, which is expressed in the adaxial mesoderm at 11hpf, revealed no changes in *mdkb* morphants and also demonstrated regular convergence movements in the analyzed embryos (Fig. 16A-D). Expression of *foxd3* in the premitigratory ncc, on the other hand, was strongly reduced (Fig. 16C,D, arrows) similar to the situation in embryos overexpressing a dominant-negative version of *mdkb* (Winkler and Moon, 2001). In contrast to the earlier dominant-negative experiments, however, I did not observe any changes in hindbrain patterning of the *mdkb* morphants. Both *egr2b*, which is expressed in rhombomeres r3 and r5, as well as *hox1a* in r4 showed no difference to uninjected control embryos (Fig. 16E-H). Likewise, expression of *foxa2* in the axial mesoderm was not altered in *mdkb* deficient embryos with reduced *foxd3* expression in the ncc (Fig. 16I-L). Expression of *dlx3* at the border between neural and non-neural ectoderm was slightly reduced possibly due to the reduced number of ncc. Importantly, however, the size of the *dlx3* domain showed no altered extension indicating that the neural plate size was not affected in *mdkb* morphants (Fig. 16L). In summary, the knockdown of *mdkb* by injection of splice MOs specifically affected the premitigratory ncc domain, but had no effect on neural plate size, neural patterning in the hindbrain and formation of mesodermal structures.

4.3.2. Mdkb regulates earliest steps of ncc induction during gastrulation

After having determined the specificity of the designed MOs, I investigated if different stages of ncc development are affected by gain or loss of *mdkb* function. To analyze the effect of *mdkb* on the formation of the earliest ncc precursors during gastrulation, I looked at *pax3* expression. At 80% epiboly, *pax3* expression demarcates the neural plate including the presumptive ncc area. There, *pax3* precedes expression of established ncc markers like *foxd3*, which overlaps with *pax3* three hours later (Lewis et al., 2004). Thus, *pax3* is a marker indicative for early ncc induction. I determined *pax3* expression at 8.5hpf (80% epiboly) in *mdkb* RNA and *mdkb* MO injected embryos (Fig. 17).

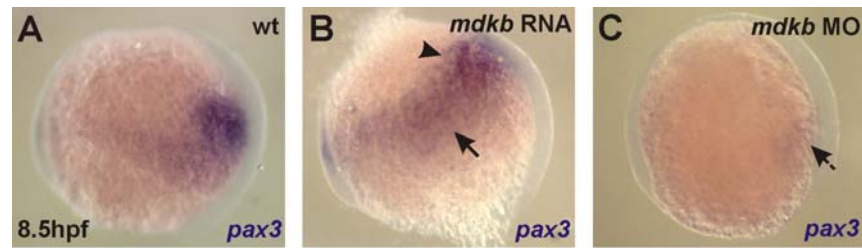


Fig. 17: Overexpression and knockdown of *mdkb* interferes with early *pax3* expression.

A-C Lateral view of *pax3* expression in a control embryo and *mdkb* RNA or *mdkb* MO injected embryos at 80% epiboly (dorsal to the right). Ectopic *pax3* expression in an embryo injected with 150pg *mdkb* mRNA (B), reduced *pax3* expression in embryo injected with *mdkb* (C). The arrows in B mark expanded *pax3* expression, the arrowheads the anterior border of *pax3* expression. Pointed arrows in C mark area with reduced *pax3* expression.

In uninjected controls at this stage, *pax3* expression is found in two bilateral domains without expression in the dorsal midline (Fig. 17A). In embryos injected with 150 pg *mdkb* RNA, this domain was ventrally expanded and expression levels were increased (48%, n=37; arrow in Fig. 17B). Furthermore, this domain was also shifted to a more anterior position in the embryo (arrowhead in Fig. 17B) suggesting that ectopic Mdkb modulates the position and size of the *pax3* positive ncc domain during gastrulation. In contrast, embryos injected with the *mdkb* MO showed a nearly complete repression of *pax3* expression (65%, n=62; Fig. 17C). Low levels of expression remained in a posterior domain of the embryo (arrowhead in Fig. 17C). This indicates that Mdkb activity is required for defining a correctly positioned ncc precursor domain during gastrulation.

4.3.3. Misexpression of *mdkb* alters expression of prominent ncc specifiers

Ncc precursors give rise to different subsets of derivatives with distinct fates and characteristic gene expression patterns (Le Douarin and Kalcheim, 1999). I analyzed expression of *foxd3*, *sox10*, *sox9b* and *snail1b*, which are ncc specifying genes and label a broad spectrum of ncc subtypes (Thisse et al., 1995; Dutton et al., 2001; Yan et al., 2005; Lister et al., 2006).

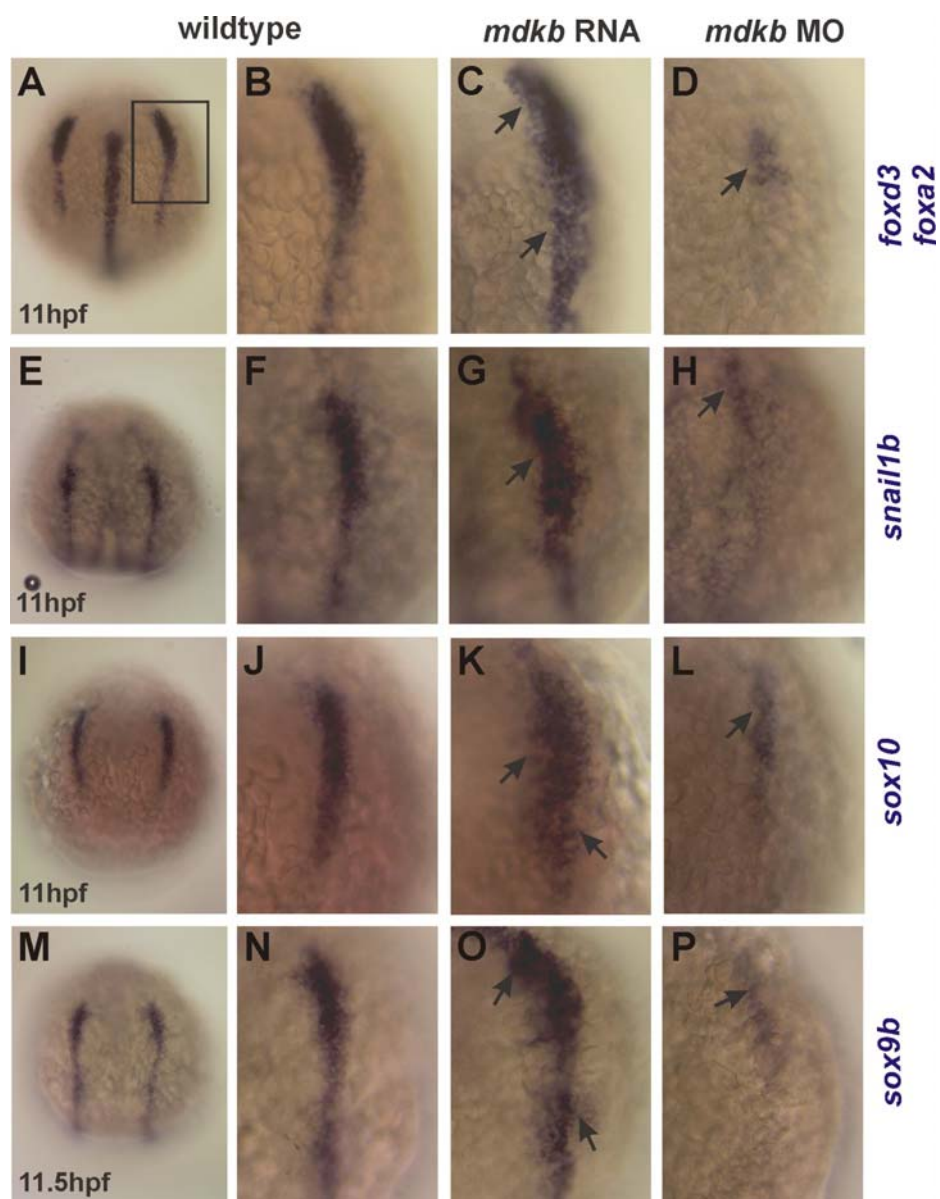


Fig. 18: *mdkb* regulates formation of different subtypes of neural crest cells.

A-D Expression of *foxd3/foxa2*, **E-H** *snail1b*, **I-L** *sox10* and **M-P** *sox9b* in uninjected wildtype embryos (first and second column), embryos injected with 150pg *mdkb* mRNA (third column) and *mdkb* splice-site Morpholinos (forth column). A, E, I and M are dorsal views of whole embryos with anterior to the top, all other pictures are higher magnification views of corresponding regions marked by box in A. Arrows indicate areas of enhanced, respectively reduced expression.

Table 1: Effect of *mdkb* misexpression on neural crest numbers

injected	marker gene	developmental time (hpf)	total number of embryos (n)	embryos with raised ncc number (n)	percentage
<i>mdkb</i> RNA	<i>pax3</i>	8.5	27	18	66.7
	<i>foxd3</i>	11	17	15	88.2
	<i>snail1b</i>	11	26	16	61.5
	<i>sox10</i>	11	17	14	82.4
	<i>sox9b</i>	11.5	17	15	88.2
total			104	78	75.0

injected	marker gene	developmental time (hpf)	total number of embryos (n)	embryos with reduced ncc number (n)	percentage
<i>mdkb</i> MO	<i>pax3</i>	8.5	62	40	64.5
	<i>foxd3</i>	11	68	50	73.5
	<i>snail1b</i>	11	38	25	65.8
	<i>sox10</i>	11	33	31	93.9
	<i>sox9b</i>	11.5	50	32	64.0
total			251	178	70.9

These markers were analyzed at 11-12hpf (1 to 3-somite stage) in embryos injected with 150 pg *mdkb* RNA or 9.4 ng of combined *mdkb* splice MOs. After injection of *mdkb* RNA, expression of all analyzed markers was strongly enhanced in a total of 75% of analyzed embryos (n=104; see Table 1; Fig. 18C,G,K,O). On the other hand, knockdown of *Mdkb* activity after MO injection resulted in a dramatic reduction of *ncc* marker expression at this stage. An average of 71% embryos showed a significantly reduced expression of all markers analyzed or even completely lacked marker expression (n=251; see Table 1; Fig. 18D,H,L,P). As expression of all four analyzed markers was altered, this suggests that most if not all different *ncc* subtypes are regulated by *Mdkb* activity.

4.3.4. Rescue of *ncc* defects in *mdkb* morphants by RNA co-injection

To analyze whether the observed effects of the *mdkb* MOs on *ncc* induction are specific, I performed RNA and MO coinjection experiments to rescue the *ncc* phenotype. For this experiment, embryos were either injected individually with 100 pg *mdkb* RNA or 9.4 ng *mdkb* MO or the RNA was co-injected approximately 20 minutes after the MO solution into the same embryo. All injected embryos were raised until the 1-somite stage (11hpf) and then subdivided into two groups.

The first group of 30 embryos was used for RNA extraction and cDNA synthesis. The different cDNAs were used for RT-PCR to determine the presence of unspliced *mdkb* transcripts. *mdkb* specific primers showed the increase of *mdkb* RNA in RNA injected embryos, as well as the presence of unspliced product resulting from MO injection (Fig 19A row 1; used primers mk-003 and mk-004). In co-injected embryos, the correctly spliced *mdkb* but unexpectedly no unspliced *mdkb* band could be observed, presumably due to an amplification advantage of the smaller products (Fig. 19A row 1, RNA x MO lane). Therefore, a second PCR with the same set of cDNAs was conducted with *mdkb* intron 3 specific primers to demonstrate the stabilization of intron 3 in *mdkb* MO and co-injected

embryos (Fig. 19A row 3; used primers *mdkb_intorn3-4_up* and *mdkb_intron3-4_down*). -RT reactions served as negative controls. Furthermore, *actin* primers were used to control cDNA loading and PCR reactions (Fig. 19A row 2 and 4). Unspliced *mdkb* transcripts were only detected in *mdkb* splice MO injected and co-injected embryos (Fig. 19A, row3 lanes 4,5). Therefore, these RT-PCR data clearly indicate the functionality of the *mdkb* splice MO in co-injected embryos.

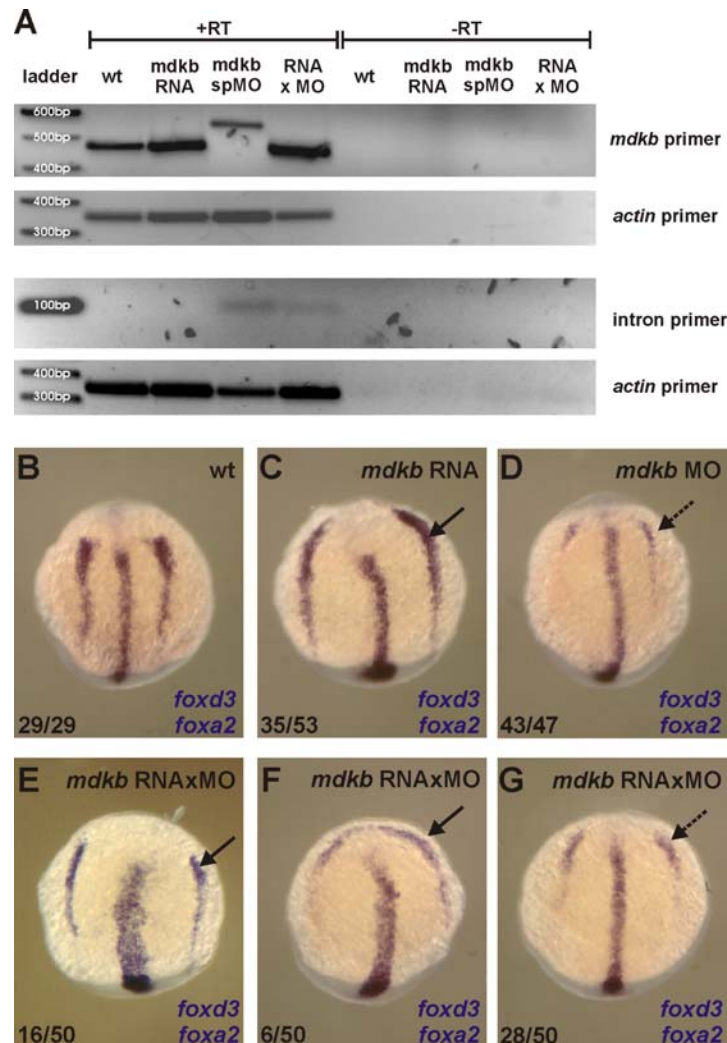


Fig. 19: RNA rescue of ncc defects in *mdkb* morphants.

A RT-PCR analysis of *mdkb* transcripts in uninjected embryos (lane 2), *mdkb*RNA (lane 3), *mdkb* splice MO (lane 4) and double injected embryos (lane 5). Top panel shows RT-PCR products using exon specific primers, third panel from top shows products using primers covering the MO targeted intron 3. Analysis of *actin* expression was used as loading control in each experiment. The right panel represents -RT controls. **B-G** Analysis of *foxd3* expression in ncc and *foxa2* in axial mesoderm. Numbers indicate embryos with respective phenotype.

The second group of embryos was used for in situ hybridization to visualize *foxd3* positive ncc, while *myod* was used as a control labeling adaxial cells in the midline (Fig. 19B-G). All

wildtype embryos showed normal ncc development (n=29, Fig. 19B), while 66% of *mdkb* RNA injected embryos showed an increased level of ncc marker expression (n=53; Fig. 19C). 91% of Morpholino injected embryos showed reduced ncc number or complete loss of ncc (n=47; Fig. 19D). Importantly, co-injection of *mdkb* RNA and MO resulted in 32% of the embryos showing normal ncc development (Fig. 19E), while 12% of embryos even showed an increased number of ncc (Fig. 19F). Only 56% of embryos exhibited a reduced number or absent ncc (n=25; Fig. 19G). This experiment indicates a partial rescue of ncc defects by co-injection of *mdkb* RNA into *mdkb* morphants. It implies that the observed defects in ncc induction are specifically caused by reduced Mdkb levels and are not unspecifically caused by the injection procedure.

4.3.5. Loss of ncc in *mdkb* morphants is not a consequence of increased apoptosis

Reduction of ncc in *mdkb* morphants might be explained by two mechanisms, impaired ncc induction or enhanced apoptosis of ncc. To challenge the hypothesis that the loss of ncc in *mdkb* morphants is due to increased apoptosis, I performed TUNEL (terminal transferase dUTP nick end labeling) in wildtype and *mdkb* MO injected embryos. To visualize ncc and for control of embryonic development an in situ hybridization for *foxd3* and *foxa2* was conducted prior to TUNEL staining.

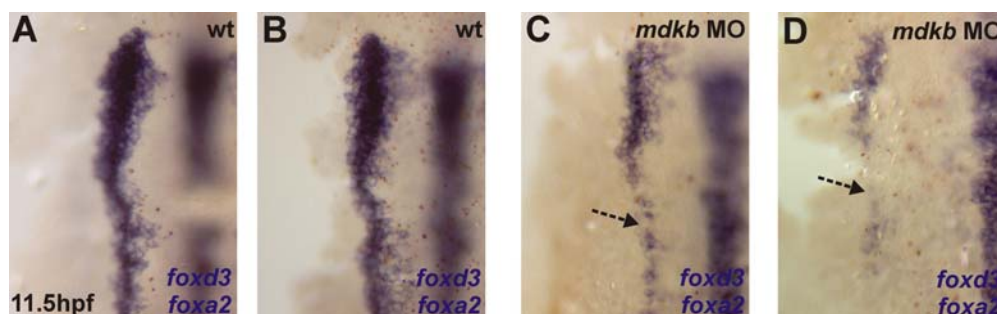


Fig. 20: Knockdown of *mdkb* does not enhance apoptosis of ncc.

A-D TUNELstain for apoptotic cells in 3 somite-stage embryos stained for expression of *foxd3* and *foxa2* in non-injected wildtype embryos (A,B) and embryos injected with *mdkb* splice-site MOs (C,D). All pictures are dorsal views on one ncc domain. Embryos with low rate of apoptosis (A, C) or slightly increased apoptosis (B, D). Dashed arrows indicate reduced ncc domains.

The *foxd3* positive ncc population at the neural border was reduced in 95% of all *mdkb* MO injected embryos (n=40; pointed arrows in Fig. 20C,D). Usually, the number of apoptotic cells in control embryos varied to some extent (Fig. 20A showing low rate of apoptosis, Fig. 20B showing slightly increased rate of apoptosis). In all analyzed morphants, no evidence for

strongly enhanced apoptosis of ncc or other cell types was found (Fig. 20C,D). Even in severely affected morphants with delayed convergence (Fig. 20D), no increase in apoptotic cell number was found in comparison to the varying levels of apoptosis in control embryos. This observation further supports the idea that loss of ncc in *mdkb* morphants is due to an impairment of ncc induction rather than survival or maintenance.

4.3.6. Analysis of ncc recovery in late embryonic stages of *mdkb* morphants

Several lines of evidence suggested the possibility that ncc have the capacity to reappear during later development even after complete ablation at early stages (Lewis et al., 2004). This regain of ncc is explained by specification of ncc through different signals during later differentiation. Lewis et.al. (2004) showed that *wnt8a* depletion in zebrafish exclusively interferes with the induction of ncc but not with the specification of later ncc derivatives. Ncc reuse Wnt signals apart from Wnt8 for differentiation. To analyze whether Mdkb similar to Wnt8a function only affects ncc induction, I investigated reestablishment of ncc and ncc derivatives at later time points during embryonic development.

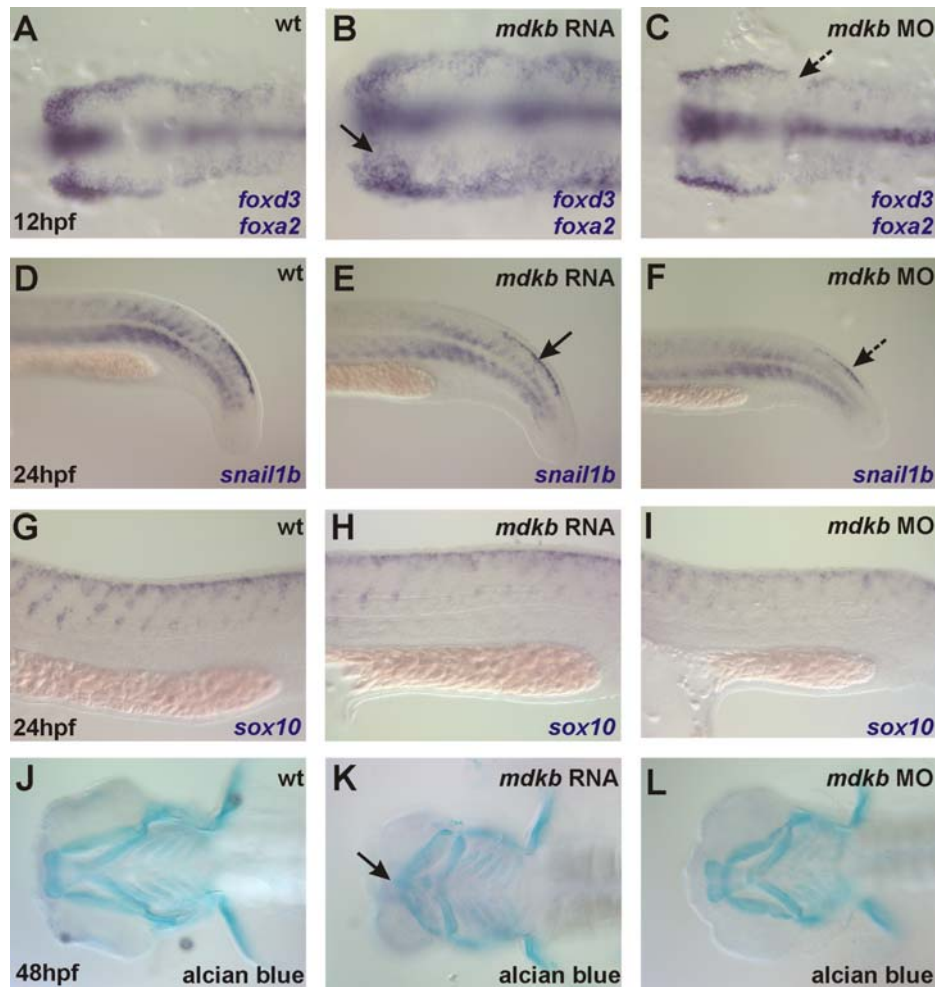


Fig. 21: *mdkb* interferes with *ncc* induction but not with *ncc* delamination or cartilage development.

A-C Expression of *foxd3* and *foxa2* in uninjected wildtype embryos (A), embryos injected with 150 pg *mdkb* mRNA (B) and *mdkb* MO (C) at the 6-somite stage. Pictures are taken of embryo preparations with focus on the cephalic *ncc* region. Arrows indicate areas of enhanced, respectively reduced expression. **D-F** Expression of *snail1b* in the tail of embryos at the 24hpf stage is detected in the mesoderm and *ncc* (D). Overexpression and knockdown of *mdkb* results only in minor changes of *ncc* number (arrows in E and F). **G-I** Delaminating *ncc* are visualized by *sox10* expression in embryos 24hpf (G). Overexpression and knockdown of *mdkb* does not interfere with *ncc* movement (H and I). **J-L** Dorsal views of alcian blue stained embryos at the 48hpf stage. Anterior head cartilage development in *mdkb* RNA injected embryos is impaired (K), while *mdkb* MO injected embryos showed no defects (L).

Recovery of *ncc* in RNA and MO injected zebrafish embryos was investigated by looking at the *ncc* number at the 6-somite stage (12hpf). *Ncc* at this stage delaminate, undergo EMT and start to move away from their place of induction (Halloran and Berndt, 2003). Premigratory *ncc* were identified by the expression of *foxd3* via in situ hybridization (Fig. 21A). 83% of *mdkb* RNA injected embryos displayed a larger cephalic *ncc* domain at this stage with increased numbers of *ncc* (n=36; arrow in Fig. 21B). Knockdown of *Mdkb* function by MO injection resulted in a reduced *ncc* number in all embryos, but a persisting population of *ncc* was still present (n=22; Fig. 21C). This experiment suggests that changed levels of *Mdkb* activity does interfere with *ncc* cell number also at the 6 somite stage.

To look into ncc differentiation at later embryonic stages, the expression of *snail1b* in non-migratory ncc and *sox10* in migratory ncc at 24hpf was determined. At this stage, *snail1b* expression is found in trunk mesodermal cells and in dorsal tail ncc in wildtype embryos (Fig. 21D; Thisse et al., 1995). This tail ncc domain is slightly enlarged in all *mdkb* RNA injected embryos (n=4; arrow in Fig. 21E). On the other hand *mdkb* knockdown resulted only in a mild reduction of non-migratory ncc at this domain (n=7; dashed arrow in Fig. 21F). Additional investigation of trunk migratory ncc moving along the lateral pathway by looking at *sox10* expression also revealed only very mild effects after *mdkb* RNA injection (n=5; Fig. 21H) or *mdkb* MO injection (n=4; Fig. 21I). While overexpression and knockdown of *mdkb* strongly affects early ncc induction, these results suggest that ncc formation is nearly completely recovered at later stages of differentiation.

To further investigate *mdkb* independent late recovery of ncc differentiation, cartilage establishment in *mdkb* RNA or MOs injected embryos was visualized by alcian blue staining. *mdkb* RNA injected embryos showed incorrect cartilage structure organization in the anterior head, but normal appearance of cartilage tissue in posterior body parts (n=5; Fig. 21K). The observed malformation, however, might be secondary effects by interference of *mdkb* overexpression with anterior head induction (Winkler and Moon, 2001). Reduced levels of Mdkb by MO injection resulted in slower embryo development but did not result in cartilage defects (n=8; Fig. 21L). In summary, these results indicate that ncc delamination and specification are only mildly affected by altered Mdkb activity. Nevertheless, Ncc induction at the neural plate border is strongly depending on Mdkb activity.

4.4. **Mdkb regulates sensory neuron specification**

Concomitantly with *ncc*, sensory neurons are induced at the outer neural plate border during gastrulation of zebrafish (Cornell and Eisen, 2000). As the initial steps of *ncc* formation are affected by altered *Mdkb* activity, I analyzed whether also sensory neuron induction requires *Mdkb* activity.

4.4.1. **Mdkb influences primary sensory neuron induction**

I initially looked at the expression of primary neuron markers *neurogenin-1* (*ngn1*), *islet-1* (*isl1*) and *islet-2* (*isl2*) in *mdkb* RNA and MO injected embryos. In the posterior neural plate at the 1 to 3 somite stage, these markers demarcate distinct medio-lateral domains containing motor-, inter- and sensory neuron precursors, respectively.

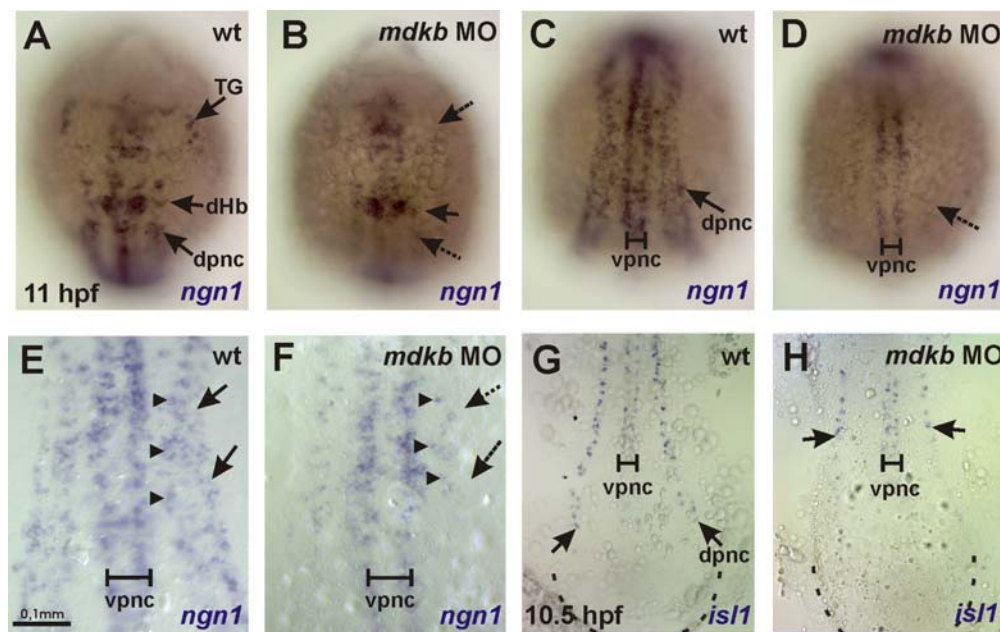


Fig. 22: *mdkb* regulates formation of sensory neurons.

A-H Dorsal views of trunk regions in uninjected (A,C,E,G) and *mdkb* MOs injected embryos (B,D,F,H) at the 1 somite stage showing *ngn1* and *isl1* expression. Dorsal proneural cells (dpnc) are reduced in injected embryos at mid-hindbrain (arrows in A,B) and trunk level (arrows in C-H), while number of ventral proneural cells (vpnc) is not affected. Note remaining interneurons (arrowheads), but absent sensory neurons (arrows) in *mdkb* morphants (in F). DHb, dorsal hindbrain; TG, trigeminal ganglia; VMB, ventral midbrain.

In control embryos, rostral *ngn1* expression is found in the trigeminal ganglion and in distinct neural progenitor domains in the head, including the diencephalon and the rhombencephalon (Fig. 22A), and caudally in the progenitor cell populations of motor neurons (ventral proneural cells, vpnc), as well as inter- and sensory neurons (dorsal proneural cells, dpnc; Fig.

22C; Blader et al., 1997). Injection of *mdkb* MOs resulted in a dramatic reduction of laterally located neural progenitors in the head, while medial cells were not affected. Reduced *ngn1* expression was found in the trigeminal ganglia and a subpopulation of dorsal neural progenitors in the hindbrain (arrows in Fig. 22B) at the 3-somite stage. In the posterior neural plate, the effect of *mdkb* knockdown was even more striking. While formation of primary motor neurons was not or only mildly affected, the number of *ngn1* positive interneurons was reduced and RB progenitors were strongly reduced or completely absent (62.5%, n=16; Fig. 22D,F). For *isll* as an additional marker for primary neurons, medially positioned motor neuron precursors were present in *mdkb* MO injected embryos, however, the number of laterally located sensory precursors (dpnc) was reduced (60%, n=15; Fig. 22G,H), similar to the situation when using a dominant-negative variant of *mdkb* (Winkler and Moon, 2001). This observations show that induction of primary sensory neurons at the neural plate border is dependent on Mdkb. Nevertheless, the observed effect of Mdkb on sensory neurons might be temporally restricted to induction and further differentiation could occur independently, as observed for *ncc*.

4.4.2. Absence of sensory neuron recovery in *mdkb* morphants

To test, if the down-regulation of *mdkb* has a long-lasting effect on sensory neuron induction or whether a regain of neuronal precursors is possible at later developmental stages, the expression of *ngn1* in embryos at the 6-somite stage (12hpf) was determined. In wildtype embryos of this stage, *ngn1* expression is found in a large number of primary neurons in distinct brain substructures (Fig. 23D; arrowhead marks the MHB), in the trigeminal ganglion (arrow in Fig. 23D) and in dorsal and ventral proneural clusters and interneurons of the spinal cord (marked in Fig. 23G). Gain of Mdkb function by injection of 150 pg RNA resulted in suppression of head formation and shortening of the AP axis (previously described in Winkler and Moon, 2001; Fig. 23B). These embryos showed an increased number of cells expressing *ngn1* in dorsal midbrain structures and in the neural tube (n=31; arrows in Fig. 23B). Remarkably more *ngn1* positive cells could be observed at the neuroectoderm border in the trigeminal ganglion precursors and in the neural tube (arrows in Fig. 23E). In the trunk, overexpression of *mdkb* increased the cell number in the dorsal proneural cluster and also of interneurons and of the ventral proneural cluster (Fig. 23H). The opposite observation, loss of *ngn1* positive primary sensory neurons, was observed in 50% of embryos injected with the *mdkb* MO (n=16). Remarkably, cells of the telencephalon (arrows in Fig. 23C and F), the trigeminal ganglia and cells of the dorsal proneural cluster were ablated (arrow in Fig. 23I),

but no change in ventral primary neuron populations were obvious. These results indicate that the neuronal effect of deregulation of *mdkb* expression levels is detectable also during later stages of neurogenesis. This, both the induction and recovery of sensory neuron precursors is dependent on Mdkb.

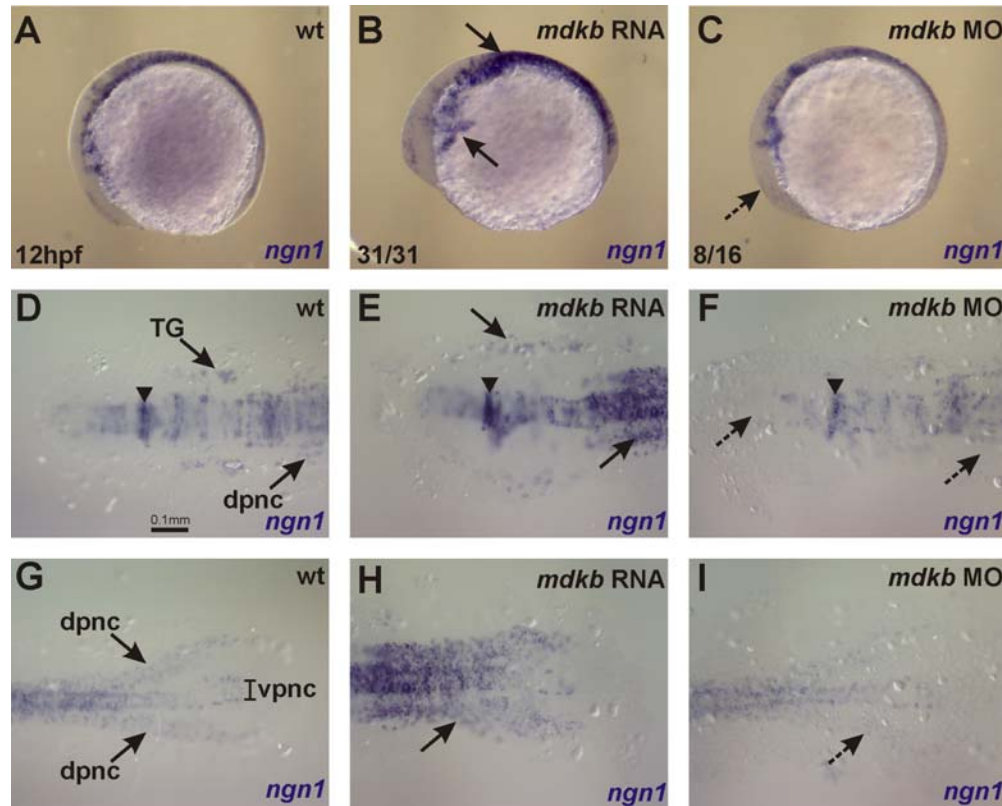


Fig. 23: Influence of *mdkb* on primary neurons at the 6-somite stage.

A-C Lateral views of whole-mount embryos marked for *ngn1* expression. **D-I** are dorsal views of the head regions (**D-F**) and tail regions (**G-I**) of dissected embryos. *mdkb* RNA injected embryos have a raised number of *ngn1* positive cells, especially in the enlarged midbrain region and the neural tube (arrows in **B,E,H**). Embryos injected with *mdkb* MO lack *ngn1* positive cells of the telencephalon, the trigeminal ganglia and the dpnc (arrows in **C,F,I**). Arrowheads mark the MHB; TG, trigeminal ganglia; dpnc, dorsal proneural cluster; vpnc, ventral proneural cluster. Numbers indicate embryos with respective phenotype.

To follow the fate of the sensory neuron precursors in the neural tube, *isl2* expression in embryos at the 18-somite stage was investigated. *isl2* is expressed in ventrally located motor neurons (arrowheads in Fig. 24) and a continuous row of RB sensory neurons in the dorsal neural tube. Injection of *mdkb* RNA had no influence on the number or regularly spaced appearance of motor neurons, but it significantly increased the number of RB neurons in the dorsal neural tube (in 79% of the analyzed embryos, n=14; arrows in Fig. 24B). In contrast, knockdown of Mdkb activity severely reduced the number of RB neurons (69%, n=26; arrows in Fig. 24C), while again no effect on motor neurons was observed (arrowheads in Fig. 24C). To determine whether differentiation of these neurons is affected by Mdkb, the presence of

acetylated-tubulin protein in the neuronal cell bodies and axons of *mdkb* injected embryos was analyzed. At 28hpf, formation of ventral motor neurons was normal in both *mdkb* RNA and MO injected embryos (Fig. 24G-I). The number of RB neurons, in contrast, was increased in *mdkb* RNA injected embryos and their position appeared irregular (76.9%, n=13; Fig. 24M). Loss of Mdkb activity, on the other hand, resulted in a significant loss of differentiated RB neurons (75%, n=20; Fig. 24N). In average 33 RB neurons on a 0.7 mm stretch of the embryonic trunk representing 4 to 5 somite segments (s.d. 3.3; n=4) were counted. Injection of *mdkb* RNA increased the RB number to 40.5 (s.d. 4.1; n=4). Injection of *mdkb* MO, on the other hand, lowered the number to 21 (s.d. 3.1; n=4).

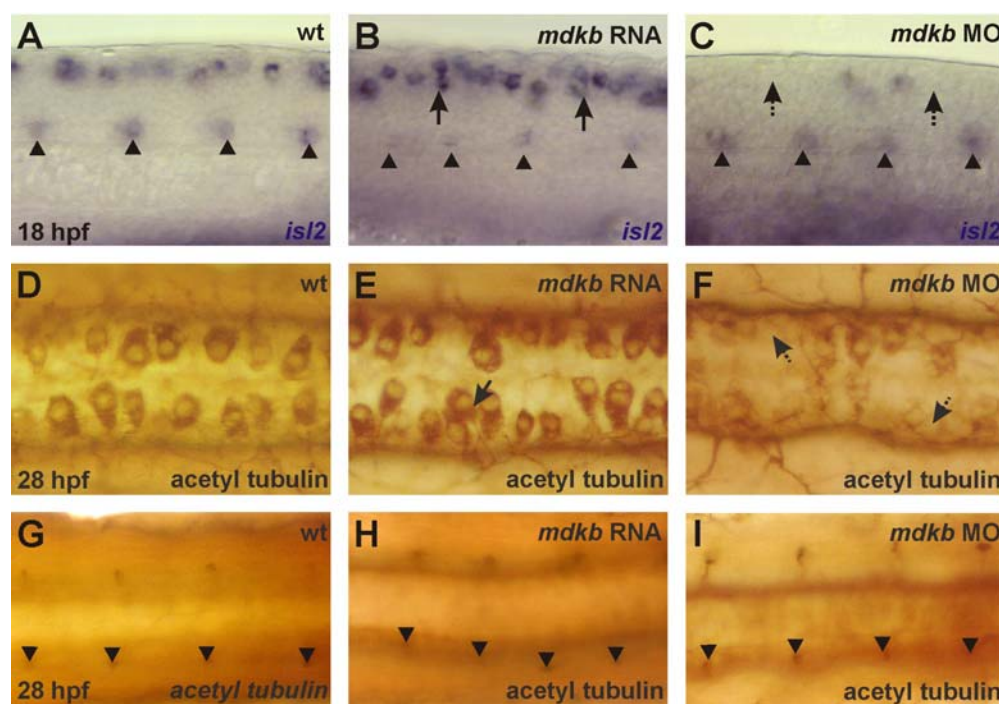


Fig. 24: *mdkb* regulates the number of differentiated RB sensory neurons.

A-C Lateral views of trunk regions in embryos at the 18-somite stage showing *isl2* expression in ventrally located motor neurons (arrowheads) and dorsal sensory RB neurons (arrows). Embryos injected with 150pg *mdkb* RNA (B) show enhanced numbers of dorsal RB, while motor neurons are not affected. In contrast, RB are reduced in *mdkb* MO injected embryos (C). **D-I** Dorsal views of embryos at 28hpf immunostained with an antibody against acetylated tubulin. (D-F) show focal planes at the level of dorsal sensory neurons, (G-I) show focal planes of the same embryos at the level of ventral motor neurons. Note increased RB cell number in *mdkb* RNA injected embryos (arrow in E) and reduced RB cell number in *mdkb* MO injected embryos (arrows in F), while number of motor neurons is not affected (arrowheads in G-I).

These results show that that Mdkb action on sensory neurons is persisting and recovery of neurons at later stages of development is absent. Taken together, our gain and loss of function studies indicate that Mdkb regulates induction of both *ncc* and RB neurons at the neural plate border in zebrafish.

4.5. Non-overlapping activities of Midkine growth factors during mid- and hindbrain formation

Mdkb activity in the early embryo greatly differs from that of its co-orthologue Mdka and therefore indicates functional divergence of both factors in the neural tube. While Mdka is essential for floor plate formation (Schafer et al., 2005), Mdkb is necessary for induction of ncc and sensory neurons (this thesis, chapter 4.4). In addition to their function in the neural tube, *mdka* and *mdkb* are also implicated in brain formation. Both genes are expressed in brain, but their exact functions during brain development have not yet been investigated. Expression of both genes in distinct brain regions during different phases of development opens the possibility of divergent functions also during brain development. Additionally, expression and function of *ptn*, the third member of the midkine family, has not been investigated in zebrafish brain development and remains elusive.

4.5.1. Mostly non-overlapping expression patterns of *mdka*, *mdkb* and *ptn* during zebrafish brain development

To investigate functional divergence of Midkine growth factors during brain development, the precise expression patterns of all three genes in the embryonic brain were determined by in situ hybridization. Detailed comparison of the expression patterns at different stages of development was expected to give first hints on possible functions in distinct brain regions.

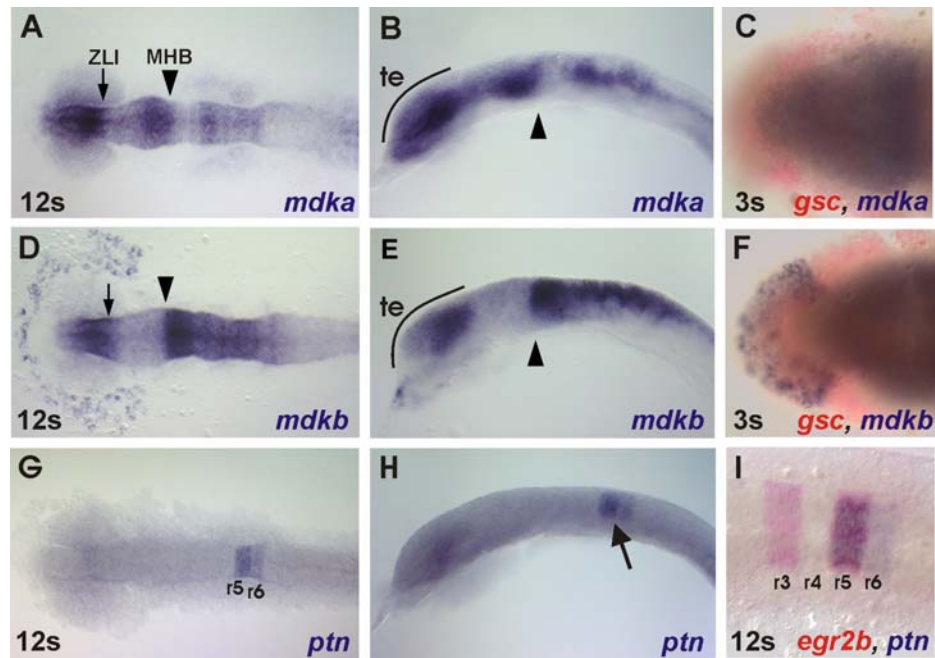


Fig. 25: Expression of *midkine* genes in early brain domains.

A,B,D,E,G,H Dorsal (pictures in row1) and lateral views (pictures in row2) of expression of *mdka* (A,B), *mdkb* (D,E) and *ptn* (G,H) at the 12-somite stage (15hpf). **C, F** are dorsal views of *mdka* and *mdkb* expression (blue) in comparison to *gsc* expression (red) in the prechordal plate at the 3-somite stage (11hpf). **I** Dorsal view on *ptn* (blue) and *egr2b* (red) expression in the rhombencephalon. Arrows in A and D mark the zona limitans intrathalamica (ZLI); arrowheads mark the MHB; te = telencephalon, r = rhombomeres. Figures A and B were kindly provided by M. Schäfer. Figure I was kindly provided by C. Neuner.

I initially looked at the expression of all three genes at the 12-somite stage (15hpf; Fig. 25). The expression of *mdka* at this stage is most prominent in the telencephalon, in the mesencephalon, anterior to the MHB, in the ventral parts of the rhombomeres (Fig. 25A,B). At the 3-somite stage (11hpf), expression of *mdka* is found close to the anterior neural ridge near the polster marked by *gsc* expression (Fig. 25C). In contrast, *mdkb* expression is found in the telencephalon, in dissociating prechordal plate cells and in the complete rhombencephalon. Expression of *mdkb* in the forebrain is more posterior than *mdka*, but surrounds the anterior ridge by its expression in the ventral prechordal cells (Fig. 25F). Therefore, *mdka* and *mdkb* expression at this stage overlap in the telencephalon while in the rhombencephalon expression of both genes is complementary. Expression of *ptn* is found at low levels in all brain areas but most prominently in rhombomeres r5 and r6 (Fig. 25G,H), as shown by colocalization with *egr2b* expression (Fig. 25I). At this stage of development, *ptn* expression therefore overlaps completely with either *mdka* or *mdkb* in the ventral, respectively dorsal portions of rhombomeres r5 and r6.

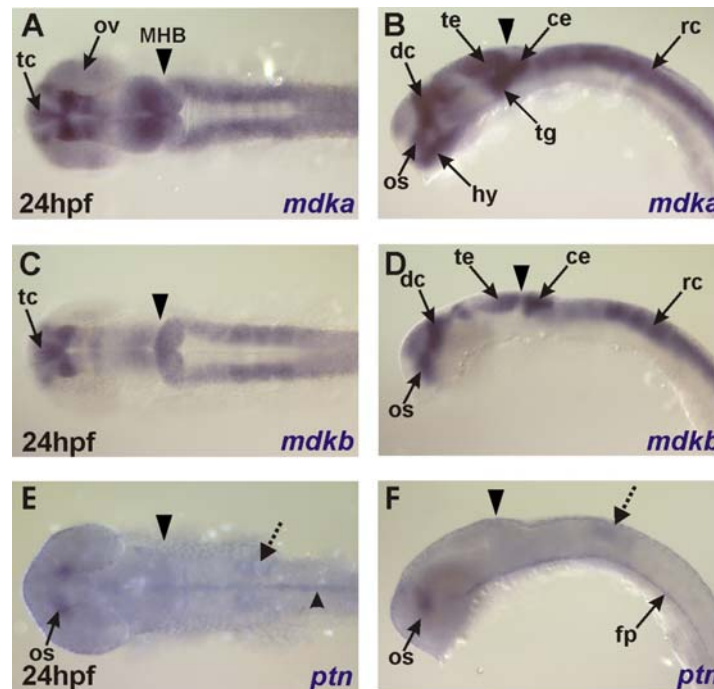


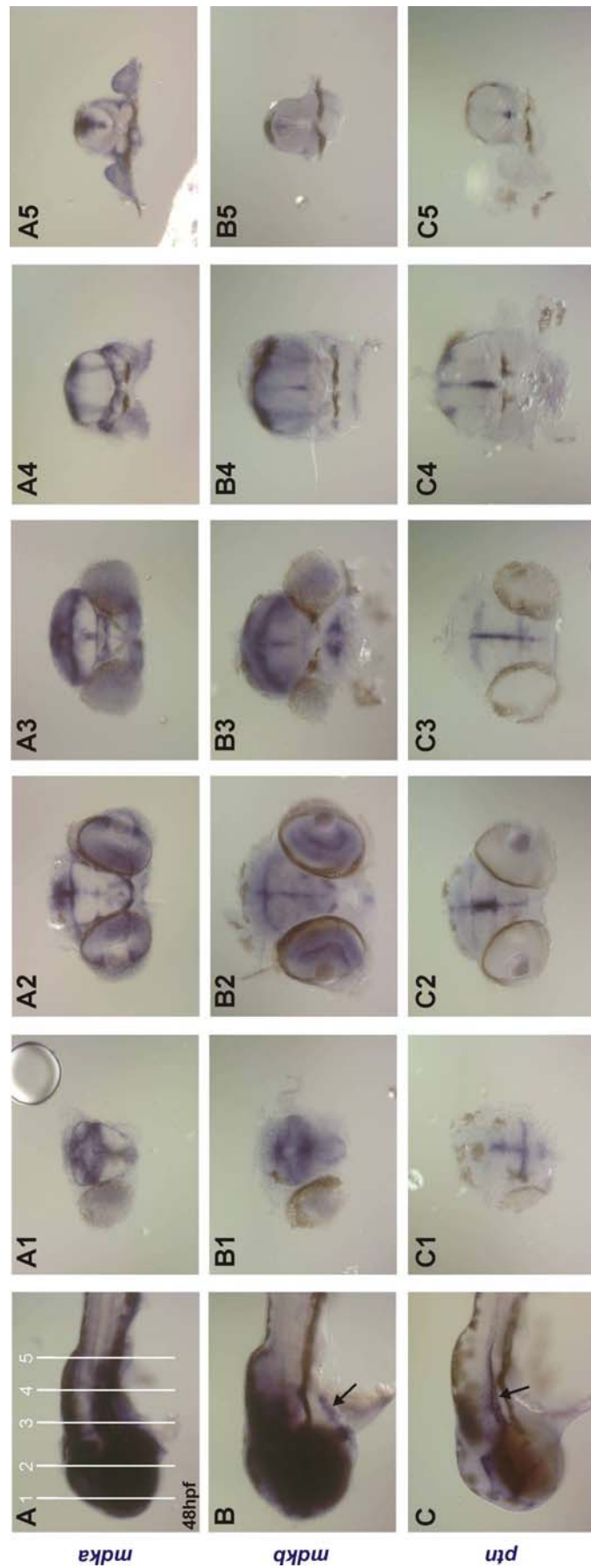
Fig. 26: Expression of *midkine* genes in the brain at 24hpf.

A-F Expression of *mdka* (A,B), *mdkb* (C,D) and *ptn* (E,F) in the head at 24hpf (dorsal views in row1, lateral views in row2). Arrowheads mark the MHB; ce = cerebellum, dc = diencephalon, fp = floor plate, hy = hypothalamus, os = optic stalk, ov = optic vesicles, rc = rhombencephalon, tc = telencephalon, te = tectum, tg = tegmentum.

Comparison of the expression patterns of all *midkine* genes after 24hpf revealed further aspects of restricted expression. Expression of *mdka* is broad in the brain (Fig. 26A,B). Expression of *mdka* is detected in the optic vesicles, the telencephalon, the hypothalamus and the posterior diencephalon. Midbrain structures like the tegmentum, the tectum and the MHB also show high levels of *mdka* expression. Also the cerebellum and the complete rhombencephalon shows high *mdka* expression.

Expression of *mdkb* (Fig. 26C,D) is observed in the telencephalon and the surrounding diencephalic tissues. *mdkb* is also strongly expressed in the dorsal telencephalon, the tectum and the cerebellum, but discontinuous at the level of the MHB. The rhombomeres show variable levels of *mdkb* expression with lower expression in the anterior and high levels in the posterior segments. At this stage, *mdka* and *mdkb* are found co-expressed in an area around the telencephalon, in the tectum, the cerebellum and the rhombomeres. Exclusive expression of *mdka* at this stage is found in the eyes and the dorsal midbrain.

In contrast to the broad expression of *mdka* and *mdkb*, *ptn* (Fig. 26E,F) is restricted to the optic stalks and the cephalic floor plate. Expression in r5 and r6 is faint but detectable (dashed arrow in Fig. 26E,F). All three *midkine* genes have overlapping expression in a small zone in the forebrain, the optic stalk at this stage.



	Section 1	Section 2	Section 3	Section 4	Section 5
<i>mdka</i>	medial telencephalon, around 3rd ventricle, diencephalon	eye and optic nerve diencephalon, ventricle borders, dorsal mesencephalon	hypothalamus, mandibular arch, dorsal mesencephalon, ventricle border	dorsal myelencephalon, ventricle border, pharyngeal arches, around aorta and notochord	dorsal rhombencephalon, ventricle border, fin buds
<i>mdkb</i>	telencephalon, around 3rd ventricle, diencephalon	eye, ventricle borders	ventricle border, around stomodeum	dorsal myelencephalon, ventricle border	dorsal rhombencephalon, ventricle border
<i>ptn</i>	around 3rd ventricle, telen-diencephalon border	ventricle borders	ventricle borders	ventricle border, floor plate	floor plate

Fig. 27: Expression of midkine genes in the brain 48hpf.

A-C Patterns of *mdka* (line A), *mdkb* (line B) and *ptn* (line C) expression are shown in a lateral overview (row 1) and in consecutive sections (1 to 5, position of section is indicated in A). Brain tissues with increased expression are listed for every gene and section in the table. Bold font type indicates tissues with overlapping expression.

Expression of *midkine* genes at 48hpf is highly diverse and non-overlapping in different brain compartments. To compare their expression patterns, sections at five different positions along the AP axis of the head of whole mount stained embryos were analyzed (indicated in Fig. 27A). The sections are shown in Fig. 27A-C and brain structures of high expression are summarized in the table in Fig. 27. Co-localization of all three *midkine* transcripts is evident, especially at ventricle borders and in the dorsal myelencephalon. Expression differences were observed for *mdkb* expression dorsal to the heart (pharyngeal pouch; arrow in Fig. 27B) or expression of *mdka* in the pectoral fin buds (Fig. 27A5). Remarkably, expression of both genes in the eye is clearly divergent. Expression of *mdka* is restricted to the nuclear layer, while *mdkb* expression is found throughout all layers of the eye but prominently in the plexiform layer (Fig. 27A2 and 27B2). Interestingly, expression of *ptn* at this later stage is very strong compared to earlier stages. Its expression is found in ventral CNS structures like the floor plate and the ventral tegmentum/tubercle (arrow in Fig. 27C). In summary, the results show that expression of all three *midkine* genes is highly dynamic during CNS development in zebrafish. Expression of all three genes is often co-localized, yet individual differences of tissue specific expression can be detected. This observation allows speculation about possible redundant functions of these factors during brain development in tissues of overlapping expression. To test this further, functional studies utilizing RNA overexpression or single and combined MO knockdowns were conducted.

4.5.2. Overexpression of *midkine* genes affects different aspects of brain patterning

To test the effect of ectopic expression of single *midkine* genes on brain patterning, 150 pg of each RNA was injected individually into 1-cell stage embryos. All injected embryos displayed similar phenotypes with shortened body axis and head malformations after 24hpf or 72hpf (Fig. 28). In a large number of embryos, this resulted in a cyclopic defect. Brain landmark structures like the MHB were detectable in these embryos, but ventricles were often missing. At 72hpf, cyclopia and brain defects were very obvious, while jaw development and eye differentiation seemed to be normal in all embryos. Secondary developmental defects like tail curling and bigger cardiac sacs were observed in all injected embryos.

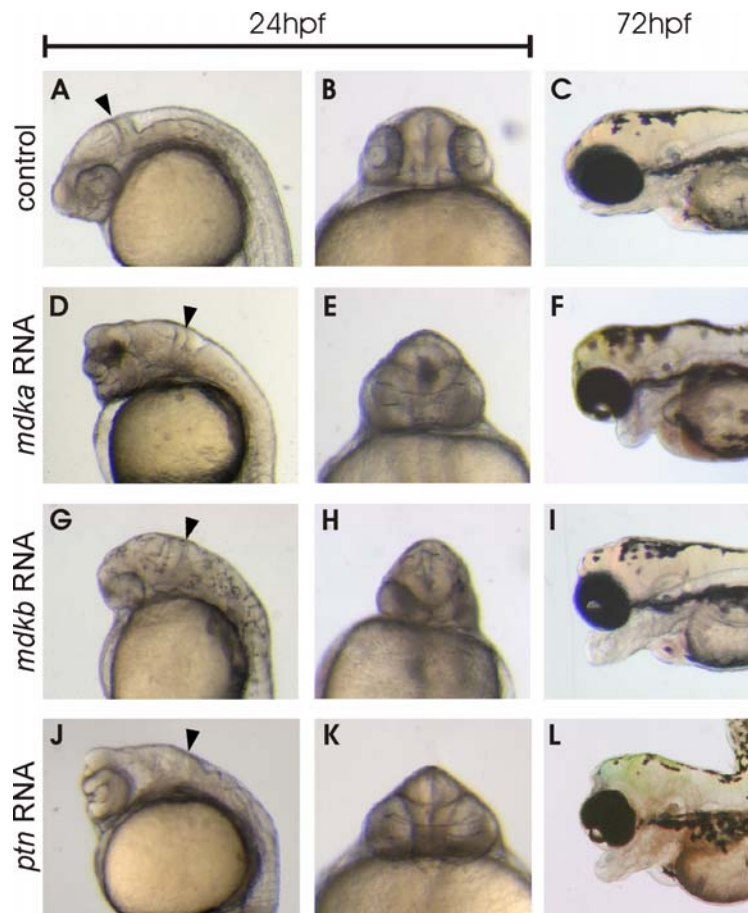


Fig. 28: Phenotypic effects of *midkine* RNA injection.

A-C uninjected wildtype embryos. D-F *mdka* RNA, G-I *mdkb* RNA, J-L *ptn* RNA injected embryos (150 pg RNA each) at 24hpf (row 1 are lateral views, row 2 are frontal views on the eye region) and 72hpf (row 3) show similar phenotypic effects. Arrowheads mark the MHB position.

To investigate the underlying changes in brain patterning in more detail and at the molecular level, in situ hybridization on embryos injected with 100 pg RNA for each gene, respectively, was performed. The expression of telencephalic (*emx3*; Morita et al., 1995), MHB (*eng2*; Fjose et al., 1992) and rhombencephalic (*egr2b*; Oxtoby and Jowett, 1993) markers in 12-somite stage embryos (15hpf) were visualized. Expression of all marker genes was present in the RNA injected embryos (Fig. 28E; *mdka*: n=17; *mdkb*: n=17; *ptn*: n=45; Fig 22, row1), but all embryos displayed a shortening of the AP axis (Winkler and Moon, 2001; Winkler et al., 2003). Remarkably, *mdka* RNA injected embryos showed an enlarged ventral outgrowth at the forebrain level in four dissected embryos, which was only visible after dissection of embryos from the yolk sack (arrow in Fig. 28E). *mdkb* RNA injection led to strong reduction of *emx3* expression in the telencephalon (58%; arrow in Fig. 22I), as previously described (Winkler and Moon, 2001). Overexpression of *ptn* resulted in ventral fusion of the *egr2b* expression domains in 31% of the embryos (arrows in Fig. 28M).

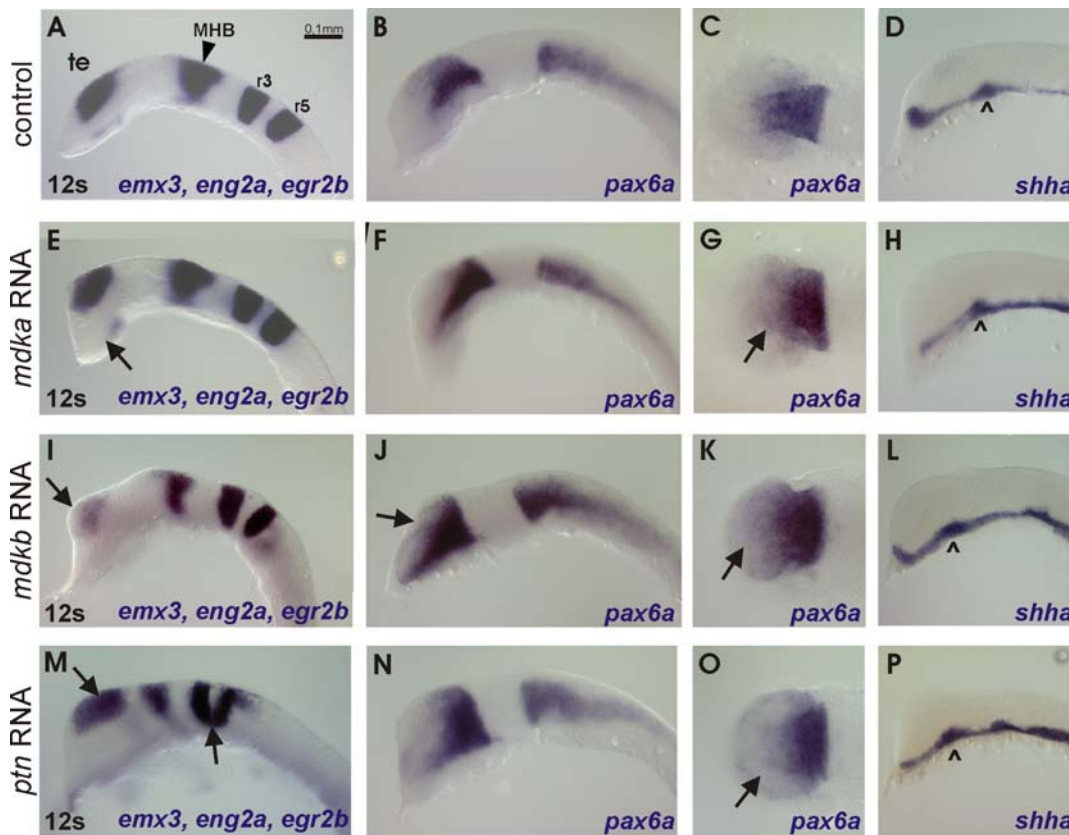


Fig. 29: Different effects of RNA injections on gene expression patterns in the head.

A-D uninjected wildtype embryos, **E-H** *mdka* RNA, **I-L** *mdkb* RNA, **M-P** *ptn* RNA injected embryos (100 pg RNA each) at the 12-somite stage. **A,E,I,M** are lateral views showing expression of *emx3* in the telencephalon, *eng2a* in the MHB and *egr2b* in r3 and r5. **B,F,J,N** are lateral views, **C,G,K,O** are dorsal views of the eye field with *pax6a* expression. **D,H,L,P** are lateral views of *shha* expression in the notochord. Arrowheads mark the ZLI position. Arrows mark expression changes.

One very prominent feature in all analyzed life embryos was eye fusion after RNA injection. To look at this defect in more detail, the expression of *pax6a* was investigated, an essential factor for eye development which is expressed in the forebrain, the posterior eye fields and the hindbrain (Nornes et al., 1998). Embryos injected with *mdka*, *mdkb* or *ptn* RNA displayed shortening of the forebrain along the AP axis (*mdka*: 100% n=9; *mdkb*: 100% n=22; *ptn*: 89% n=37; Fig. 29 A,E,I,M). Some injected embryos completely missed the telencephalic region and expressed *pax6a* in anterior regions (*mdkb*: 50%, arrow Fig. 29J; *ptn*: 19%). In many cases, the forebrain shortening resulted in an expanded expression of *pax6a* in the ventral diencephalon, sometimes reaching to the anterior embryo border (Fig. 29F,J,N). This effect is also visible in dorsal views of the eye fields of injected embryos (Fig. 29G,K,O). Furthermore, these dorsal views show that distinct eye fields are not properly formed. This suggests that the observed cyclopic effect is due to impaired anterior movement of diencephalic cells, which subsequently results in improper division of the eye fields. Further

possible reasons for the observed effect might be the loss of forebrain parts or missing signals from the underlying prechordal plate.

To control correct formation of the prechordal plate, *shha* expression in RNA injected embryos was analysed. The expression of *shha* in all injected embryos looked normal, except for slightly shorter distances between the anterior embryonic border and the ZLI and an overall shortened axis (*mdka*: 97% shortened embryos, but with normal *shha* expression, n=35; *mdkb*: 85% shortened embryos but *shha* expression normal, n=20; *ptn*: 96% shortened embryo but *shha* expression normal, n=64; Fig. 29D,H,L,P). In summary, these results imply that overexpression of *midkine* genes have individually different effects on brain patterning, as for example gain of *Mdkb* function reduces the telencephalon and *Ptn* overexpression reduces r4 size. Nevertheless, all factors share some common activities on forebrain development and eye field formation.

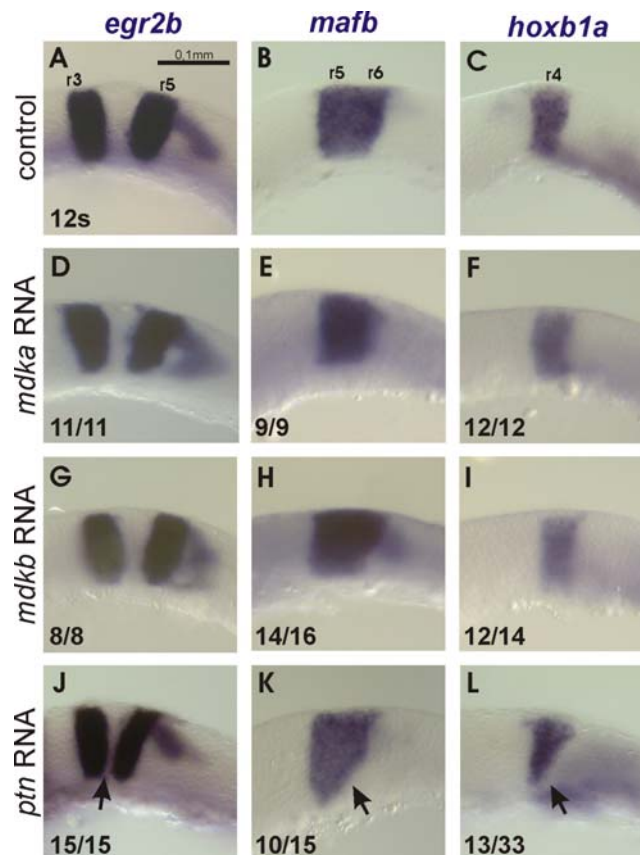


Fig. 30: Injection of *ptn* RNA alters rhombomere size.

A-C uninjected control embryos, D-F *mdka* RNA, G-I *mdkb* RNA, J-L *ptn* RNA injected embryos (100 pg RNA each) at the 12-somite stage. All pictures are lateral views showing expression of *egr2b* in r3 and r5 (A,D,G,J), *mafb* in r5 and r6 (B,E,H,K) and *hoxb1a* in r4 (C,F,I,L) Arrows mark areas with altered expression. Numbers indicate embryos with respective phenotype.

To look in more detail at alterations in the rhombencephalon, the expressions of *egr2b* in r3 and r5, *mafb* (formerly known as *valentino*) in r5 and r6 and *hoxb1a* in r4 in RNA injected embryos were determined (Fig. 30). Overexpression of *mdka* and *mdkb* had little influence on the establishment of their correct expression domains (75 pg RNA; *mdka*: 100% overall normal rhombomere shape, n=36, Fig. 30D-F; *mdkb*: 89% normal, n=38; Fig. 30G-I). In contrast to this, gain of Ptn function led to a ventral reduction of r4 and r6 tissues in many of the embryos, while r5 and r3 were not changed in size (75 pg RNA; overall changes in rhombomere shape: 49%, n=78; Fig. 30J-L). These overexpression data open the possibility that *ptn* plays a role in formation of r4, the hindbrain organizer.

4.5.3. Double and triple knockdown of Midkine factors: Design and activity of *mdka* and *ptn* splice Morpholinos

In addition to gain of function experiments, gene knockdown of *mdka*, *mdkb* and *ptn* were performed to reveal functions of each factor during brain patterning. For this purpose, MO microinjections with subsequent in situ hybridization were conducted.

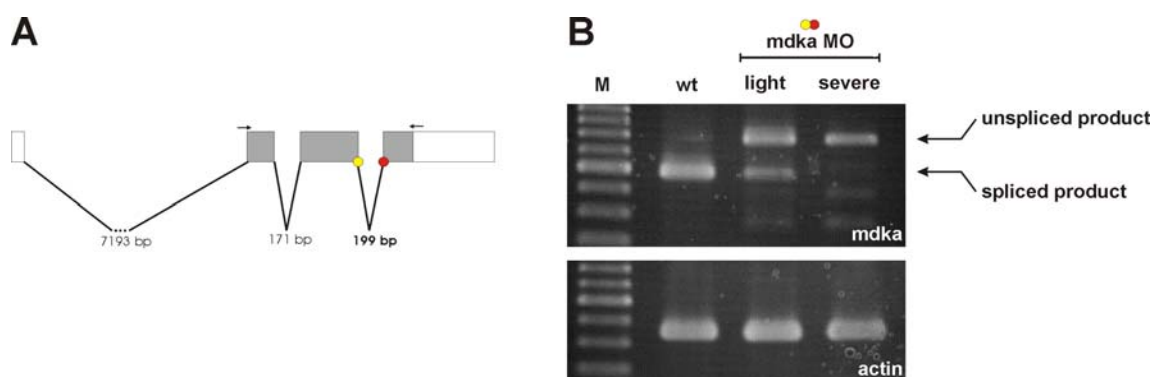


Fig. 31: Design and activity of *mdka* splice MOs.

A Organization of the *mdka* pre-mRNA with indicated MO binding sites (red and yellow spots), intron sizes and regions of primer binding. **B** RT-PCR analysis of *mdka* transcription in uninjected embryos (lane 2), embryos injected with *mdka* MOs showing light phenotypic effects (lane 3) or severe phenotypic effects (lane 4). Lane M represents a 100bp DNA size ladder. Figure B was kindly provided by M. Schäfer.

First, *mdka* splice MOs directed against the splice acceptor and the splice donor site of intron 3 of the pre-mRNA were designed (Fig. 31A). Injection of both MOs resulted in stabilization of a 199 bp intron in the pre-mRNA and therefore likely abolished *Mdka* function. The intron stabilization could be detected by RT-PCR with *mdka* specific primers in MO injected embryos (Fig. 31B; used primers mkESTup and mk3-2). The abundance of unspliced products could be correlated with the severeness of the induced phenotypes. A mild phenotype in the embryos was accompanied with the appearance of a correctly spliced band

(Fig. 31B). A nearly complete block of correct *mdka* splicing resulted in severe phenotypic effects.

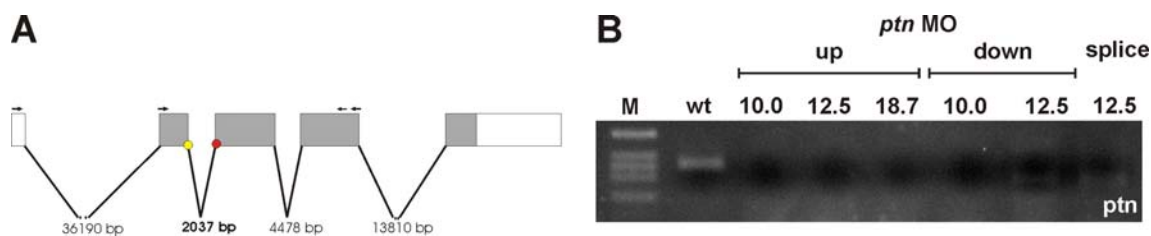


Fig. 32: Design and function of *ptn* splice MO.

A Organization of the *ptn* pre-mRNA with indicated MO binding sites (red and yellow spots), intron sizes and regions of primer binding. **B** Nested RT-PCR analysis of *ptn* transcription in uninjected embryos (lane 2) and embryos injected with different concentrations of the individual *ptn* MOs or a combination of both splice MOs (lanes 3-8; numbers indicate overall MO concentration in mg/ml; for splice MO injection *ptn* up and *ptn* down MO were mixed at a 1:1 ratio and injected, resulting in a single MO concentration of 6.25 mg/ml). Lane M represents a 1kb DNA size ladder.

Second, splice MOs directed against the zebrafish *ptn* gene were designed (Fig. 32A). The MOs were directed against the 3' border of exon 2 and the 5' border of exon 3 of the *ptn* pre-mRNA and therefore should lead to stabilization of intron 2 with a size of 4,475 bp. Incorrect splicing could be shown by nested RT-PCR utilizing two pairs of primers spanning the Mo binding sites at the exon border (used primers for first amplification *tfptnf101* and *tfptnf102*; used primers for second amplification *ptnMO01* and *ptnMO02*). The correctly spliced *ptn* band is lost in all *ptn* MO injected embryos, indicating blocking of correct *ptn* pre-mRNA splicing and subsequent transcript decay (Fig. 32B). These experiments show the efficiency of the designed *mdka* and *ptn* splice MOs.

4.5.4. Single knockdown of *midkine* genes reveals non-overlapping functions during brain patterning

For investigation of the brain patterning after single knockdown of *mdk* or *ptn* functions, a combination of telencephalic (*emx3*), MHB (*eng2*) and rhombencephalic (*egr2b*) marker genes was utilized in expression analysis of MO injected embryos at the 12s stage.

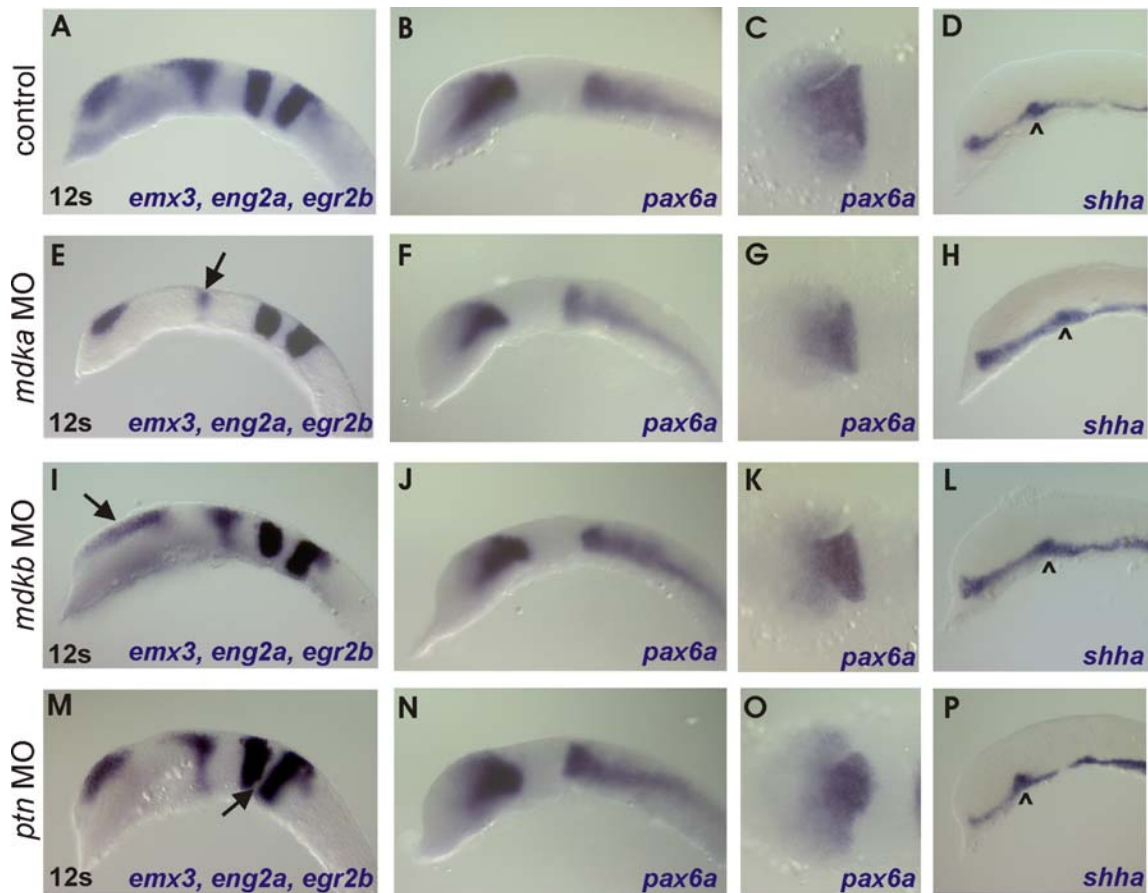


Fig. 33: Diverse effects of *mdka*, *mdkb* and *ptn* knockdown on gene expression in the developing brain.

A-D non-injected wildtype embryos, E-H *mdka* MO, I-L *mdkb* MO, M-P *ptn* MO injected embryos (each 6.25 μ g) at the 12-somite stage. A,E,I,M are lateral views showing expression of *emx3* in the telencephalon, *eng2a* in the MHB and *egr2b* in r3 and r5. B,F,J,N are lateral views, C,G,K,O are dorsal eye field views of *pax6a* expression. D,H,L,P are lateral views of *shha* expression in the notochord. Arrowheads mark the ZLI position; arrows mark expression changes in the MHB and telencephalon, respectively.

Reduction of *Mdka* activity resulted in decrease of *eng2* expression at the MHB in 54% of the analyzed embryos, while fore- and hindbrain structures were not affected (n=24; arrow in Fig. 33E). *mdkb* morphant embryos showed expanded expression of *emx3*, indicative for an enlargement of the telencephalon in 67% of all embryos, but no changes in mid- or hindbrain structures (n=24; Fig. 33I). This is consistent with earlier observations, when injection of a dominant negative variant of *mdkb* also resulted in an elongated expression domain of *emx3* (Winkler and Moon, 2001). However, in contrast to the dominant negative experiments, no change in *egr2b* expression was detectable in *mdkb* morphants. Knockdown of *ptn* expression shortened the AP axis of injected embryos and resulted in a compression of the expression domains and reduction of r4 (n=17; Fig. 33M).

In all morphants, *pax6a* expression was present and showed no significantly altered pattern when compared to the controls (100%: *mdka* n=43; *mdkb* n=26; *ptn* n=61; Fig. 33F,J,N). Only

a slight elongation of the midbrain domain was observed in *mdkb* morphants and an overall compression of expression in the *ptn* morphants. The division of the eye field was normal in all morphants, as analyzed in live embryos and by *pax6a* expression. Development of ventral signaling structures like the notochord and the ZLI marked by *shha* expression were also not influenced in the morphants (*mdka*: 94% normal, n=36; *mdkb*: 96% normal, n=26; *ptn*: 100% normal, n=23; Fig. 33H,L,P). These observations show that knockdown of *mdka*, *mdkb* and *ptn* lead to gene specific alterations in brain patterning. First, *mdka* seems to influence MHB establishment. Second, *mdkb* function influences correct telencephalon formation. Last, r4 size is influenced by *ptn* action.

4.5.5. Combined knockdown reveals an exclusive role of *mdka* during MHB establishment

To detect possible redundant activities of *mdka*, *mdkb* and *ptn* during MHB development, each splice MO individually, as well as all possible combinations of the MOs were injected into 1 cell-stage embryos and subsequently determined expression of *eng2* in the MHB (see Table 3 for summary of all MO injections).

Table 3: Effects of individual and combined *midkine* knockdown on MHB formation.

Loss of MHB establishment was observed in embryos by *eng2* in situ hybridization at the 12-somite stage after injection of MO, triple = *mdka/mdkb/ptn* MO combination; u.d. = undiluted.

MO combination	overall MO concentration	single MO concentration	injected embryos [n]	loss of <i>eng2</i> expression
<i>mdka</i>	12.5 µg/µl	12.5 µg/µl	17	94.12%
<i>mdkb</i>	12.5 µg/µl	12.5 µg/µl	20	20.00%
<i>ptn</i>	12.5 µg/µl	12.5 µg/µl	18	50.00%
<i>mdka/mdkb</i>	25.0 µg/µl	12.5 µg/µl	15	100.00%
<i>mdka/ptn</i>	25.0 µg/µl	12.5 µg/µl	17	82.35%
<i>mdkb/ptn</i>	25.0 µg/µl	12.5 µg/µl	28	10.71%
triple u.d.*	25.0 µg/µl	8.3 µg/µl	41	78.05%

In situ hybridizations showed that knockdown of *mdka* or a combined knockdown of *mdka/ptn* or *mdka/mdkb* each resulted in reduced *eng2* expression in more than 80% of the analyzed embryos (Fig. 34C,Di,J,K,L). In contrast to this, injection of single *mdkb* and *ptn* MO or the *mdkb* x *ptn* combination resulted in significantly less embryos with reduced *eng2* expression (Fig. 34E-H,M,N and Table 3; Fig. 27M and N show disturbed convergence but

normal levels of *eng2* expression). Simultaneous knockdown of all three factors resulted in a high number of embryos with reduced *eng2* expression (78%; Fig. 34O,F), comparable to the situation in *mdka* MO injected embryos.

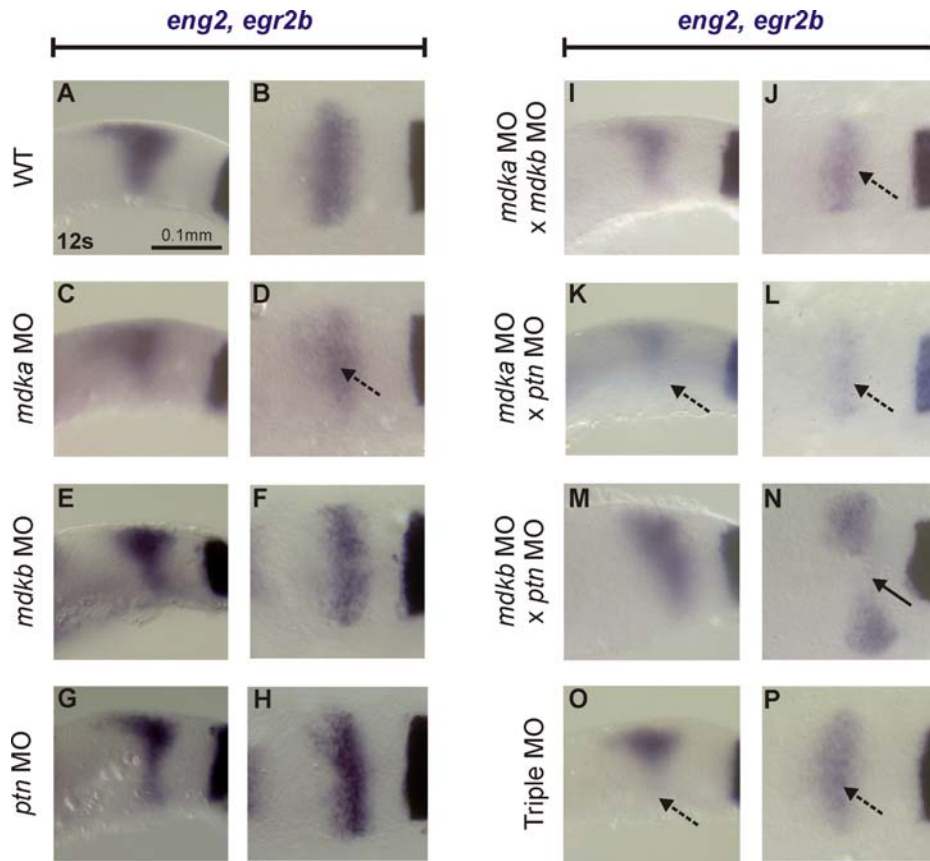


Fig. 34: Combined effects of *midkine* genes on MHB establishment.

A-X Expression of *eng2* (combined with *egr2b*; row 1 and 4 lateral views; row 2 and 5 dorsal views) in wildtype (A-C), single morphants (D-F *mdka* MO; G-I *mdkb* MO; J-L *ptn* MO), as well as double morphants (M-O *mdka/mdkb* MO; P-R *mdka/ptn* MO; S-U *mdkb/ptn* MO) and triple morphants (V-X).

These knockdown experiments thus revealed an exclusive role for *mdka* during the establishment of the MHB organizer. This *mdka* function seems to be independent from that of *mdkb* or *ptn*, because a combined knockdown did not result in any stronger repression of the remaining *eng2* expression or in an increased number of affected embryos.

4.5.6. Knockdown of *ptn* function results in hindbrain patterning defects

In addition to MHB development, also the establishment of the rhombencephalic organizer *r4* in single, double and triple morphants was investigated. To look at hindbrain patterning defects caused by reduced levels of *midkine* activities, I injected single MOs and

combinations of splice MOs and subsequently performed in situ hybridization (Fig. 35 and table 4).

Table 4: Effects of *mdk/ptn* knockdown on hindbrain patterning.

Loss of rhombencephalic integrity observed by *egr2b* and *maf3* in situ hybridization in embryos at the 12-somite stage after injection of MO; triple = *mdka/mdkb/ptn* MO combination; u.d. = undiluted.

MO combination	overall MO concentration	single MO concentration	injected embryos [n]	compressed r4	injected embryos [n]	reduced <i>maf3</i> expression
<i>mdka</i>	12.5 µg/µl	12.5 µg/µl	17	0.00%	11	0.00%
<i>mdkb</i>	12.5 µg/µl	12.5 µg/µl	20	25.00%	29	13.79%
<i>ptn</i>	12.5 µg/µl	12.5 µg/µl	18	66.67%	16	6.25%
<i>mdka/mdkb</i>	25.0 µg/µl	12.5 µg/µl	15	0.00%	7	0.00%
<i>mdka/ptn</i>	25.0 µg/µl	12.5 µg/µl	16	87.50%	7	28.57%
<i>mdkb/ptn</i>	25.0 µg/µl	12.5 µg/µl	28	89.29%	9	22.22%
triple u.d.*	25.0 µg/µl	8.3 µg/µl	41	78.05%	10	10.00%

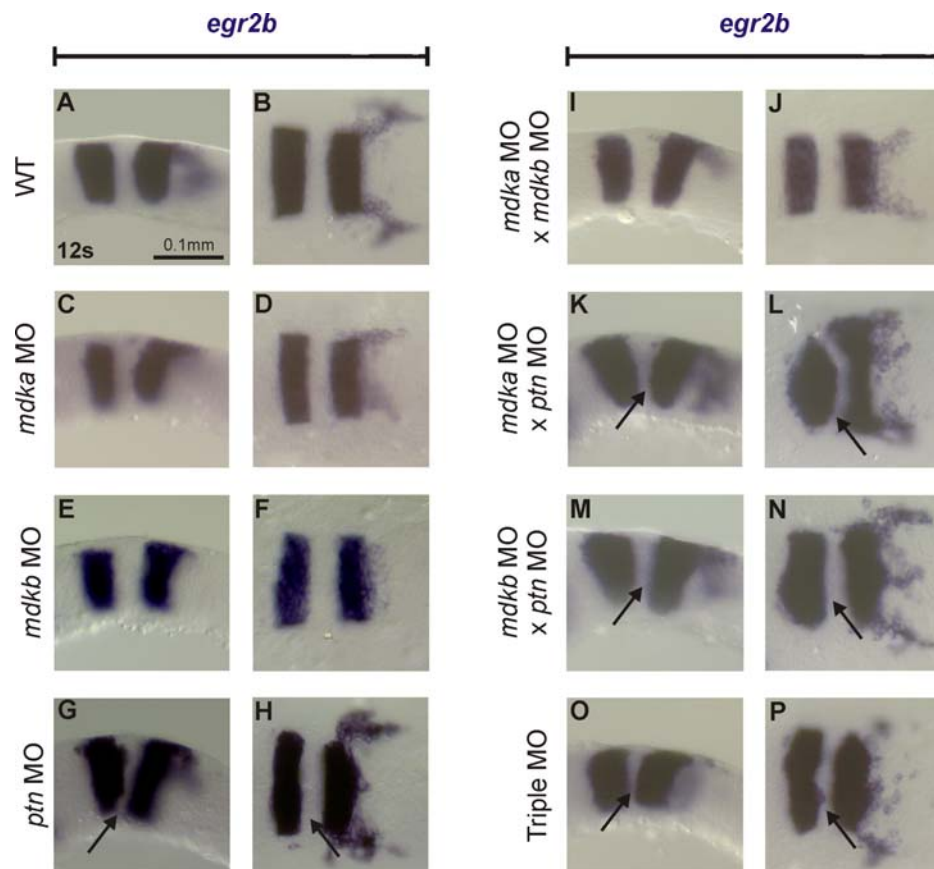


Fig. 35: Effects on hindbrain development after single and combined midkine knockdown.

A-P Expression of *egr2b* (row 1 and 3 lateral views; row 2 and 4 dorsal views) in wildtype (A and B), single gene morphants (C and D *mdka* MO; E and F *mdkb* MO; G and H *ptn* MO) and combined gene morphants (I and J *mdka/mdkb* MO; K and L *mdka/ptn* MO; M and N *mdkb/ptn* MO, O and P triple MO).

As markers, two prominent hindbrain patterning genes were used, *egr2b* and *mafb* (Oxtoby and Jowett, 1993; Moens et al., 1996). *egr2b* is expressed in r3 and r5, while *mafb* expression is found in r5 and r6. The size of r4 was reduced in 66.66% of *ptn* MOs injected embryos (Fig. 35G,H). Also, injection of a combination of *mdka/ptn* MOs, *mdkb/ptn* MOs or the triple knockdown of *mdka/mdkb/ptn* resulted in over 75% of embryos with a smaller r4 (Fig. 35K-P). As the extents of *egr2b* expression in r3 and r5 were not significantly affected, this suggests a defect specifically in r4. Accordingly, irregular expression of *mafb* in r5 and r6 was only detected in a small fraction of the analyzed embryos (lower than 30%; Table 4). No obvious expression change of *egr2b* was found in *mdka*, *mdkb* or *mdka/mdkb* MO injected embryos (Fig. 35C-F, I,J). These data suggest that loss of *ptn* function results in defects during the establishment of the hindbrain organizer r4. Minor combinatorial effects of *ptn* with *mdka* or *mdkb* on r4 size are suggested by the increased numbers of double morphant embryos with reduced r4.

In conclusion, our gain and loss of function studies of *midkine* genes during head development indicate that all three genes have different roles during formation of distinct brain compartments. *mdka* functions during MHB establishment, *mdkb* regulates telencephalon formation, and *ptn* function is required for specification of r4, the hindbrain organizer. Cooperative effects of these genes during brain development were only observed during r4 formation, as r4 defects were pronounced in double and triple morphants than in *ptn* single morphants.

4.6. Somitogenesis is regulated by *ptn*

4.6.1. Combined knockdown of *mdka*, *mdkb* and *ptn* results in somite fusion

In the *mdka*, *mdkb* and *ptn* triple morphants, surprisingly a strong effect on somite formation was observed (Fig. 36) in addition to the brain patterning defects. 84.7% of the triple morphants lacked most or all somite boundaries along the AP axis (n=92; Fig. 36B right arrow). The paraxial mesoderm seemed to be present in these embryos, but it completely lacked its correct segmentation. In contrast, the formation of midline structures, like the notochord and the neural tube, was not disturbed. Non-transparent cell aggregates in these embryos indicated necrosis and was often observed but not further investigated (Fig. 36B, left arrow).

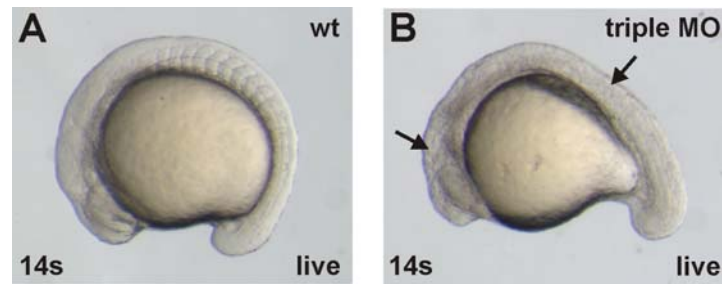


Fig. 36: Loss of somites and impaired brain development in *midkine* triple morphants.

A Lateral view of a living zebrafish embryo at the 14 somite stage. **B** Triple *midkine* morphant embryos at the same stage with impaired brain development, loss of tissue transparency (left arrow) and disturbed somite development (right arrow).

4.6.2. Expression of *midkine* genes during somitogenesis in the paraxial and presomitic mesoderm (PSM)

To test whether the spatial expression pattern of *midkine* genes is consistent with a putative role during somitogenesis, the expression of all three *midkine* genes in the tail bud and the paraxial mesoderm of embryos at the 14-somite stage (16hpf) were determined.

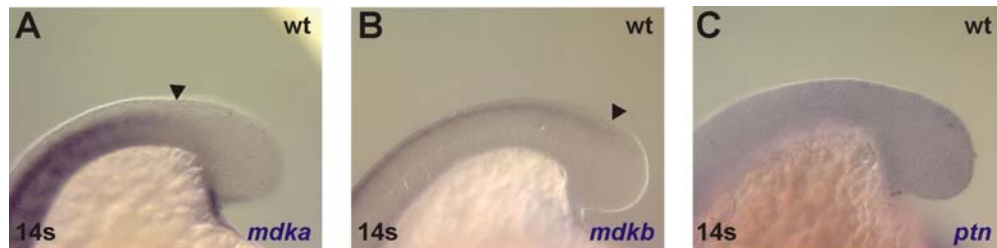


Fig. 37: Expression of zebrafish *midkine* genes in trunk and tail bud.

A-C Lateral views with focus on the paraxial mesoderm and the tail bud of 14-somite stage embryos. **A** *mdka* expression in the somites, the neural tube and in the ventral finfold ectoderm. **B** Expression of *mdkb* in the dorsal neural tube and in neural tube precursor cells of the tail bud. **C** Expression of *ptn* is ubiquitous but very weak in the tail bud. Arrowheads demarcate the posterior edge of expression.

At this stage, *mdka* is expressed in the somites, the neural tube and in the ventral finfold ectoderm (Fig. 37A). From earlier studies, it is known that overexpression of *mdka* inhibits correct somite formation (Winkler and Moon, 2001). Nevertheless, *mdka* expression is not found in the tail bud itself, but in the segmented paraxial mesoderm (Fig. 37A). *mdka* is expressed in a wave like fashion sweeping from anterior to posterior in the trunk, declining at the level of somite budding (Schafer et al., 2005). *mdkb* transcripts are detected in the dorsal neural tube and in dorsal cells of the tail bud but not in its mesodermal compartment (Fig. 37B). The expression of *ptn* is generally weak and found ubiquitously at low levels in the tail

bud (Fig. 37C). In conclusion, *mdka* and *ptn* are expressed in the somites or the PSM, respectively and are therefore possible regulators of somite formation.

4.6.3. Knockdown of *ptn* inhibits somite formation

To analyze whether the loss of somite boundaries is a particular feature of triple morphants, visual inspection of living embryos injected with one MO or a combination of MOs at 14 to 16 h after injection (12 to 14-somite stage) was conducted (Table 5). Changes in somite formation were never observed in wildtype control embryos, and in embryos injected with *mdka*, *mdkb* or combined *mdka/mdkb* MO. In contrast to this, high numbers of embryos lacking correct somite formation were found after injection with the *ptn* MO or in any MO combination including the *ptn* MO. Thus, reduction of Ptn function seems to result in loss of somite boundaries.

Table 5: Effects of *midkine* knockdown on somite formation.

Phenotypic observation for loss of somite boundaries in living embryos was made 14 to 16hpf; triple = *mdka/mdkb/ptn* MO combination; u.d. = undiluted.

MO combination	overall MO concentration	single MO concentraion	injected embryos [n]	embryos lacking somites [%]
<i>mdka</i>	5 mg/ml	5 mg/ml	86	0.00
<i>mdkb</i>	5 mg/ml	5 mg/ml	151	0.00
<i>ptn</i>	5 mg/ml	5 mg/ml	107	48.60
<i>mdka/mdkb</i>	10 mg/ml	5 mg/ml	107	0.00
<i>mdka/ptn</i>	10 mg/ml	5 mg/ml	73	100.00
<i>mdkb/ptn</i>	10 mg/ml	5 mg/ml	104	92.31
triple	15 mg/ml	5 mg/ml	92	84.78
triple u.d.	25 mg/ml	8.3 mg/ml	152	92.11

Somitogenesis is driven by a complex molecular mechanism and can be subdivided into three distinct steps: prepatterning of somite precursors in the tail bud, AP polarity establishment and somite epithelialization (Pourquie, 2001). To classify the somite defects observed after *mdk* and *ptn* knockdown according to these steps, I determined the expression of indicative marker genes in the different morphants (single MO injection concentration: 12.5 ng/nl; triple MO concentration each MO 5.0 ng/nl, overall MO concentration 15.0 ng/nl). *myod* expression was used to determine segment boundary formation and the shape of formed somites. Additionally, *myod* is also expressed in adaxial cells and therefore a good marker for correct convergence movements. To control for tail bud formation and convergence, expression of *ntl*

(Schulte-Merker et al., 1992) in the notochord and tail bud cells was analyzed in the morphants. The regular oscillations of the somitogenesis clock and correct pre patterning of PSM cells were analyzed by determining cycling expression of *her1* in the PSM (Muller et al., 1996). In the same embryos, expression of *foxd3* in *ncc* and anterior somites served as control for regular convergence and formation of the tail bud (Odenthal and Nusslein-Volhard, 1998). Finally, *mespb* expression in the somitomeres demarcates the anterior identity of newly forming and future somites at the anterior PSM border (S-1, S0 and S1 somite; Sawada et al., 2000).

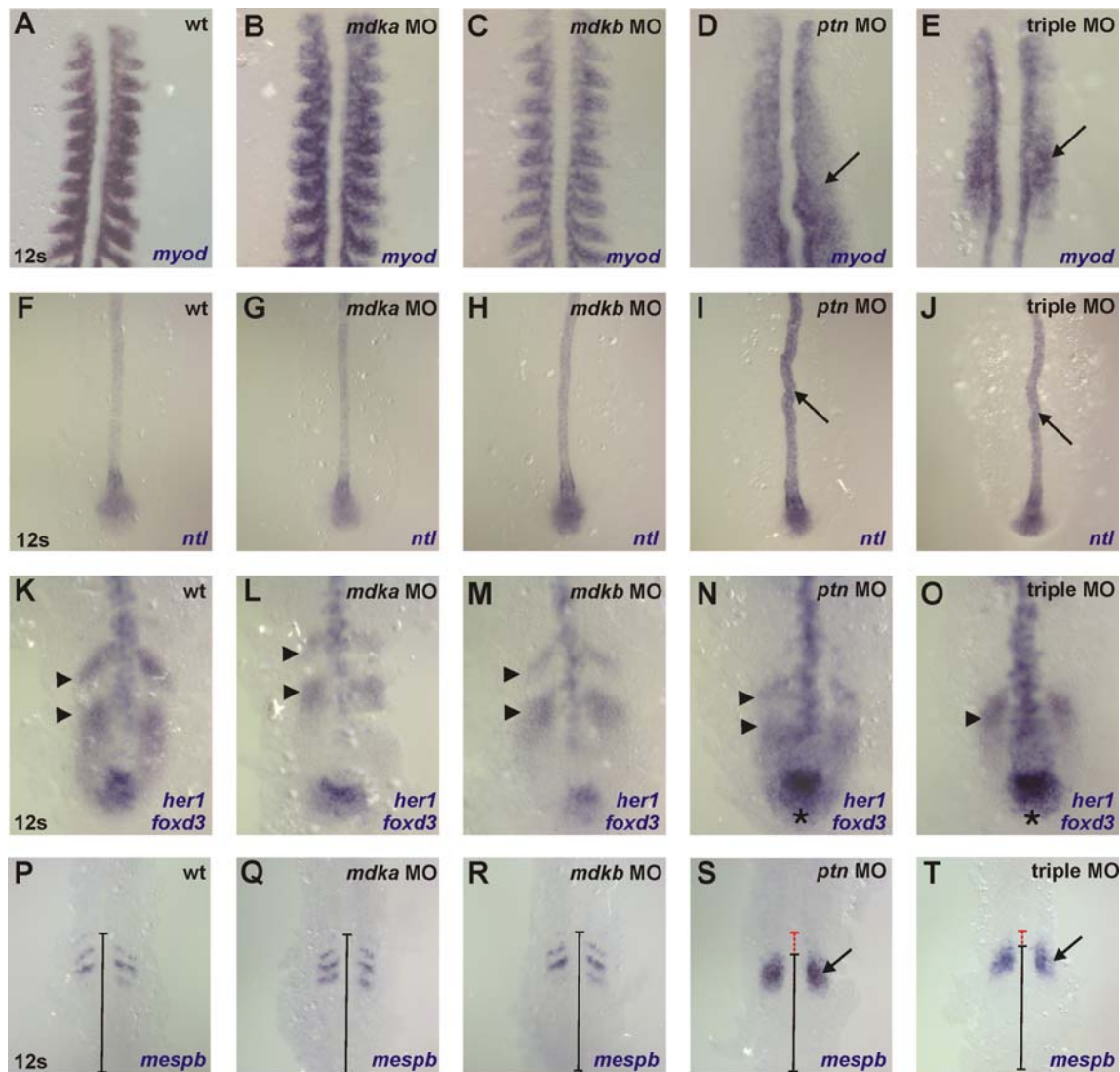


Fig. 38: Knockdown of *ptn* affects somite boundary formation and the somitogenesis clock.

A-E Dorsal views of regular *myod* expression in the somites and adaxial cells of wildtype (A), *mdka* (B) and *mdkb* (C) morphants. Loss of segmentation, fusion of somites (arrows in D and E) and bending of the midline can be observed in *ptn* (D) and triple morphants (E). **F-J** Development of notochord and tail bud cells marked by *ntl* expression is not disturbed in injected embryos, but the midline shows bending in *ptn* and triple morphants (arrows in D and E). **K-O** Oscillating expression of *her1* is regular in wildtype (K), *mdka* (L) and *mdkb* (M) morphants (arrowheads mark distinct expression

waves). *ptn* (N) and triple morphants (O) show fuzzy and impaired *her1* oscillation in the PSM and an increased number of *foxd3* positive tail bud cells (asterisk in N and O). **P-T** Expression of *mespb* in somitomeres and newly formed somites is normal in wildtype (P), *mdka* (Q) and *mdkb* (R) morphants (bars mark the distance between the posterior end of the tail bud and the latest formed somite expressing *mespb*). In *ptn* (S) and triple morphants (T) expression of *mespb* is not segmented and lacks anterior extension, as indicated by the red bar marking the difference between wildtype and morphant distance between the posterior end of the tail bud and the latest formed somite.

Expression of *myod* was not affected in wildtype, *mdka* and *mdkb* single morphants and thus indicated regular somite formation (*mdka*: n=25; *mdkb*: n=21; Fig. 38A,B,C). Surprisingly, in *ptn* single or *mdka/mdkb/ptn* triple morphants, a fusion of *myod* expression domains was observed in the paraxial mesoderm of the trunk (*ptn* MO: 79% embryos with fused somites, n=24; triple: 86% fused somites, n=7; Fig. 38D,E). This suggested a lack of somite boundaries that was often observed along the complete AP axis, and less frequently in only a restricted number of somites. Adaxial expression of *myod* was present in all MO injected embryos, but often appeared bended in *ptn* and triple morphants. The midline bending effect in the *ptn* and triple morphants was also observed in embryos stained for *ntl* expression (arrows in Fig. 38I,J), while expression of *ntl* in the tail bud was not affected in any case (overall n=73; Fig. 38F- J). Noteworthy, overall cell density in the notochord of *ptn* and triple morphants seemed to be increased (data not shown).

Interestingly, *ptn* morphants or triple morphant embryos showed impaired cycling of *her1* expression in the PSM, while regular cycling of *her1* was observed in all embryos injected with *mdka* or *mdkb* MOs (*mdka*: n=12; *mdkb*: n=48, *ptn*: 72% altered *her1* expression, n=25; triple 53% altered *her1* expression, n=19; Fig. 38K-O). In the *ptn* and triple morphants, oscillatory expression of *her1* is correctly initiated in the posterior PSM but not maintained anteriorly. Thus, these embryos lack correct *her1* stripe formation at the anterior end of the PSM (arrowheads in Fig. 38N and O mark the last stripe of *her1* expression). This indicates an incorrect output of the somite clockwork. In all morphants, expression of *foxd3* is present in ncc and dorsal tail bud cells, but in *ptn* MO and triple MO injected embryos the *foxd3* positive cell population in the tail bud is enlarged (asterisk in Fig. 38N,O). Somite fusion, as evident by *foxd3* expression in the anterior trunk somites, is detected in all embryos that lack correct *her1* expression in the tail bud (data not shown).

In wildtype embryos, as well as *mdka* and *mdkb* morphants, *mespb* expression in the newly forming somites is normal and correctly separated (*mdka*: n=12; *mdkb*: n=16; Fig. 38P,Q,R). In *ptn* and triple morphants, the *mespb* stripes fuse to one large domain (*ptn*: 70% with fused stripes, n=10; triple: 66%, n=9; Fig. 38S,T). The position of the fused stripes in *ptn* and triple morphants is slightly shifted to posterior in comparison to the front of somite budding (indicated by red bar in Fig. 38S,T). In conclusion, this experiment shows that the somite

defects observed in triple morphants were likely caused by the knockdown of *ptn*. This knockdown apparently interfered with the somitogenesis clock in the tailbud and resulted in a delayed propagation of the oscillatory wave of *her1* gene expression. Consequently, this led to an impaired pre patterning of tailbud cells and the lack of somite boundary formation.

5. Discussion

Midkine genes in vertebrates encode small secreted heparin-binding growth factors with neurotrophic activities. The *midkine* gene family consists of only two members, *midkine* (*mdk*) and *pleiotrophin* (*ptn*; Muramatsu, 2002). In zebrafish, the *midkine* gene locus has been duplicated during an ancient fish specific genome duplication which resulted in two functional genes, *mdka* and *mdkb* (Winkler et al., 2003). These two co-orthologues show functional divergence and exhibit distinct *in vivo* activities during zebrafish neuronal development. While *Mdka* function recently was shown to be essential for floor plate induction in zebrafish (Schafer et al., 2005), previous studies had postulated an influence of *Mdkb* on *ncc* and early neurogenesis (Winkler and Moon, 2001). However, closer investigation of the steps of neural crest cell (*ncc*) induction and maintenance were missing. In contrast to *mdk*, the *ptn* gene is not duplicated in zebrafish (Winkler et al., 2003). Thus far, its expression during zebrafish development was only rudimentarily described and besides its ability to induce axonal outgrowth *in vivo* (Chang et al., 2004) little is known about its functions. Furthermore, in depth studies of the interactions of all three zebrafish genes *in vivo* are completely lacking.

This thesis provides a detailed description of *mdkb* expression and function during *ncc* and sensory neuron induction. In addition, determination and comparison of the expression of *mdka*, *mdkb* and *ptn* during early phases of brain development was performed. Furthermore, exclusive and overlapping roles of *midkine* genes during brain patterning and somitogenesis were elucidated.

5.1. Functions of *Mdkb* in neural crest and sensory neuron induction

5.1.1. **Spatiotemporal expression of *mdkb* is consistent with a role during *ncc* and sensory neuron induction at the neural plate border**

To understand the spatiotemporal relation between *ncc*, respectively sensory neuron induction and *mdkb* expression, *in situ* hybridizations with known *ncc* and primary neuron markers were performed. Expression of *mdkb* was detected in close proximity to zones of earliest steps of *ncc* induction, marked by anterior *pax3* expression during gastrulation at the neural plate border (Lewis et al., 2004). *Pax3* (in a cooperative function with *Zic1* and *Msx1*) is one prominent early inducer of *ncc* during *Xenopus* gastrulation (Monsoro-Burq et al., 2005; Sato et al., 2005). Like in *Xenopus*, *pax3* expression in zebrafish precedes expression of *ncc*

differentiation genes like *foxd3*, *sox10*, *sox9b* and *snail2* (Thisse et al., 1995; Odenthal and Nusslein-Volhard, 1998; Seo et al., 1998; Dutton et al., 2001; Li et al., 2002). Expression of these ncc differentiation genes is initiated two hours later in two domains at the neural plate border overlapping with *mdkb* expression (Fig. 8). At the same time, several neuronal cell populations are specified at the neural plate border of zebrafish, e.g. precursors of the dorsal sensory neurons, that will later form Rohon-Beard (RB) neurons and the trigeminal ganglia (Solnica-Krezel, 2002). Induction of these primary neuronal precursors is initiated by expression of the bHLH gene *ngn1* and the LIM homeodomain gene *isll* (Korz et al., 1993; Korzh et al., 1998). At this stage, *mdkb* transcripts can be detected surrounding these earliest sensory neuron precursors near the neural plate border (Fig. 10). Several lines of evidence suggest that Delta-Notch signals are essential to single out neuronal cells out of a common ncc/sensory neuron precursor cell pool (Artinger et al., 1999; Cornell and Eisen, 2000; Filippi et al., 2005), which may also be characterized by *mdkb* expression.

After closure of the neural tube (18hpf), ncc begin to migrate to their target tissue and continue differentiation (Raible and Eisen, 1994; Halloran and Berndt, 2003). At the same time, RB sensory neurons in the dorsal neural tube initiate axon outgrowth. At this later stage of ncc development, *mdkb* expression in the dorsal CNS is found adjacent to these cells and may serve as a secreted growth factor influencing the further development of these cells.

5.1.2. *mdkb* expression is regulated by known ncc-inducing signals, but not by Delta-Notch signaling

Concluding from this spatiotemporal pattern, *mdkb* is expressed at the right time and place to act as a secreted signaling factor during induction of ncc and sensory neurons. Therefore, expression of *mdkb* might therefore also be influenced by the same signals, that induce ncc and sensory neurons. To test this hypothesis, interference with known pathways essential for ncc and sensory neuron development at the neural plate border were performed and the effects on *mdkb* expression were determined.

Cutback of retinoid signaling reduces *mdkb* expression

Members of the *midkine* gene family were originally identified in a screen for retinoic acid (RA) induced genes in murine embryonic carcinoma cells (Muramatsu, 1992). Interestingly, studies in *Xenopus* (Villanueva et al., 2002) and other vertebrates (Aybar and Mayor, 2002) have shown that retinoid signaling is involved in early ncc induction. However, little is known

about the role of RA during ncc development in zebrafish. For example, *neckless* mutants deficient for *raldh2*, the enzyme responsible for conversion of retinal to retinoic acid, show only a mild ncc phenotype with increased levels of apoptosis in the fourth and fifth branchial arches (Begemann et al., 2001). Therefore, investigations were conducted whether RA signaling affects *mdkb* expression. Previous studies have shown that high doses of exogenously applied RA (10^{-6} M RA final concentration in the incubation media) completely repress *mdkb* expression, while lower doses (10^{-8} M RA) enhance endogenous *mdkb* transcription (Winkler and Moon, 2001). This is consistent with the idea that a gradient of endogenous RA signaling defines a regionally restricted pattern of *mdkb* expression in the zebrafish embryo during gastrulation. To further support this, I used the inhibitor of the retinaldehyde dehydrogenase DEAB and showed that *mdkb* expression is strongly reduced in the absence of endogenous RA signaling. The observed residual *mdkb* transcription in dorsal regions can be explained by an incomplete inhibition of endogenous RA signaling under our experimental conditions (Fig. 10). Alternatively, it is also possible that RA signaling is required for maintaining *mdkb* expression, but that other factors are responsible for the induction of *mdkb* transcription. I was able to rule out the possibility that the observed repression of *mdkb* expression is due to a loss of the neural plate, because DEAB treated embryos have normal *tfap2* expression in the non-neural ectoderm, while *mdkb* expression is lost simultaneously (Fig. 11).

Repression of FGF signals ablates *mdkb* expression

FGFs are known to be crucial for ncc formation (Mayor et al., 1997; Monsoro-Burq et al., 2003). In *Xenopus*, FGF8 secreted from the paraxial mesoderm is essential for the induction of ncc markers (Monsoro-Burq et al., 2003). In zebrafish, however, the role of FGF8 during ncc development remains unclear, as the zebrafish *fgf8* mutant *acerebelar* exhibits no apparent ncc phenotype (Reifers et al., 1998). It is possible that other FGFs compensate for the loss of FGF8 function during neural crest induction in these mutants. Further studies for roles of other FGFs during zebrafish ncc induction are missing. Consistent with a postulated role in ncc induction, *mdkb* expression in *acerebelar* is normal, except that it is lost in the cerebellum which is lacking in these mutants (Winkler and Moon, 2001). To investigate whether any other members of the FGF family regulate *mdkb* expression, I used the chemical inhibitor SU5402 to block all FGF signaling (Mohammadi et al., 1997). Inhibition starting from mid-gastrulation stages efficiently repressed *mdkb* expression (Fig. 10). This may be due to direct repression of *mdkb* transcription, but can also be the consequence of incorrect

formation of the neural plate or interference with FGF function during mesoderm development (Griffin and Kimelman, 2003). Loss of the neural plate was indicated by enlarged *tfap2* expression in the non-neural ectoderm of treated embryos (Fig. 11; see also Furthauer et al., 2004). Further experiments using single or combined gene knockdown of different FGFs need to be done to get better insight into the mechanisms at work.

Overexpression of *fgf8* by mRNA injection resulted in an enlarged neural plate in zebrafish (Furthauer et al., 2004). By performing a similar injection experiment, I showed that ectopic Medaka *fgf8* expression expands *mdkb* expression throughout the complete gastrulating embryo, also into non-neural areas (Fig. 10). Taken together, these findings suggest that during gastrulation *mdkb* transcription at the neural plate border is directly induced by FGF signaling at the correct dorso-ventral position. However, at present it is impossible to distinguish whether this postulated FGF/*mdkb* interaction is only indirect, as modulated FGF signaling per se alters the size of the neural plate. Promoter analysis of *mdkb* and specific knockdown of single FGFs will be necessary to finally proof dependence of *mdkb* expression on FGF signaling. Together these studies indicate that *mdkb* expression during gastrulation is regulated by BMP (previously shown by Winkler and Moon (2001), RA and FGF signaling (Fig. 39)).



Fig. 39: *mdkb* expression is regulated by several signaling pathways during gastrulation.

Positive regulation of *mdkb* expression by Wnt signals

FGFs are thought to cooperate with canonical Wnt/ β -catenin signaling during ncc formation (LaBonne and Bronner-Fraser, 1998b; Villanueva et al., 2002). Moreover, Wnts are also involved in later cell fate determination of ncc precursors into either the pigment or neuron/glia lineages (Dorsky et al., 1998; Lewis et al., 2004). By incubating embryos in LiCl which activates the Wnt cascade by inhibition of GSK-3 beta activity (Klein and Melton, 1996) I found that activation of the Wnt pathway dramatically increased *mdkb* expression in neural tissues (Fig. 12). This effect was observed whether embryos were treated during early gastrulation prior to organizer formation or during later gastrulation after organizer formation, indicating a Wnt responsiveness of *mdkb* expression throughout development. LiCl treatment

blocks GSK-3 beta activity, but also other non-Wnt related kinases and therefore broadly influences cell signaling (Cohen and Goedert, 2004). More experiments are needed, like e.g. heat-shock inducible expression of a dominant-negative TCF3 (Lewis et al., 2004), to establish a direct Wnt-dependent regulation of *mdkb*. The same transgenic line could in addition be used to determine if ectopic *mdkb* expression after Wnt signal ablation is able to reestablish ncc formation. This would clarify, whether Mdkb acts downstream or independently of Wnt/ β -catenin signaling.

Regulation of *mdkb* expression is independent of Delta-Notch signals

Several studies implicated Delta-Notch signaling in ncc formation (Cornell and Eisen, 2000; Endo et al., 2002) and work in zebrafish established a link between Delta-Notch and Wnt signaling during this process (Ishitani et al., 2005). Furthermore, it was shown that the Delta-Notch downstream component Olig3 is implicated in cell fate decisions between ncc and sensory neuron fates at the neural plate border (Filippi et al., 2005). As *mdkb* affects formation of both cell types after overexpression and gene knockdown (Winkler and Moon, 2001), I tested whether lateral inhibition might influence *mdkb* expression by looking at Delta-Notch deficient *mindbomb* (*mib*) mutants. *mib* mutants have dramatically enhanced numbers of primary neurons at the expense of ncc (Cornell and Eisen, 2000, 2002). However, no significant difference in *mdkb* expression was observed in *mib* versus wildtype embryos (Fig. 13). Thus, *mdkb* expression does not appear to be a target of Delta-Notch mediated regulation or be influenced by lateral inhibition. As ncc are absent in *mib* mutants, in which *mdkb* expression is normal, I rather speculate that *mdkb* acts prior to the Delta-Notch mediated cell fate decision between ncc and sensory neurons.

In summary, my results suggest that *mdkb* is positioned downstream of BMP, FGF, Wnt and RA signaling cascades, which are essential for ncc induction during gastrulation and early segmentation. I propose that BMP and RA signaling define the lateral extensions of *mdkb* expression at an intermediate position along the DV axis in the gastrulating zebrafish embryo. This lateral limit of its expression domain corresponds to the neural plate border zone where ncc and primary neurons are induced. At later stages of ncc differentiation and cell fate decisions at the neural plate border, Wnt and Delta-Notch signals are needed. Wnt signals have a positive effect, while Delta-Notch signals have no effect on *mdkb* transcription.

5.1.3. Mdkb regulates neural crest and sensory neuron induction at the neural plate border

To investigate the function of Mdkb on induction of ncc, I determined the expression of different ncc markers after increase or reduction of Mdkb activity. Initial experiments used a dominant-negative approach to interfere with Mdkb function (Winkler and Moon, 2001). However, at that time it was not possible to exclude that the C-terminally truncated Mdkb variants also interact with other Midkine ligands, like Mdka or Ptn. I therefore chose a more specific Morpholino approach, and in fact found that certain dominant-negative effects, e.g. defects in hindbrain patterning, cannot be attributed to reduced Mdkb activity (Fig. 17). Efficiency, stability and specificity of the *mdkb* splice Morpholinos (MOs) and the induced effects were shown by RT-PCR and by RNA rescue experiments (Fig. 15, 16 and 19). A knockdown of correctly spliced *mdkb* transcripts of at least 40% was observed in the analyzed embryos (Fig. 17). The reduction of Mdkb function by the MOs resulted in specific loss of ncc, but did not interfere with neural plate size, neural patterning or formation of mesodermal structures (Fig. 16).

Mdkb is required for the induction of earliest ncc precursors during gastrulation

In *mdkb* morphants the earliest effects on ncc were observed at 80% epiboly. At this stage, the MO injected embryos showed a significant reduction of the *pax3* expression domain, while overexpression of *mdkb* resulted in a shift of *pax3* expression to the animal pole and an increase in *pax3* expressing cells (Fig. 18). *pax3* is one of the earliest markers for ncc in zebrafish (Seo et al., 1998; Lewis et al., 2004). Influence of Mdkb on the expression of this early ncc inducer suggest that Mdkb regulates the earliest steps of ncc induction and may also affect subsequent steps of ncc differentiation.

During segmentation stages, expression of ncc differentiation markers, including *sox10*, *sox9b*, *snail1b* and *foxd3* was significantly reduced in *mdkb* morphants (see Table 1 and Fig. 18). Concomitantly, all these markers showed increased expression after *mdkb* overexpression. Interference with appearance of all these ncc differentiation factors by altered Mdkb function underline the importance of Mdkb in ncc development and implies a broad range of defects in *mdkb* morphants during later development. In conclusion, this broad range of effects indicates on one hand that *mdkb* is an early factor involved in ncc induction, rather than a factor acting exclusively on later ncc differentiation. On the other hand, it suggests that

Mdkb might act on a postulated common ncc/sensory neuron precursor population at the neural plate border.

Mdkb is essential for sensory neuron induction

My studies on primary neuron induction in *mdkb* morphants clearly show that Mdkb also regulates formation of Rohon-Beard (RB) sensory neurons. Their precursors are positioned directly adjacent to premigratory trunk ncc at more medial positions relative to ncc (Cornell and Eisen, 2000). RB neurons, like ncc, thus are specified at roughly the same ectodermal position and time. Interestingly, the number of RB neurons is also drastically increased in *mib* mutants, while ncc are lost. RB neuron formation is increased at the expense of ncc by disruption of lateral inhibition (Cornell and Eisen, 2000). In contrast to the situation in *mib* mutants, *mdkb* morphants show a reduction of both ncc and RB neurons, suggesting that *mdkb* is required for the formation of precursors for both cell lineages (see Table 1; Fig. 22). Reciprocally, overexpression of *mdkb* also expanded the numbers of both cell types as well. In addition, this finding supports the idea that Mdkb regulates cell fate induction at the neural plate border, where *mdkb* is co-expressed with *ngn1* (Fig. 8). Importantly, *ngn1* and *isll* positive cells in the medial neural plate, which later differentiate into motoneurons and cells of the MHB are not affected by altered Mdkb activities (Fig. 21 and 22). The effect of Mdkb on sensory neurons is persisting and alterations of sensory neuron numbers were also detected at later stages (Fig. 22 and 23). The specific effect on dorsal sensory neurons can be explained by a loss of the neural plate boundary or ablation of a progenitor cell population for trunk ncc and sensory neurons. An influence on the neural plate border can be observed by slightly reduced expression of *dlx3b* (Fig. 14), required for the specification of sensory neurons and the trigeminal placode (Woda et al., 2003; Kaji and Artinger, 2004).

Similar observations on RB neuron formation were made with altered *prdm1/blimp1* activity, a SET/zinc-finger domain transcription factor (Roy and Ng, 2004; Hernandez-Lagunas et al., 2005). Like *mdkb*, *prdm1/blimp1* expression starts at 90% epiboly at the neural plate border, where it is co-expressed with *ngn1* and *foxd3*. *ubo* (*u-boot*; *narrowminded*) mutants with deficiencies in *prdm1/blimp1* and the corresponding morphants show a loss of ncc derivatives and RB. Conversely, ectopic *prdm1/blimp1* expression leads to an increased number of these cell types. Future studies have to show, whether Mdkb and Prdm1/Blimp1 act in the same cascade during ncc and RB induction.

Recovery of ncc derivatives at later developmental stages indicates Mdkb independent ncc differentiation

The knockdown of *mdkb* and the subsequent loss of ncc marker expression indicates a severe morphant phenotype at later developmental stages. Nevertheless, the morphants developed quite normally, except for a slight developmental delay. This mild phenotype might be due to an incomplete ncc ablation. Residual ncc marker expression is observed in anterior domains during early segmentation stages (11hpf), e.g. in the cephalic ncc region (Fig. 18). Likewise, *mdkb* morphants at slightly later developmental stages display reduced numbers of ncc, but never a complete loss of ncc (Fig. 21). Interestingly, migrating ncc at 24hpf are observed along the body axis in nearly normal numbers, while the remaining population of non-migratory ncc in the tail at this stage as well is only slightly reduced (Fig. 21). Derivatives like head cartilage do form normally in *mdkb* morphants, thereby indicating a regain of ncc (Fig. 21). This may be explained by an incomplete gene knockdown after Morpholino injection with robust appearance of single ncc precursor cells that give rise to persisting ncc populations during later stages. Alternatively, additional factors might be present that induce ncc independently of *mdkb* at this stages of development. One possible explanation may be that Mdkb mainly functions in the maintenance of ncc and sensory neuron fates. However, this argument is weakened by the observation that no enhanced levels of apoptosis cannot be detected in ncc during segmentation stages in *mdkb* morphants (Fig. 19). Furthermore, the strong reduction of *pax3* positive cells during gastrulation stages argue against a maintenance role of Mdkb and instead suggest a function during the earliest steps of ncc induction at the neural plate border. A similar regain of ncc derivatives after complete depletion of ncc induction is observed after knockdown of *wnt8a* (Lewis et al., 2004), implying functional correlation between both factors during ncc induction and possibly a common mechanisms of ncc recovery.

5.1.4. Model of Mdkb action on cell induction at the neural plate border

While Midkine shows a variety of activities in cell culture assays (Muramatsu, 2002), its *in vivo* functions remain unclear as knockout mice lack any early phenotype (Nakamura et al., 1998). Previous studies showed that the two duplicated *mdk* genes in zebrafish exhibit divergent activities (Winkler et al., 2003). On the one hand, Mdka regulates formation of the medial floor plate (Schafer et al., 2005). On the other hand, Mdkb is required for the formation of ncc and sensory neurons (Winkler and Moon, 2001). Based on the observations

in this study, I propose that several signaling pathways essential for ncc induction and neural plate border specification, regulate expression of *mdkb* (Fig. 40).

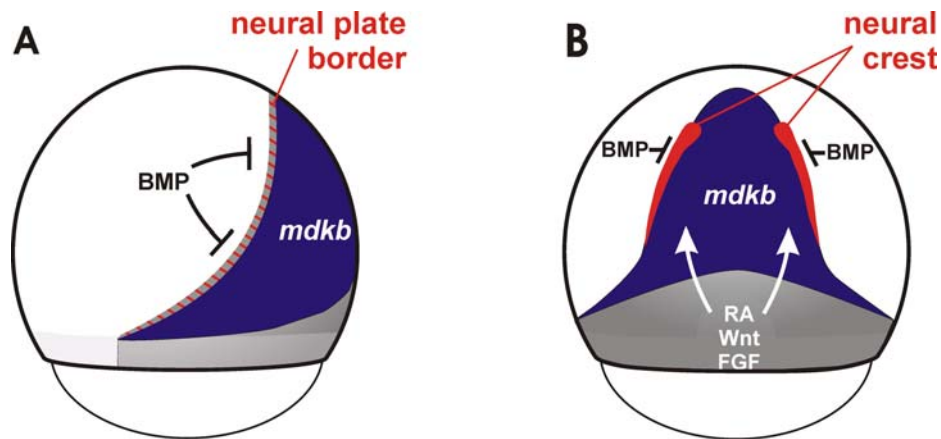


Fig. 40: Model of *mdkb* regulation and activity during ncc and sensory neuron formation.

A,B Schematic lateral (A) and dorsal (B) views of zebrafish gastrulae at 80% epiboly. Ventral to dorsal BMP gradients and posterior to anterior gradients of RA, Wnt and FGF activity establish a zone of competence at the neural plate border, where ncc are formed. *mdkb* expression is restricted to the neural plate by inhibitory and stimulatory activities of BMP, RA, Wnt and FGF signaling, respectively. At the neural plate border, Mdkb controls specification of neural crest cells and sensory neurons.

Mdkb is likely to act downstream of these pathways in order to specify different cell fates at the neural plate border. Similar to *prdm1/blimp1* (Artinger et al., 1999; Roy and Ng, 2004; Hernandez-Lagunas et al., 2005), altered Mdkb activity affects all analyzed subsets of ncc, as well as sensory neuron formation and is not regulated by Delta-Notch. I therefore speculate that Mdkb controls the earliest steps of cell induction at the neural plate border. The future identification of the downstream pathways activated by Mdkb will help to gain insight into these induction processes at the neural plate border. Furthermore, it will be of great interest to determine whether Mdkb interacts with other factors involved in promoting the appearance of an anticipated common precursor population of ncc and RBs at the neural plate border (Hernandez-Lagunas et al., 2005). Time and place of *mdkb* expression are consistent with the proposed idea that ectodermally derived factors control ncc induction during gastrulation in zebrafish (Lewis et al., 2004; Ragland and Raible, 2004).

5.2. Restricted expression patterns of *midkine* genes during early brain development

The expression of *mdk* and *ptn* were well studied in mouse and rat and show spatially and temporally strictly controlled patterns (Kadomatsu et al., 1988; Rauvala, 1989; Kadomatsu et al., 1990; Li et al., 1990; Merenmies and Rauvala, 1990). Both genes are expressed in overlapping patterns during early mouse development in the early ectoderm, the neural plate and the neural tube (Fan et al., 2000). Additional studies revealed RNA expression and protein localization in the cortex (Matsumoto et al., 1994b) and the cerebellum of the developing rat brain (Matsumoto et al., 1994a). Functional studies in primary cell cultures showed neurotrophic activities for Mdk (Michikawa et al., 1993) and for Ptn (Li et al., 1990; Mi et al., 2007). Subsequently, a wide array of additional activities during brain development has been proposed, like neurite outgrowth (Chang et al., 2004), neuronal movement (Rauvala et al., 2000) and neural stem cell differentiation (Rauvala et al., 2000). This suggests the possibility that all three orthologues show significant activities during brain development in zebrafish as well.

5.2.1. Comparison of *mdka*, *mdkb* and *ptn* expression during early brain development

In mice, *midkine* genes are not expressed in the adult CNS (Fan et al., 2000). In contrast to this, earlier studies in zebrafish revealed restricted expression of *mdka* and *mdkb* in the adult zebrafish brain in non-overlapping patterns (Winkler et al., 2003). Also *ptn* expression was detectable at high levels in the adult brain by RT-PCR (Chang et al., 2004). However, a detailed analysis of expression patterns in the embryonic brain has been lacking until now. Transcripts of all three zebrafish genes could be detected by in situ hybridization in non-overlapping patterns from the 12-somite stage onwards in several brain structures (Fig. 24, 25 and 26).

mdka and *mdkb* expression is found to be localized in close proximity, but most times in not overlapping patterns throughout brain development in zebrafish. Expression of *mdka* was found anterior to the MHB in the midbrain, while *mdkb* expression was restricted to the hindbrain at posterior positions to the MHB (Fig. 25 and 26). This observation indicates a possible regulation of both genes by secreted signaling factors from the MHB, like FGF8 or Wnt1 (Reifers et al., 1998; Lekven et al., 2003). Influence of FGF8 has been shown for *mdkb* expression in *acerebelar* mutants lacking a functional *fgf8* gene (Winkler and Moon, 2001).

These mutants, however, completely lack the MHB and the cerebellum due to a loss of FGF8's maintenance function (Reifers et al., 1998). What is more, non-overlapping expression of *mdka* and *mdkb* at the MHB might be a first hint to indicate divergent functions for the establishment of the MHB, either as positional cues or as maintenance factors.

A second example of non overlapping expression of *mdka* and *mdkb* is evident in the rhombencephalon. Expression of *mdkb* in dorsal rhombencephalic tissues does not overlap with ventral *mdka* expression in the hindbrain (Fig. 25). This indicates divergent roles of both factors during hindbrain patterning, similar to the different functions of both factors during dorso-ventral neural tube patterning (this study, Schafer et al., 2005). Differences in *mdka* and *mdkb* expression are also detectable in non-neural tissues: *mdka* is broadly expressed in dorsal and pectoral fins, while *mdkb* is exclusively expressed in cells surrounding the hatching gland precursors (Fig. 26).

In contrast to *mdka* and *mdkb*, the expression of *ptn* is very weak and ubiquitous in the CNS. Zones of abundant *ptn* expression are first found at 15hpf in the optic stalk and in rhombomeres r5 and r6. The expression in the hindbrain shows an AP gradient. It is strong in r5 and weak in r6 (Fig. 24). *ptn* expression in the hindbrain is transient and disappears fast during later development (Fig. 25). This temporally limited expression suggests a transient function of Ptn during this short time window during formation of the posterior rhombomeres, similar to *Mafb* function in zebrafish (Moens et al., 1996; Moens et al., 1998). Zebrafish *valentino* mutants, deficient for *mafb*, lack r5 and r6 and the boundary between r4 and r7 (Moens et al., 1996). In addition to this, correct establishment of AP rhombomere identity is lost in these mutants by interference with correct *hox* gene expression (Prince et al., 1998).

Interestingly, *ptn* expression in the optic stalk persists over a long time and overlaps completely with the expression of *mdka* and *mdkb*. The optic stalk is a transient tubular structure that collects the axons of the retinal ganglion cells into the optic nerve and allows the blood vessels to reach the eye (Lupo et al., 2000). Coexpression of all three factors in the optic stalk (Fig. 26) and expression of *mdka* and *mdkb* in different layers in the eye (Fig. 27) hint to prominent roles of zebrafish *midkine* genes during axonal growth in the developing eye. Expression of *mdk* and *ptn* is also found in eye tissues of *Xenopus* (Sekiguchi et al., 1995) and rat (Miyashiro et al., 1998) and eye specific functions have been investigated in retinal progenitor differentiation (Roger et al., 2006) and photoreceptor regeneration (Unoki et al., 1994; Masuda et al., 1995).

At 48hpf, additional expression of *ptn* is found at the ventricle borders, again overlapping with *mdka* and *mdkb* at this stage (Fig. 26). Ventricle borders are well known zones of high cell proliferation during adult neurogenesis in zebrafish (Mueller and Wullimann, 2003; Zupanc et al., 2005). They are therefore suspected to contain neural stem cells (Zupanc et al., 2005; Grandel et al., 2006). To show a correlation of proliferating neural stem cells and *mdk* gene expression, BrdU-pulse labeling needs to be done. Furthermore, a comparison of *mdk* expression with that of genes essential for secondary neurogenesis, like e.g. *neuroD*, *ngn1*, *notch-1a*, would be interesting to link *mdk* expression with zones of high neurogenic activity (Mueller and Wullimann, 2003).

Importantly, non-overlapping expression of *ptn* in the floorplate was observed (Fig. 27) and might be a first clue to a possible function of *ptn* during late spinal cord patterning similar to the early roles of *mdka* and *mdkb* in the neural tube (this study, Schafer et al., 2005).

In summary, I could show that all three *midkine* genes have restricted expression patterns during embryonic brain development in zebrafish. Non overlapping expression of the three genes at prominent brain signaling centers like the MHB and posterior to r4 suggest putative combinatorial activities of *Mdka*, *Mdkb* and *Ptn* during of patterning of the embryonic brain.

5.2.2. Different aspects of zebrafish brain patterning are regulated by Midkine growth factors

To investigate the functions of *mdka*, *mdkb* and *ptn* during brain pattern formation and the establishment of signaling centers in the brain, I utilized RNA overexpression and splice MO knockdown experiments to interfere with endogenous levels of *mdka*, *mdkb* and *ptn*. RT-PCR analyses were performed to detect incorrectly spliced transcripts thereby showing efficiency of the MOs (Fig. 15, 30 and 31). Subsequent in situ hybridization was used to analyze alterations in marker expression and irregular brain patterning in the injected embryos (Fig. 29 and 33). Effects observed on brain patterning after single knockdown were compared to those obtained in double and triple *mdka/mdkb/ptn* morphants (Fig. 34, 35 and Table 3, 4). A special emphasis was placed on marker expression in the Mid-Hindbrain boundary (MHB) and rhombomere 4 (r4) organizers in these morphants. This allowed presuming whether Midkine proteins interact as heterodimers in order to establish correct brain patterning.

Overlapping activities of midkine/pleiotrophin during forebrain formation

Injection of *mdka*, *mdkb* and *ptn* RNAs resulted in strong and very similar morphological defects, e.g. loss of forebrain structures, in all groups of injected embryos (Fig. 28). The occurrence of identical or highly similar phenotypes suggests overlapping activities or binding to a common receptor of all three proteins. Midkine and Pleiotrophin proteins are highly similar (minimum 40% identities at amino acid level) and share common protein domain motives with conserved residues (Muramatsu, 2002).

Another common result of RNA injections was that the formation of the optic vesicles was impaired, as indicated by fusion of the *pax6a* expression domains (Fig. 29). In addition, expression of *pax6a* was found in anterior positions in the forebrain after *mdka*, *mdkb* or *ptn* RNA injection. These results indicate that the process of eye development at this stage is impaired. Usually, a single field of retinal precursor cells in the neural plate separates into left and right eyes by an anterior movement of posterior diencephalic precursors (Solnica-Krezel, 2002). Interference with the movement of the diencephalic cells results in impaired separation of the primordial eye field and therefore leads to cyclopia (Varga et al., 1999). The signals essential for correct diencephalic movement partly originate from the underlying cells of the axial mesoderm (Macdonald et al., 1995). *shha* expression in the prechordal plate of *mdka*, *mdkb* and *ptn* RNA injected embryos indicated normal midline formation and presence of the prechordal plate (Fig. 29). Nevertheless, the performed experiments can not exclude that essential signals from the axial mesoderm might be missing. Further explanations for the failure in anterior extension of diencephalic cells may be incorrect induction or movement of the diencephalic cells as consequence of impaired forebrain development. Interference with organizer function like that of the anterior neural ridge and the MHB as major forebrain organizers results in failures in forebrain patterning (Houart et al., 1998). Ablation of the anterior neural ridge in zebrafish results in the absence of *emx3* expression in the telencephalon and altered expression of *shh* in the forebrain (Houart et al., 1998). However, *midkine* RNA injections never resulted in complete ablation of *emx3* expression and therefore indicate normal anterior neural ridge appearance.

While the similar activities of overexpressed RNAs suggested a common activity during forebrain development, MO injections showed only mild alterations in the expression of the forebrain markers, *emx3* and *pax6a* (Fig. 33) Only knockdown of *mdkb* resulted in elongation of the *emx3* domain in 67% of the injected embryos and thereby resembles results previously obtained with a dominant-negative version of Mdkb (Winkler and Moon, 2001). Elongation

of the anterior head is consistent with a posteriorizing activity of *Mdkb* during CNS development, as postulated earlier.

MHB establishment depends on *Mdka* function

A second important organizer for brain patterning is the isthmus organizer, also called the MHB, which is specified at its correct position during gastrulation by combined action of *otx2* and *gbx2* (Simeone et al., 1992; Muller et al., 1996). MHB formation is initiated slightly later by the three factors *Wnt1*, *Pax2.1* and *Fgf8* that act in parallel (Lun and Brand, 1998; Reifers et al., 1998). These factors also drive pattern formation in the surrounding neuronal tissues and are important for MHB maintenance (Wurst and Bally-Cuif, 2001). MHB establishment was analyzed by looking at the expression of the homeobox gene *eng2a*, a downstream target of *Pax2.1* and *Wnt/β-catenin* (Fjose et al., 1992; Buckles et al., 2004). Reduction of *eng2a* expression at the MHB in embryos deficient for *Mdka* alone or in *mdka/mdkb* or *mdka/ptn* double knockdown embryos suggested a non-overlapping function of *Mdka* in either induction or maintenance of the MHB (Fig. 33 and 34). A *Mdka* function during MHB induction is less likely, because expression of *wnt1* is still present in the MHB of *mdka* morphants (data not shown). Additionally, observations of living morphants showed that knockdown of *Mdka* does not ablate the MHB at 24hpf. Finally, also *eng2* expression is not completely lost in the morphants but is strongly reduced (Fig. 33 and 34). This rather suggests that *Mdka* might be implicated in the later maintenance of MHB cells. Maintenance of the MHB is regulated by a complex interplay of *Wnt1*, *Fgf8* and *Pax2.1/Eng2a/Eng3* during the segmentation period (Wurst and Bally-Cuif, 2001; Solnica-Krezel, 2002). At this stage, *Eng2a* function is needed synergistically with *Eng3* to maintain the MHB (Scholpp and Brand, 2001; Wurst and Bally-Cuif, 2001). Combined loss of *Eng2a* and *Eng3/Pbx* function result in ablation of a correctly folded MHB by lack of maintenance functions (Scholpp and Brand, 2001; Erickson et al., 2007), similar to the situation in zebrafish *no isthmus* mutants lacking *pax2.1* (Lun and Brand, 1998). Therefore, the observed effect of *Mdka* on *eng2a* expression suggests that also *eng3* and *pbx* expression might be reduced and MHB maintenance is impaired. This reduced maintenance could result in partial but not complete ablation of the MHB, as observed in *mdka* morphants.

Ptn is essential for rhombomere 4 organizer formation

One remarkable observation was that gain and loss of Ptn activity similar to combined reduction of Ptn and Mdk activity had a strong effect on hindbrain segmentation (Fig. 29, 30 and 31). Most prominently, rhombomere 4 (r4) displayed a change in its size, obvious by the reduced distance between r3 and r5 marked by *egr2b* or by misshaped expression of *hoxb1a* in r4 (Fig. 29). Thus, Ptn has an effect on the establishment of r4, which is an important hindbrain signaling center (Maves et al., 2002; Walshe et al., 2002). R4 is a center for morphogen secretion, including FGF3 and FGF8, which together are required for correct cell identity establishment in the posteriorly positioned rhombomeres r5 and r6 (Maves et al., 2002). While single knockdown of *fgf3* or *fgf8* only mildly affects expression of posterior hindbrain markers like *egr2b* in r5 and *mafb* in r5 and r6, combined knockdown of both *fgfs* completely abolishes their expression. Expression of r4 markers like *hoxb1a* was not altered in *fgf3/fgf8* double morphants indicating normal r4 establishment (Prince et al., 1998). In contrast to these effects after interfering with r4 signals, Ptn function only acts on r4 shape, while appearance of posterior rhombomeres expressing *egr2b* or *mafb* is not inhibited (Fig. 2, 23, 26, 28, Table 4). This observation suggests that Ptn function is unlikely involved in Fgf signal progression of r4, but either interferes with r4 induction or maintenance. Induction of r4 is not completely ablated in *ptn* morphants, because *hoxb1a* expression is still present (data not shown). Interestingly, knockdown of *hoxb1a* and its orthologue *hoxb1b* results in altered r4 size (McClintock et al., 2002) comparable to that seen in *ptn* morphants, suggesting a similar mode of action. A function of Ptn during r4 maintenance could not be excluded by my experiments and has to be investigated in additional experiments.

Expression of *ptn* in r5 and r6 is comparable to *mafb* (the mouse *kreisler* homologue) expression in the same rhombomeres, suggesting a possible functional connection of both genes. Loss of *mafb* in zebrafish *valentino* mutants leads to a shortening of the rhombencephalon and appearance of one fused r5/6 rhombomere that lacks the r4/r7 boundaries (Moens et al., 1996; Moens et al., 1998). To test for potential effects of Ptn on r5 and r6 establishment, I investigated expression of *mafb* in *ptn* morphants, which was overall normal (Table 4). Nevertheless, slight alterations of ventral *val* expression was observed in *ptn* RNA injected embryos (Fig. 30). These results and the observation, that r5 expression of *egr2b* appears normal, exclude a functional interaction between *mafb* and *ptn*.

Interestingly, overexpression of *ptn* resulted in a typical wedge shape of r4 (Fig. 30). These results suggest possible effects on dorso-ventral patterning of r4, which may be explained by interference of Ptn with ventral signals from the underlying mesoderm. *ptn* expression is

found at higher levels in the dorsal regions of r5 and r6 (Fig. 25), indicating the possibility of a DV gradient of secreted Ptn in r4. This gradient might regulate patterning in r4, similar to the situation of *Mdka* and *Mdkb* in the neural tube.

To conclude, I was able to show that MHB formation depends on *Mdka* function and that hindbrain segmentation is affected after knockdown of *ptn*. Combined loss of *ptn* and *mdka* or *mdkb* resulted in an increased number of affected embryos. This indicates a possible interaction of Mdk and Ptn (Fig. 34). Finally, forebrain development was exclusively affected by *mdkb* knockdown, but further information on a possible interaction with *Mdka* and Ptn on this brain structure is necessary (Fig. 41).

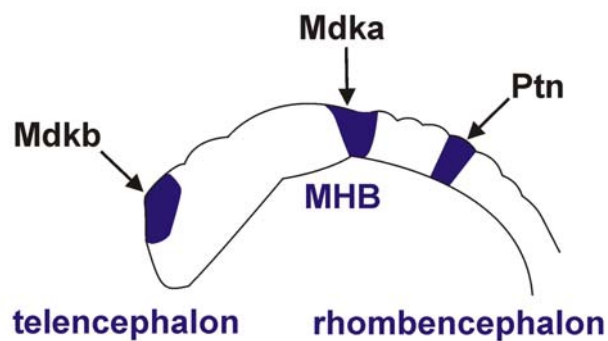


Fig. 41: Summary of the observed combinatorial effects of *Mdka*, *Mdkb* and *Ptn* on different brain regions.

5.3. Ptn is essential for somite boundary formation

Cells in the anterior PSM dissociate from adjacent cells and form a segmental boundary, thereby generating an epithelialized somite. Positional identity of these cells is predetermined in the PSM and is maintained in the newly formed somites. Several models have been proposed to explain the reiterative appearance of somites, including the clock and wavefront model (Cooke and Zeeman, 1976; Pourquie, 2001; Holley and Takeda, 2002). Studies in diverse model organisms have revealed several essential cellular components of both, clock and wavefront. Nevertheless, many of the implicated genetic factors and aspects of the molecular mechanism remain unclear. For example, it remains elusive which mechanisms are responsible for the differences between anterior and posterior somite appearance (Holley, 2006, 2007).

5.3.1. Combined knockdown of midkine and pleiotrophin function interferes with somitogenesis

An interesting and unexpected effect of simultaneously knocking down all three *midkine* genes was that somite boundaries were completely absent in the triple morphants (Fig. 28). Paraxial mesoderm and notochord structures were present in these embryos, suggesting a loss of somite boundaries rather than tissue ablation. The loss of somite boundaries in these embryos was visible in living zebrafish larvae (Fig. 35) and was also observed when somite markers were analyzed by in situ hybridization against *myod* (Fig. 38), *mespb* (Fig. 38) or *papc* (Fig. 43). It is remarkable that all somites along the AP axis were affected, indicating interference with initial processes of somitogenesis during gastrulation and/or interference with induction of somitic precursors in the PSM. The observed somitic fusions were very similar to those observed in zebrafish *fused somite (fss)* mutants, which lack *tbx24* activity (van Eeden et al., 1996; Nikaido et al., 2002). *fss* mutants show no polarity in the presomitic mesoderm and therefore lack correct somite maturation (Oates et al., 2005). *Tbx24* itself was shown to be involved in establishment of segment polarity and induces caudalized cell fates at the anterior end of the PSM. Thus, it affects a rather late step of somite formation (Durbin et al., 2000).

5.3.2. Triple knockdown of *mdka*, *mdkb* and *ptn* does not interfere with initiation of the somitogenesis clock but affects somitomere maturation

Cyclic expression of genes controlled by the somitogenesis clock was investigated to analyze the initial PSM pre patterning events in the triple morphants. *her1* expression is cycling in the PSM of zebrafish and is directly regulated by Delta-Notch signaling (Holley et al., 2002; Oates and Ho, 2002). Simultaneous knockdown of all three *midkine* genes resulted in severe changes in the somitogenesis clock output (Fig. 37O). The initiation of oscillating clock genes was not disturbed in the triple morphants, as single, but diffuse *her1* stripes were emerging from the tail bud. However, oscillation of *her1* was not maintained leading to a reduced number of *her1* stripes in the anterior PSM. This effect is different from that of *her1* expression in zebrafish mutants deficient for Delta-Notch signals, which show a salt-and-pepper like expression (van Eeden et al., 1996; Holley et al., 2000). In addition, triple morphants lack anterior and posterior somites, while Delta-Notch mutants, like *after-eight*, *deadly seven* and *beamter*, lack only posterior somites (Holley, 2006). It is therefore unlikely

that a direct interference with the Delta-Notch pathway is the reason for the observed triple knockdown effect on somites.

her1 expression in the triple morphants resembles that seen in mutants with alterations in the wavefront activity (Sawada et al., 2001). This wavefront regulates the progression of tissue maturation and cell differentiation in a head-to-tail direction along the AP axis of the embryo. The wavefront is built up by FGF8 and Tbx24 (Holley and Takeda, 2002). To visualize the position of the maturation front in the morphants, I examined expression of *mespb* in the anterior domain of the PSM, immediately posterior to the last epithelialized somites (Sawada et al., 2000). A posterior shift in position of the last formed somite was evident by altered *mespb* expression in the morphants (indicated by the red bar in Fig. 37T). These observations also resemble the situation in *fs* mutants, where impaired stabilization of oscillating expression occurs at the maturation front (Nikaido et al., 2002). However, in contrast to *fs* mutants where rostral *mespb* expression is lost (Sawada et al., 2000; Oates et al., 2005), *mespb* expression in triple morphants persists, although at more posterior positions. A possible explanation for the posterior shift of *mespb* expression is interference with the mechanisms that determine the position of the maturation front. This is established by an FGF8 activity gradient in the PSM (Dubrulle et al., 2001; Holley and Takeda, 2002). Thus, one possible reason for the observed effects is an effect of Mdk/Ptn on FGF8 signaling. The proposed function of Mdk/Ptn during positioning of the maturation front is indicated by *mdka* expression in the paraxial mesoderm close to the position of the wavefront in the anterior PSM (Schafer et al., 2005). Furthermore, overexpression experiments suggested that *mdka* might play a prominent role during somitogenesis (Winkler et al., 2003).

5.3.3. Knockdown of Ptn function is responsible for somite ablation in triple morphants

Interestingly, no alteration in somitogenesis was observed after single knockdown of either *mdka* or *mdkb* (Fig. 38; Schafer et al., 2005). The data presented in this thesis now show that only combined loss of *mdka/mdkb* and *ptn* function at increased MO dose interferes with somitogenesis in a high percentage of embryos (Table 5). Single knockdown of Ptn function also resulted in fusion of somites, but at a lower rate. This result was surprising, because *ptn* expression, in contrast to *mdka* and *mdkb* expression, is only weak in the areas of somite formation (Fig. 36). The high percentage of embryos with somite fusion after combined ablation of midkine and pleiotrophin indicates that knockdown of either *mdka* or *mdkb* is able to interfere with somitogenesis only in combination with Ptn reduction. This indicates a

combinatorial effect of the factors during somitogenesis or a predominant function of *Ptn*, which is supported by *Mdka/Mdkb*. Single knockdown of *ptn* resulted in effects comparable to triple morphants (Fig. 38) but at a lower number of injected embryos. This observation points to a prominent function of *ptn* during somitogenesis.

5.3.4. Enhanced numbers of *foxd3* positive cells in the tail bud suggest possible cell fate changes in *ptn* morphants

It is noteworthy, that raised numbers of *foxd3* positive cells were detected in the tail bud of *ptn* and triple morphants (Fig 38N,O). This observation opens up the possibility that more cells in the PSM of these morphants remain in an unspecified fate in this stem cell area (Pan et al., 2006; Pan and Thomson, 2007). The fate of these dorsal *foxd3* positive cells in the tail bud of zebrafish is unknown so far (Odenthal and Nusslein-Volhard, 1998), but interestingly injection of a *foxd3* MO showed ectopic *myf5* expression in the PSM (Lee et al., 2006). This suggests that *foxd3* represses myogenic fates in the tail bud. Instead, it keeps these cells in an undifferentiated state. Additional analysis of *ntl* expression in the *ptn* and triple morphants showed no enhanced levels of *ntl* positive cells in the tail bud (Fig. 38I,J). However, cell density in the notochord of *ptn* and triple morphants seem to be increased, indicated by a stronger *ntl* signal (Fig. 38I,J) and by preliminary notochord cell counting (data not show). It is not clear, whether the increased number of *foxd3* expressing cells in the tail bud is correlated with the increase in notochord cell number.

Additionally, I observed a wavy midline expression of *ntl* after knockdown of *ptn*. This might also be due to defects in mesoderm cell specification resulting in a higher number of cells in the midline. Interference of single *ptn* knockdown with cell adhesion or adaxial and paraxial mesoderm specification are indicated by reduction of *papc* expression in the PSM (Fig. 43F). *Papc* is a cell adhesion molecule (Protocadherin; reviewed in Frank and Kemler, 2002) acting as a downstream effector of *spadetail* in zebrafish to regulate cell movement in the mesoderm (Yamamoto et al., 1998). Moreover, *Papc* function is well studied during somitogenesis of *Xenopus* (Kim et al., 2000) and zebrafish (Yamamoto et al., 1998). Nevertheless, this midline defect could also be caused secondarily by the loss of somite integrity. Statistical analysis of notochord cell numbers, investigation of mesoderm induction and visualization of cell movements are required to shed light on this problem.

5.3.5. The efficiency of the *ptn* MO is increased by a second binding site in the intron of the pre-mRNA target

To test for the specificity of phenotypes induced by the used splice MO, I injected a second ATG MO to independently knockdown *ptn*. This experiment did not result in pronounced somite fusion after injection of an equal amount of MO (Fig. 42). Somite fusion was only observed in single somites and in a mild way. Higher amounts of the *ptn* ATG MO (> 5.0 pg) resulted in increased mortality of the injected embryos. Therefore, I can not exclude that the *ptn* ATG MO knockdown was insufficient to completely block Ptn translation. To further test the MO efficiency and to show that the observed somite fusion is not due to an unspecific effect, individual injections of the splice Up and Down MOs were made. Both splice MOs were able to interfere with somite formation, but the efficiency of the Down MO, blocking the splice acceptor, was clearly more potent and resulted in somite fusion along the complete AP axis (Fig. 43C). Injection of the *ptn* MO Up, in contrast, resulted only in mild and partial fusion of somites. Nevertheless, budding of somites at the anterior PSM border was clearly affected (Fig. 43E).

The search for additional binding sequences for the *ptn* MO down in the zebrafish genome revealed a second, completely homologous sequence of 25bp in intron 1 of the *ptn* gene (Fig. 44). This very surprising observation may explain the increased efficiency of the *ptn* down MO. The second MO binding site may result in enhanced binding of the MO to the pre-mRNA and may result in more efficient blockage or degradation of the *ptn* transcript. To test this hypothesis, further RT-PCR experiments should reveal a lower level of *ptn* mRNA in *ptn* MO down injected embryos in contrast to *ptn* MO up, *ptn* ATG MO or control MO injected embryos.

In conclusion, I showed that Ptn alone or more robust in combination with *Mdka* or *Mdkb* function is essential for correct somite formation. Ptn function either interferes with the establishment of the maturation front or interferes with cell adhesion in the PSM. Therefore, my data indicate that *ptn* is a novel molecular control element for mesoderm segmentation in zebrafish.

6. Future perspectives

Further experiments should aim at identifying and characterizing the receptor(s) for *Mdka*, *Mdkb* and *Ptn*. Determination of their expression and function will give insight into the integration of several Midkine signals into either one common or alternatively several different pathways. It will be important to analyze possible interactions between Wnt and Midkine/Pleiotrophin signaling through *Lrp5/6* in diverse processes including neural crest induction. Identification of the receptors should be accompanied by investigation of downstream targets of single and combined *Mdk/Ptn* signaling, e.g. by microarray analyses to reveal signaling targets and to identify the effectors of the described developmental effects.

In a next step, the transcriptional regulation of all three genes is to be determined by in depth promoter analyses and investigation of possible miRNA binding sites. Identification of conserved sequences in the promoter or in the UTR region of *midkine* genes will result in a better understanding of the complex spatiotemporal patterns during development and will possibly identify the upstream regulators responsible for tight control of these highly homologous genes. For gain-of-function experiments, the establishment of transgenic lines with inducible *mdk* and *ptn* expression would be a valuable tool. These will allow to tightly control the levels of expression at distinct stages and places during development.

7. References

- Amacher, S. L., Draper, B. W., Summers, B. R. and Kimmel, C. B. (2002). The zebrafish T-box genes no tail and spadetail are required for development of trunk and tail mesoderm and medial floor plate. *Development* **129**, 3311-23.
- Amet, L. E., Lauri, S. E., Hienola, A., Croll, S. D., Lu, Y., Levorse, J. M., Prabhakaran, B., Taira, T., Rauvala, H. and Vogt, T. F. (2001). Enhanced hippocampal long-term potentiation in mice lacking heparin-binding growth-associated molecule. *Mol Cell Neurosci* **17**, 1014-24.
- Amores, A., Force, A., Yan, Y. L., Joly, L., Amemiya, C., Fritz, A., Ho, R. K., Langeland, J., Prince, V., Wang, Y. L. et al. (1998). Zebrafish hox clusters and vertebrate genome evolution. *Science* **282**, 1711-4.
- Amsterdam, A. and Hopkins, N. (2006). Mutagenesis strategies in zebrafish for identifying genes involved in development and disease. *Trends Genet* **22**, 473-8.
- Amsterdam, A., Nissen, R. M., Sun, Z., Swindell, E. C., Farrington, S. and Hopkins, N. (2004). Identification of 315 genes essential for early zebrafish development. *Proc Natl Acad Sci U S A* **101**, 12792-7.
- Artinger, K. B., Chitnis, A. B., Mercola, M. and Driever, W. (1999). Zebrafish narrowminded suggests a genetic link between formation of neural crest and primary sensory neurons. *Development* **126**, 3969-79.
- Aulehla, A. and Herrmann, B. G. (2004). Segmentation in vertebrates: clock and gradient finally joined. *Genes Dev* **18**, 2060-7.
- Aulehla, A., Wehrle, C., Brand-Saberi, B., Kemler, R., Gossler, A., Kanzler, B. and Herrmann, B. G. (2003). Wnt3a plays a major role in the segmentation clock controlling somitogenesis. *Dev Cell* **4**, 395-406.
- Aybar, M. J. and Mayor, R. (2002). Early induction of neural crest cells: lessons learned from frog, fish and chick. *Curr Opin Genet Dev* **12**, 452-8.
- Baker, R. E., Schnell, S. and Maini, P. K. (2006). A clock and wavefront mechanism for somite formation. *Dev Biol* **293**, 116-26.
- Bang, A. G., Papalopulu, N., Kintner, C. and Goulding, M. D. (1997). Expression of Pax-3 is initiated in the early neural plate by posteriorizing signals produced by the organizer and by posterior non-axial mesoderm. *Development* **124**, 2075-85.
- Barenbaum, M. and Bronner-Fraser, M. (2005). Early steps in neural crest specification. *Semin Cell Dev Biol* **16**, 642-6.
- Barth, K. A., Kishimoto, Y., Rohr, K. B., Seydler, C., Schulte-Merker, S. and Wilson, S. W. (1999). Bmp activity establishes a gradient of positional information throughout the entire neural plate. *Development* **126**, 4977-87.
- Begemann, G., Marx, M., Mebus, K., Meyer, A. and Bastmeyer, M. (2004). Beyond the neckless phenotype: influence of reduced retinoic acid signaling on motor neuron development in the zebrafish hindbrain. *Dev Biol* **271**, 119-29.
- Begemann, G., Schilling, T. F., Rauch, G. J., Geisler, R. and Ingham, P. W. (2001). The zebrafish neckless mutation reveals a requirement for raldh2 in mesodermal signals that pattern the hindbrain. *Development* **128**, 3081-94.
- Beis, D. and Stainier, D. Y. (2006). In vivo cell biology: following the zebrafish trend. *Trends Cell Biol* **16**, 105-12.
- Belting, H. G., Hauptmann, G., Meyer, D., Abdelilah-Seyfried, S., Chitnis, A., Eschbach, C., Soll, I., Thisse, C., Thisse, B., Artinger, K. B. et al. (2001). spiel ohne grenzen/pou2 is required during establishment of the zebrafish midbrain-hindbrain boundary organizer. *Development* **128**, 4165-76.
- Bernhardt, R. R., Chitnis, A. B., Lindamer, L. and Kuwada, J. Y. (1990). Identification of spinal neurons in the embryonic and larval zebrafish. *J Comp Neurol* **302**, 603-16.
- Blader, P., Fischer, N., Gradwohl, G., Guillemot, F. and Strahle, U. (1997). The activity of neurogenin1 is controlled by local cues in the zebrafish embryo. *Development* **124**, 4557-69.
- Brand, M., Heisenberg, C. P., Jiang, Y. J., Beuchle, D., Lun, K., Furutani-Seiki, M., Granato, M., Haffter, P., Hammerschmidt, M., Kane, D. A. et al. (1996). Mutations in zebrafish genes affecting the formation of the boundary between midbrain and hindbrain. *Development* **123**, 179-90.
- Brent, A. E. (2005). Somite formation: where left meets right. *Curr Biol* **15**, R468-70.
- Brent, A. E. and Tabin, C. J. (2002). Developmental regulation of somite derivatives: muscle, cartilage and tendon. *Curr Opin Genet Dev* **12**, 548-57.
- Briscoe, J. and Ericson, J. (1999). The specification of neuronal identity by graded Sonic Hedgehog signalling. *Semin Cell Dev Biol* **10**, 353-62.
- Briscoe, J., Pierani, A., Jessell, T. M. and Ericson, J. (2000). A homeodomain protein code specifies progenitor cell identity and neuronal fate in the ventral neural tube. *Cell* **101**, 435-45.
- Buckles, G. R., Thorpe, C. J., Ramel, M. C. and Lekven, A. C. (2004). Combinatorial Wnt control of zebrafish midbrain-hindbrain boundary formation. *Mech Dev* **121**, 437-47.
- Burns, C. G., Milan, D. J., Grande, E. J., Rottbauer, W., MacRae, C. A. and Fishman, M. C. (2005). High-throughput assay for small molecules that modulate zebrafish embryonic heart rate. *Nat Chem Biol* **1**, 263-4.
- Carney, T. J., Dutton, K. A., Greenhill, E., Delfino-Machin, M., Dufourcq, P., Blader, P. and Kelsh, R. N. (2006). A direct role for Sox10 in specification of neural crest-derived sensory neurons. *Development* **133**, 4619-30.
- Chang, C. and Hemmati-Brivanlou, A. (1998). Neural crest induction by Xwnt7B in *Xenopus*. *Dev Biol* **194**, 129-34.
- Chang, M. H., Huang, C. J., Hwang, S. P., Lu, I. C., Lin, C. M., Kuo, T. F. and Chou, C. M. (2004). Zebrafish heparin-binding neurotrophic factor enhances neurite outgrowth during its development. *Biochem Biophys Res Commun* **321**, 502-9.
- Chiang, E. F., Pai, C. I., Wyatt, M., Yan, Y. L., Postlethwait, J. and Chung, B. (2001). Two sox9 genes on duplicated zebrafish chromosomes: expression of similar transcription activators in distinct sites. *Dev Biol* **231**, 149-63.
- Chizhikov, V. V. and Millen, K. J. (2005). Roof plate-dependent patterning of the vertebrate dorsal central nervous system. *Dev Biol* **277**, 287-95.
- Cohen, P. and Goedert, M. (2004). GSK3 inhibitors: development and therapeutic potential. *Nat Rev Drug Discov* **3**, 479-87.

- Cooke, J. and Zeeman, E. C.** (1976). A clock and wavefront model for control of the number of repeated structures during animal morphogenesis. *J Theor Biol* **58**, 455-76.
- Cordes, S. P. and Barsh, G. S.** (1994). The mouse segmentation gene *kr* encodes a novel basic domain-leucine zipper transcription factor. *Cell* **79**, 1025-34.
- Cornell, R. A. and Eisen, J. S.** (2000). Delta signaling mediates segregation of neural crest and spinal sensory neurons from zebrafish lateral neural plate. *Development* **127**, 2873-82.
- Cornell, R. A. and Eisen, J. S.** (2002). Delta/Notch signaling promotes formation of zebrafish neural crest by repressing Neurogenin 1 function. *Development* **129**, 2639-48.
- Culp, P., Nusslein-Volhard, C. and Hopkins, N.** (1991). High-frequency germ-line transmission of plasmid DNA sequences injected into fertilized zebrafish eggs. *Proc Natl Acad Sci U S A* **88**, 7953-7.
- Dale, K. J. and Pourquie, O.** (2000). A clock-work somite. *Bioessays* **22**, 72-83.
- De Robertis, E. M.** (2006). Spemann's organizer and self-regulation in amphibian embryos. *Nat Rev Mol Cell Biol* **7**, 296-302.
- De Robertis, E. M. and Kuroda, H.** (2004). Dorsal-ventral patterning and neural induction in *Xenopus* embryos. *Annu Rev Cell Dev Biol* **20**, 285-308.
- Diez del Corral, R., Olivera-Martinez, I., Goriely, A., Gale, E., Maden, M. and Storey, K.** (2003). Opposing FGF and retinoid pathways control ventral neural pattern, neuronal differentiation, and segmentation during body axis extension. *Neuron* **40**, 65-79.
- Diez del Corral, R. and Storey, K. G.** (2004). Opposing FGF and retinoid pathways: a signalling switch that controls differentiation and patterning onset in the extending vertebrate body axis. *Bioessays* **26**, 857-69.
- Dockter, J. L.** (2000). Sclerotome induction and differentiation. *Curr Top Dev Biol* **48**, 77-127.
- Dooley, K. and Zon, L. I.** (2000). Zebrafish: a model system for the study of human disease. *Curr Opin Genet Dev* **10**, 252-6.
- Dorsky, R. I., Moon, R. T. and Raible, D. W.** (1998). Control of neural crest cell fate by the Wnt signalling pathway. *Nature* **396**, 370-3.
- Driever, W., Solnica-Krezel, L., Schier, A. F., Neuhauss, S. C., Malicki, J., Stemple, D. L., Stainier, D. Y., Zwartkruis, F., Abdellah, S., Rangini, Z. et al.** (1996). A genetic screen for mutations affecting embryogenesis in zebrafish. *Development* **123**, 37-46.
- Dubrulle, J., McGrew, M. J. and Pourquie, O.** (2001). FGF signaling controls somite boundary position and regulates segmentation clock control of spatiotemporal Hox gene activation. *Cell* **106**, 219-32.
- Dubrulle, J. and Pourquie, O.** (2002). From head to tail: links between the segmentation clock and antero-posterior patterning of the embryo. *Curr Opin Genet Dev* **12**, 519-23.
- Dubrulle, J. and Pourquie, O.** (2004a). Coupling segmentation to axis formation. *Development* **131**, 5783-93.
- Dubrulle, J. and Pourquie, O.** (2004b). *fgf8* mRNA decay establishes a gradient that couples axial elongation to patterning in the vertebrate embryo. *Nature* **427**, 419-22.
- Durbin, L., Sordino, P., Barrios, A., Gering, M., Thisse, C., Thisse, B., Brennan, C., Green, A., Wilson, S. and Holder, N.** (2000). Anteroposterior patterning is required within segments for somite boundary formation in developing zebrafish. *Development* **127**, 1703-13.
- Dutton, K. A., Pauliny, A., Lopes, S. S., Elworthy, S., Carney, T. J., Rauch, J., Geisler, R., Haffter, P. and Kelsh, R. N.** (2001). Zebrafish colourless encodes *sox10* and specifies non-ectomesenchymal neural crest fates. *Development* **128**, 4113-25.
- Ellingsen, S., Laplante, M. A., Konig, M., Kikuta, H., Furmanek, T., Hoivik, E. A. and Becker, T. S.** (2005). Large-scale enhancer detection in the zebrafish genome. *Development* **132**, 3799-811.
- Endo, Y., Osumi, N. and Wakamatsu, Y.** (2002). Bimodal functions of Notch-mediated signaling are involved in neural crest formation during avian ectoderm development. *Development* **129**, 863-73.
- Erickson, T., Scholpp, S., Brand, M., Moens, C. B. and Waskiewicz, A. J.** (2007). Pbx proteins cooperate with Engrailed to pattern the midbrain-hindbrain and diencephalic-mesencephalic boundaries. *Dev Biol* **301**, 504-17.
- Fan, Q. W., Muramatsu, T. and Kadomatsu, K.** (2000). Distinct expression of midkine and pleiotrophin in the spinal cord and placental tissues during early mouse development. *Dev Growth Differ* **42**, 113-9.
- Filippi, A., Tiso, N., Deflorian, G., Zecchin, E., Bortolussi, M. and Argenton, F.** (2005). The basic helix-loop-helix olig3 establishes the neural plate boundary of the trunk and is necessary for development of the dorsal spinal cord. *Proc Natl Acad Sci U S A* **102**, 4377-82.
- Fjose, A., Njolstad, P. R., Nornes, S., Molven, A. and Krauss, S.** (1992). Structure and early embryonic expression of the zebrafish engrailed-2 gene. *Mech Dev* **39**, 51-62.
- Force, A., Lynch, M., Pickett, F. B., Amores, A., Yan, Y. L. and Postlethwait, J.** (1999). Preservation of duplicate genes by complementary, degenerative mutations. *Genetics* **151**, 1531-45.
- Frank, M. and Kemler, R.** (2002). Protocadherins. *Curr Opin Cell Biol* **14**, 557-62.
- Furthauer, M., Thisse, C. and Thisse, B.** (1997). A role for FGF-8 in the dorsoventral patterning of the zebrafish gastrula. *Development* **124**, 4253-64.
- Furthauer, M., Van Celst, J., Thisse, C. and Thisse, B.** (2004). Fgf signalling controls the dorsoventral patterning of the zebrafish embryo. *Development* **131**, 2853-64.
- Gavalas, A. and Krumlauf, R.** (2000). Retinoid signalling and hindbrain patterning. *Curr Opin Genet Dev* **10**, 380-6.
- Gilbert, S. F.** (2000). *Developmental Biology*, 6th Edition. Sunderland (MA): Sinauer Associates, Inc.
- Giudicelli, F. and Lewis, J.** (2004). The vertebrate segmentation clock. *Curr Opin Genet Dev* **14**, 407-14.
- Grandel, H., Kaslin, J., Ganz, J., Wenzel, I. and Brand, M.** (2006). Neural stem cells and neurogenesis in the adult zebrafish brain: origin, proliferation dynamics, migration and cell fate. *Dev Biol* **295**, 263-77.
- Griffin, K. J. and Kimelman, D.** (2003). Interplay between FGF, one-eyed pinhead, and T-box transcription factors during zebrafish posterior development. *Dev Biol* **264**, 456-66.

- Haffter, P. and Nusslein-Volhard, C.** (1996). Large scale genetics in a small vertebrate, the zebrafish. *Int J Dev Biol* **40**, 221-7.
- Halloran, M. C. and Berndt, J. D.** (2003). Current progress in neural crest cell motility and migration and future prospects for the zebrafish model system. *Dev Dyn* **228**, 497-513.
- Hatta, K., Kimmel, C. B., Ho, R. K. and Walker, C.** (1991). The cyclops mutation blocks specification of the floor plate of the zebrafish central nervous system. *Nature* **350**, 339-41.
- Hauptmann, G. and Gerster, T.** (1994). Two-color whole-mount in situ hybridization to vertebrate and Drosophila embryos. *Trends Genet* **10**, 266.
- Hawley, S. H., Wunnenberg-Stapleton, K., Hashimoto, C., Laurent, M. N., Watabe, T., Blumberg, B. W. and Cho, K. W.** (1995). Disruption of BMP signals in embryonic Xenopus ectoderm leads to direct neural induction. *Genes Dev* **9**, 2923-35.
- Heeg-Truesdell, E. and LaBonne, C.** (2004). A slug, a fox, a pair of sox: transcriptional responses to neural crest inducing signals. *Birth Defects Res C Embryo Today* **72**, 124-39.
- Helms, A. W. and Johnson, J. E.** (2003). Specification of dorsal spinal cord interneurons. *Curr Opin Neurobiol* **13**, 42-9.
- Hernandez-Lagunas, L., Choi, I. F., Kaji, T., Simpson, P., Hershey, C., Zhou, Y., Zon, L., Mercola, M. and Artinger, K. B.** (2005). Zebrafish narrowminded disrupts the transcription factor *prdm1* and is required for neural crest and sensory neuron specification. *Dev Biol* **278**, 347-57.
- Holley, S. A.** (2006). Anterior-posterior differences in vertebrate segments: specification of trunk and tail somites in the zebrafish blastula. *Genes Dev* **20**, 1831-7.
- Holley, S. A.** (2007). The genetics and embryology of zebrafish metamerism. *Dev Dyn*.
- Holley, S. A., Geisler, R. and Nusslein-Volhard, C.** (2000). Control of *her1* expression during zebrafish somitogenesis by a delta-dependent oscillator and an independent wave-front activity. *Genes Dev* **14**, 1678-90.
- Holley, S. A., Julich, D., Rauch, G. J., Geisler, R. and Nusslein-Volhard, C.** (2002). *her1* and the notch pathway function within the oscillator mechanism that regulates zebrafish somitogenesis. *Development* **129**, 1175-83.
- Holley, S. A. and Takeda, H.** (2002). Catching a wave: the oscillator and wavefront that create the zebrafish somite. *Semin Cell Dev Biol* **13**, 481-8.
- Houart, C., Westerfield, M. and Wilson, S. W.** (1998). A small population of anterior cells patterns the forebrain during zebrafish gastrulation. *Nature* **391**, 788-92.
- Ikeya, M. and Takada, S.** (1998). Wnt signaling from the dorsal neural tube is required for the formation of the medial dermomyotome. *Development* **125**, 4969-76.
- Ingham, P. W. and Kim, H. R.** (2005). Hedgehog signalling and the specification of muscle cell identity in the zebrafish embryo. *Exp Cell Res* **306**, 336-42.
- Ishitani, T., Matsumoto, K., Chitnis, A. B. and Itoh, M.** (2005). Nrarp functions to modulate neural-crest-cell differentiation by regulating LEF1 protein stability. *Nat Cell Biol* **7**, 1106-12.
- Itoh, M., Kim, C. H., Palardy, G., Oda, T., Jiang, Y. J., Maust, D., Yeo, S. Y., Lorick, K., Wright, G. J., Ariza-McNaughton, L. et al.** (2003). Mind bomb is a ubiquitin ligase that is essential for efficient activation of Notch signaling by Delta. *Dev Cell* **4**, 67-82.
- Iwasaki, W., Nagata, K., Hatanaka, H., Inui, T., Kimura, T., Muramatsu, T., Yoshida, K., Tasumi, M. and Inagaki, F.** (1997). Solution structure of midkine, a new heparin-binding growth factor. *Embo J* **16**, 6936-46.
- Jessell, T. M.** (2000). Neuronal specification in the spinal cord: inductive signals and transcriptional codes. *Nat Rev Genet* **1**, 20-9.
- Kadomatsu, K., Huang, R. P., Suganuma, T., Murata, F. and Muramatsu, T.** (1990). A retinoic acid responsive gene MK found in the teratocarcinoma system is expressed in spatially and temporally controlled manner during mouse embryogenesis. *J Cell Biol* **110**, 607-16.
- Kadomatsu, K. and Muramatsu, T.** (2004). Midkine and pleiotrophin in neural development and cancer. *Cancer Lett* **204**, 127-43.
- Kadomatsu, K., Tomomura, M. and Muramatsu, T.** (1988). cDNA cloning and sequencing of a new gene intensely expressed in early differentiation stages of embryonal carcinoma cells and in mid-gestation period of mouse embryogenesis. *Biochem Biophys Res Commun* **151**, 1312-8.
- Kaji, T. and Artinger, K. B.** (2004). *dlx3b* and *dlx4b* function in the development of Rohon-Beard sensory neurons and trigeminal placode in the zebrafish neurula. *Dev Biol* **276**, 523-40.
- Kawakami, Y., Raya, A., Raya, R. M., Rodriguez-Esteban, C. and Belmonte, J. C.** (2005). Retinoic acid signalling links left-right asymmetric patterning and bilaterally symmetric somitogenesis in the zebrafish embryo. *Nature* **435**, 165-71.
- Kelsh, R. N., Brand, M., Jiang, Y. J., Heisenberg, C. P., Lin, S., Haffter, P., Odenthal, J., Mullins, M. C., van Eeden, F. J., Furutani-Seiki, M. et al.** (1996). Zebrafish pigmentation mutations and the processes of neural crest development. *Development* **123**, 369-89.
- Kilpelainen, I., Kaksonen, M., Kinnunen, T., Avikainen, H., Fath, M., Linhardt, R. J., Raulo, E. and Rauvala, H.** (2000). Heparin-binding growth-associated molecule contains two heparin-binding beta -sheet domains that are homologous to the thrombospondin type I repeat. *J Biol Chem* **275**, 13564-70.
- Kim, S. H., Jen, W. C., De Robertis, E. M. and Kintner, C.** (2000). The protocadherin PAPC establishes segmental boundaries during somitogenesis in xenopus embryos. *Curr Biol* **10**, 821-30.
- Kim, S. H., Shin, J., Park, H. C., Yeo, S. Y., Hong, S. K., Han, S., Rhee, M., Kim, C. H., Chitnis, A. B. and Huh, T. L.** (2002). Specification of an anterior neuroectoderm patterning by Frizzled8a-mediated Wnt8b signalling during late gastrulation in zebrafish. *Development* **129**, 4443-55.
- Kimmel, C. B., Ballard, W. W., Kimmel, S. R., Ullmann, B. and Schilling, T. F.** (1995). Stages of embryonic development of the zebrafish. *Dev Dyn* **203**, 253-310.
- Klein, P. S. and Melton, D. A.** (1996). A molecular mechanism for the effect of lithium on development. *Proc Natl Acad Sci U S A* **93**, 8455-9.
- Knecht, A. K. and Bronner-Fraser, M.** (2002). Induction of the neural crest: a multigene process. *Nat Rev Genet* **3**, 453-61.

- Kojima, S., Inui, T., Muramatsu, H., Suzuki, Y., Kadomatsu, K., Yoshizawa, M., Hirose, S., Kimura, T., Sakakibara, S. and Muramatsu, T. (1997). Dimerization of midkine by tissue transglutaminase and its functional implication. *J Biol Chem* **272**, 9410-6.
- Kojima, T., Katsumi, A., Yamazaki, T., Muramatsu, T., Nagasaka, T., Ohsumi, K. and Saito, H. (1996). Human ryudocan from endothelium-like cells binds basic fibroblast growth factor, midkine, and tissue factor pathway inhibitor. *J Biol Chem* **271**, 5914-20.
- Korzh, V., Edlund, T. and Thor, S. (1993). Zebrafish primary neurons initiate expression of the LIM homeodomain protein Isl-1 at the end of gastrulation. *Development* **118**, 417-25.
- Korzh, V., Sleptsova, I., Liao, J., He, J. and Gong, Z. (1998). Expression of zebrafish bHLH genes *ngn1* and *nrd* defines distinct stages of neural differentiation. *Dev Dyn* **213**, 92-104.
- Krauss, S., Johansen, T., Korzh, V. and Fjose, A. (1991). Expression of the zebrafish paired box gene *pax[zf-b]* during early neurogenesis. *Development* **113**, 1193-206.
- Krumlauf, R., Marshall, H., Studer, M., Nonchev, S., Sham, M. H. and Lumsden, A. (1993). Hox homeobox genes and regionalisation of the nervous system. *J Neurobiol* **24**, 1328-40.
- LaBonne, C. (2002). Vertebrate development: wnt signals at the crest. *Curr Biol* **12**, R743-4.
- LaBonne, C. and Bronner-Fraser, M. (1998a). Induction and patterning of the neural crest, a stem cell-like precursor population. *J Neurobiol* **36**, 175-89.
- LaBonne, C. and Bronner-Fraser, M. (1998b). Neural crest induction in *Xenopus*: evidence for a two-signal model. *Development* **125**, 2403-14.
- Lallier, T. E. and Bronner-Fraser, M. (1988). A spatial and temporal analysis of dorsal root and sympathetic ganglion formation in the avian embryo. *Dev Biol* **127**, 99-112.
- Le Douarin, N. and Kalcheim, C. (1999). *The Neural Crest*. New York: Cambridge University Press.
- Le Douarin, N. M. and Dupin, E. (2003). Multipotentiality of the neural crest. *Curr Opin Genet Dev* **13**, 529-36.
- Lee, H. C., Huang, H. Y., Lin, C. Y., Chen, Y. H. and Tsai, H. J. (2006). Foxd3 mediates zebrafish *myf5* expression during early somitogenesis. *Dev Biol* **290**, 359-72.
- Leimeister, C., Dale, K., Fischer, A., Klamt, B., Hrabe de Angelis, M., Radtke, F., McGrew, M. J., Pourquie, O. and Gessler, M. (2000). Oscillating expression of *c-Hey2* in the presomitic mesoderm suggests that the segmentation clock may use combinatorial signaling through multiple interacting bHLH factors. *Dev Biol* **227**, 91-103.
- Lekven, A. C., Buckles, G. R., Kostakis, N. and Moon, R. T. (2003). Wnt1 and *wnt10b* function redundantly at the zebrafish midbrain-hindbrain boundary. *Dev Biol* **254**, 172-87.
- Lewis, J. L., Bonner, J., Modrell, M., Ragland, J. W., Moon, R. T., Dorsky, R. I. and Raible, D. W. (2004). Reiterated Wnt signaling during zebrafish neural crest development. *Development* **131**, 1299-308.
- Li, M., Zhao, C., Wang, Y., Zhao, Z. and Meng, A. (2002). Zebrafish *sox9b* is an early neural crest marker. *Dev Genes Evol* **212**, 203-6.
- Li, W. and Cornell, R. A. (2007). Redundant activities of *Tfap2a* and *Tfap2c* are required for neural crest induction and development of other non-neural ectoderm derivatives in zebrafish embryos. *Dev Biol* **304**, 338-54.
- Li, Y. S., Milner, P. G., Chauhan, A. K., Watson, M. A., Hoffman, R. M., Kodner, C. M., Milbrandt, J. and Deuel, T. F. (1990). Cloning and expression of a developmentally regulated protein that induces mitogenic and neurite outgrowth activity. *Science* **250**, 1690-4.
- Lieschke, G. J. and Currie, P. D. (2007). Animal models of human disease: zebrafish swim into view. *Nat Rev Genet* **8**, 353-67.
- Lister, J. A., Cooper, C., Nguyen, K., Modrell, M., Grant, K. and Raible, D. W. (2006). Zebrafish Foxd3 is required for development of a subset of neural crest derivatives. *Dev Biol* **290**, 92-104.
- Lu, K. V., Jong, K. A., Kim, G. Y., Singh, J., Dia, E. Q., Yoshimoto, K., Wang, M. Y., Cloughesy, T. F., Nelson, S. F. and Mischel, P. S. (2005). Differential induction of glioblastoma migration and growth by two forms of pleiotrophin. *J Biol Chem* **280**, 26953-64.
- Lun, K. and Brand, M. (1998). A series of no isthmus (*noi*) alleles of the zebrafish *pax2.1* gene reveals multiple signaling events in development of the midbrain-hindbrain boundary. *Development* **125**, 3049-62.
- Lupo, G., Andreazzoli, M., Gestri, G., Liu, Y., He, R. Q. and Barsacchi, G. (2000). Homeobox genes in the genetic control of eye development. *Int J Dev Biol* **44**, 627-36.
- Lupo, G., Harris, W. A. and Lewis, K. E. (2006). Mechanisms of ventral patterning in the vertebrate nervous system. *Nat Rev Neurosci* **7**, 103-14.
- Macdonald, R., Barth, K. A., Xu, Q., Holder, N., Mikkola, I. and Wilson, S. W. (1995). Midline signalling is required for Pax gene regulation and patterning of the eyes. *Development* **121**, 3267-78.
- Maeda, N., Ichihara-Tanaka, K., Kimura, T., Kadomatsu, K., Muramatsu, T. and Noda, M. (1999). A receptor-like protein-tyrosine phosphatase PTPzeta/RPTPbeta binds a heparin-binding growth factor midkine. Involvement of arginine 78 of midkine in the high affinity binding to PTPzeta. *J Biol Chem* **274**, 12474-9.
- Manzanares, M., Trainor, P. A., Nonchev, S., Ariza-McNaughton, L., Brodie, J., Gould, A., Marshall, H., Morrison, A., Kwan, C. T., Sham, M. H. et al. (1999). The role of kreisler in segmentation during hindbrain development. *Dev Biol* **211**, 220-37.
- Marshall, H., Nonchev, S., Sham, M. H., Muchamore, I., Lumsden, A. and Krumlauf, R. (1992). Retinoic acid alters hindbrain Hox code and induces transformation of rhombomeres 2/3 into a 4/5 identity. *Nature* **360**, 737-41.
- Masuda, K., Watanabe, I., Unoki, K., Ohba, N. and Muramatsu, T. (1995). Functional Rescue of photoreceptors from the damaging effects of constant light by survival-promoting factors in the rat. *Invest Ophthalmol Vis Sci* **36**, 2142-6.
- Matsumoto, K., Wanaka, A., Mori, T., Taguchi, A., Ishii, N., Muramatsu, H., Muramatsu, T. and Tohyama, M. (1994a). Localization of pleiotrophin and midkine in the postnatal developing cerebellum. *Neurosci Lett* **178**, 216-20.
- Matsumoto, K., Wanaka, A., Takatsuji, K., Muramatsu, H., Muramatsu, T. and Tohyama, M. (1994b). A novel family of heparin-binding growth factors, pleiotrophin and midkine, is expressed in the developing rat cerebral cortex. *Brain Res Dev Brain Res* **79**, 229-41.

- Maves, L., Jackman, W. and Kimmel, C. B. (2002). FGF3 and FGF8 mediate a rhombomere 4 signaling activity in the zebrafish hindbrain. *Development* **129**, 3825-37.
- Mayor, R., Guerrero, N. and Martinez, C. (1997). Role of FGF and noggin in neural crest induction. *Dev Biol* **189**, 1-12.
- McClintock, J. M., Kheirbek, M. A. and Prince, V. E. (2002). Knockdown of duplicated zebrafish *hoxb1* genes reveals distinct roles in hindbrain patterning and a novel mechanism of duplicate gene retention. *Development* **129**, 2339-54.
- Meinhardt, H. (2006). Primary body axes of vertebrates: generation of a near-Cartesian coordinate system and the role of Spemann-type organizer. *Dev Dyn* **235**, 2907-19.
- Merenmies, J. and Rauvala, H. (1990). Molecular cloning of the 18-kDa growth-associated protein of developing brain. *J Biol Chem* **265**, 16721-4.
- Meulemans, D. and Bronner-Fraser, M. (2004). Gene-regulatory interactions in neural crest evolution and development. *Dev Cell* **7**, 291-9.
- Meyer, A. and Malaga-Trillo, E. (1999). Vertebrate genomics: More fishy tales about Hox genes. *Curr Biol* **9**, R210-3.
- Meyer, A. and Schartl, M. (1999). Gene and genome duplications in vertebrates: the one-to-four (-to-eight in fish) rule and the evolution of novel gene functions. *Curr Opin Cell Biol* **11**, 699-704.
- Mi, R., Chen, W. and Hoke, A. (2007). Pleiotrophin is a neurotrophic factor for spinal motor neurons. *Proc Natl Acad Sci U S A* **104**, 4664-9.
- Michikawa, M., Xu, R. Y., Muramatsu, H., Muramatsu, T. and Kim, S. U. (1993). Midkine is a mediator of retinoic acid induced neuronal differentiation of embryonal carcinoma cells. *Biochem Biophys Res Commun* **192**, 1312-8.
- Milner, P. G., Li, Y. S., Hoffman, R. M., Kodner, C. M., Siegel, N. R. and Deuel, T. F. (1989). A novel 17 kD heparin-binding growth factor (HBGF-8) in bovine uterus: purification and N-terminal amino acid sequence. *Biochem Biophys Res Commun* **165**, 1096-103.
- Miyashiro, M., Kadomatsu, K., Ogata, N., Yamamoto, C., Takahashi, K., Uyama, M., Muramatsu, H. and Muramatsu, T. (1998). Midkine expression in transient retinal ischemia in the rat. *Curr Eye Res* **17**, 9-13.
- Moens, C. B., Cordes, S. P., Giorgianni, M. W., Barsh, G. S. and Kimmel, C. B. (1998). Equivalence in the genetic control of hindbrain segmentation in fish and mouse. *Development* **125**, 381-91.
- Moens, C. B. and Prince, V. E. (2002). Constructing the hindbrain: insights from the zebrafish. *Dev Dyn* **224**, 1-17.
- Moens, C. B., Yan, Y. L., Appel, B., Force, A. G. and Kimmel, C. B. (1996). *valentino*: a zebrafish gene required for normal hindbrain segmentation. *Development* **122**, 3981-90.
- Mohammadi, M., McMahon, G., Sun, L., Tang, C., Hirth, P., Yeh, B. K., Hubbard, S. R. and Schlessinger, J. (1997). Structures of the tyrosine kinase domain of fibroblast growth factor receptor in complex with inhibitors. *Science* **276**, 955-60.
- Mollaaghababa, R. and Pavan, W. J. (2003). The importance of having your SOX on: role of SOX10 in the development of neural crest-derived melanocytes and glia. *Oncogene* **22**, 3024-34.
- Monsoro-Burq, A. H., Fletcher, R. B. and Harland, R. M. (2003). Neural crest induction by paraxial mesoderm in *Xenopus* embryos requires FGF signals. *Development* **130**, 3111-24.
- Monsoro-Burq, A. H., Wang, E. and Harland, R. (2005). *Msx1* and *Pax3* cooperate to mediate FGF8 and WNT signals during *Xenopus* neural crest induction. *Dev Cell* **8**, 167-78.
- Montero-Balaguer, M., Lang, M. R., Sachdev, S. W., Knappmeyer, C., Stewart, R. A., De La Guardia, A., Hatzopoulos, A. K. and Knapik, E. W. (2006). The mother superior mutation ablates *foxd3* activity in neural crest progenitor cells and depletes neural crest derivatives in zebrafish. *Dev Dyn* **235**, 3199-212.
- Moreno, T. A. and Kintner, C. (2004). Regulation of segmental patterning by retinoic acid signaling during *Xenopus* somitogenesis. *Dev Cell* **6**, 205-18.
- Morita, T., Nitta, H., Kiyama, Y., Mori, H. and Mishina, M. (1995). Differential expression of two zebrafish *emx* homeoprotein mRNAs in the developing brain. *Neurosci Lett* **198**, 131-4.
- Mueller, T. and Wullimann, M. F. (2003). Anatomy of neurogenesis in the early zebrafish brain. *Brain Res Dev Brain Res* **140**, 137-55.
- Muller, M., v Weizsacker, E. and Campos-Ortega, J. A. (1996). Expression domains of a zebrafish homologue of the *Drosophila* pair-rule gene *hairy* correspond to primordia of alternating somites. *Development* **122**, 2071-8.
- Muramatsu, H., Zou, K., Sakaguchi, N., Ikematsu, S., Sakuma, S. and Muramatsu, T. (2000). LDL receptor-related protein as a component of the midkine receptor. *Biochem Biophys Res Commun* **270**, 936-41.
- Muramatsu, H., Zou, P., Kurosawa, N., Ichihara-Tanaka, K., Maruyama, K., Inoh, K., Sakai, T., Chen, L., Sato, M. and Muramatsu, T. (2006). Female infertility in mice deficient in midkine and pleiotrophin, which form a distinct family of growth factors. *Genes Cells* **11**, 1405-17.
- Muramatsu, T. (1992). Retinoic acid regulates the expression of a new heparin binding growth differentiation factor. *J Nutr Sci Vitaminol (Tokyo) Spec No*, 485-7.
- Muramatsu, T. (2002). Midkine and pleiotrophin: two related proteins involved in development, survival, inflammation and tumorigenesis. *J Biochem (Tokyo)* **132**, 359-71.
- Nakamura, E., Kadomatsu, K., Yuasa, S., Muramatsu, H., Mamiya, T., Nabeshima, T., Fan, Q. W., Ishiguro, K., Igakura, T., Matsubara, S. et al. (1998). Disruption of the midkine gene (*Mdk*) resulted in altered expression of a calcium binding protein in the hippocampus of infant mice and their abnormal behaviour. *Genes Cells* **3**, 811-22.
- Nasevicius, A. and Ekker, S. C. (2000). Effective targeted gene 'knockdown' in zebrafish. *Nat Genet* **26**, 216-20.
- Ng, L. J., Wheatley, S., Muscat, G. E., Conway-Campbell, J., Bowles, J., Wright, E., Bell, D. M., Tam, P. P., Cheah, K. S. and Koopman, P. (1997). SOX9 binds DNA, activates transcription, and coexpresses with type II collagen during chondrogenesis in the mouse. *Dev Biol* **183**, 108-21.
- Nguyen, V. H., Schmid, B., Trout, J., Connors, S. A., Ekker, M. and Mullins, M. C. (1998). Ventral and lateral regions of the zebrafish gastrula, including the neural crest progenitors, are established by a *bmp2b*/swirl pathway of genes. *Dev Biol* **199**, 93-110.
- Niehrs, C. (2004). Regionally specific induction by the Spemann-Mangold organizer. *Nat Rev Genet* **5**, 425-34.
- Nieuwkoop, P. D. (1973). The organization center of the amphibian embryo: its origin, spatial organization, and morphogenetic action. *Adv Morphog* **10**, 1-39.

- Nikaido, M., Kawakami, A., Sawada, A., Furutani-Seiki, M., Takeda, H. and Araki, K.** (2002). Tbx24, encoding a T-box protein, is mutated in the zebrafish somite-segmentation mutant fused somites. *Nat Genet* **31**, 195-9.
- Nornes, S., Clarkson, M., Mikkola, I., Pedersen, M., Bardsley, A., Martinez, J. P., Krauss, S. and Johansen, T.** (1998). Zebrafish contains two pax6 genes involved in eye development. *Mech Dev* **77**, 185-96.
- Oates, A. C. and Ho, R. K.** (2002). Hairy/E(spl)-related (Her) genes are central components of the segmentation oscillator and display redundancy with the Delta/Notch signaling pathway in the formation of anterior segmental boundaries in the zebrafish. *Development* **129**, 2929-46.
- Oates, A. C., Rohde, L. A. and Ho, R. K.** (2005). Generation of segment polarity in the paraxial mesoderm of the zebrafish through a T-box-dependent inductive event. *Dev Biol* **283**, 204-14.
- Odenthal, J. and Nusslein-Volhard, C.** (1998). fork head domain genes in zebrafish. *Dev Genes Evol* **208**, 245-58.
- Odenthal, J., van Eeden, F. J., Haffter, P., Ingham, P. W. and Nusslein-Volhard, C.** (2000). Two distinct cell populations in the floor plate of the zebrafish are induced by different pathways. *Dev Biol* **219**, 350-63.
- Oxtoby, E. and Jowett, T.** (1993). Cloning of the zebrafish krox-20 gene (krx-20) and its expression during hindbrain development. *Nucleic Acids Res* **21**, 1087-95.
- Pan, G., Li, J., Zhou, Y., Zheng, H. and Pei, D.** (2006). A negative feedback loop of transcription factors that controls stem cell pluripotency and self-renewal. *Faseb J* **20**, 1730-2.
- Pan, G. and Thomson, J. A.** (2007). Nanog and transcriptional networks in embryonic stem cell pluripotency. *Cell Res* **17**, 42-9.
- Persson, M., Stamataki, D., te Welscher, P., Andersson, E., Bose, J., Ruther, U., Ericson, J. and Briscoe, J.** (2002). Dorsal-ventral patterning of the spinal cord requires Gli3 transcriptional repressor activity. *Genes Dev* **16**, 2865-78.
- Peterson, R. T., Link, B. A., Dowling, J. E. and Schreiber, S. L.** (2000). Small molecule developmental screens reveal the logic and timing of vertebrate development. *Proc Natl Acad Sci U S A* **97**, 12965-9.
- Phillips, B. T., Kwon, H. J., Melton, C., Houghtaling, P., Fritz, A. and Riley, B. B.** (2006). Zebrafish msxB, msxC and msxE function together to refine the neural-non-neural border and regulate cranial placodes and neural crest development. *Dev Biol* **294**, 376-90.
- Pla, P., Moore, R., Morali, O. G., Grille, S., Martinozzi, S., Delmas, V. and Larue, L.** (2001). Cadherins in neural crest cell development and transformation. *J Cell Physiol* **189**, 121-32.
- Pourquie, O.** (2001). Vertebrate somitogenesis. *Annu Rev Cell Dev Biol* **17**, 311-50.
- Prince, V. E., Moens, C. B., Kimmel, C. B. and Ho, R. K.** (1998). Zebrafish hox genes: expression in the hindbrain region of wild-type and mutants of the segmentation gene, valentino. *Development* **125**, 393-406.
- Purves, D., Augustine, G. J., Fitzpatrick, D., Katz, L. C. and LaMantia, A.-S. M., James O.; Williams, S. Mark.** (2001). Neuroscience, 2nd Edition. Sunderland (MA): Sinauer Associates, Inc.
- Ragland, J. W. and Raible, D. W.** (2004). Signals derived from the underlying mesoderm are dispensable for zebrafish neural crest induction. *Dev Biol* **276**, 16-30.
- Raible, D. W.** (2006). Development of the neural crest: achieving specificity in regulatory pathways. *Curr Opin Cell Biol* **18**, 698-703.
- Raible, D. W. and Eisen, J. S.** (1994). Restriction of neural crest cell fate in the trunk of the embryonic zebrafish. *Development* **120**, 495-503.
- Raible, D. W. and Ragland, J. W.** (2005). Reiterated Wnt and BMP signals in neural crest development. *Semin Cell Dev Biol* **16**, 673-82.
- Raible, D. W., Wood, A., Hodsdon, W., Henion, P. D., Weston, J. A. and Eisen, J. S.** (1992). Segregation and early dispersal of neural crest cells in the embryonic zebrafish. *Dev Dyn* **195**, 29-42.
- Raible, F. and Brand, M.** (2001). Tight transcriptional control of the ETS domain factors Erm and Pea3 by Fgf signaling during early zebrafish development. *Mech Dev* **107**, 105-17.
- Rauvala, H.** (1989). An 18-kd heparin-binding protein of developing brain that is distinct from fibroblast growth factors. *Embo J* **8**, 2933-41.
- Rauvala, H., Huttunen, H. J., Fages, C., Kaksonen, M., Kinnunen, T., Imai, S., Raulo, E. and Kilpelainen, I.** (2000). Heparin-binding proteins HB-GAM (pleiotrophin) and amphoterin in the regulation of cell motility. *Matrix Biol* **19**, 377-87.
- Reifers, F., Bohli, H., Walsh, E. C., Crossley, P. H., Stainier, D. Y. and Brand, M.** (1998). Fgf8 is mutated in zebrafish acerebellar (ace) mutants and is required for maintenance of midbrain-hindbrain boundary development and somitogenesis. *Development* **125**, 2381-95.
- Rhinn, M., Picker, A. and Brand, M.** (2006). Global and local mechanisms of forebrain and midbrain patterning. *Curr Opin Neurobiol* **16**, 5-12.
- Roger, J., Brajeul, V., Thomasseau, S., Hienola, A., Sahel, J. A., Guillonnet, X. and Goureau, O.** (2006). Involvement of Pleiotrophin in CNTF-mediated differentiation of the late retinal progenitor cells. *Dev Biol* **298**, 527-39.
- Roy, S. and Ng, T.** (2004). Blimp-1 specifies neural crest and sensory neuron progenitors in the zebrafish embryo. *Curr Biol* **14**, 1772-7.
- Rubenstein, J. L., Shimamura, K., Martinez, S. and Puelles, L.** (1998). Regionalization of the prosencephalic neural plate. *Annu Rev Neurosci* **21**, 445-77.
- Saint-Jeannet, J. P., He, X., Varmus, H. E. and Dawid, I. B.** (1997). Regulation of dorsal fate in the neuraxis by Wnt-1 and Wnt-3a. *Proc Natl Acad Sci U S A* **94**, 13713-8.
- Sakaguchi, N., Muramatsu, H., Ichihara-Tanaka, K., Maeda, N., Noda, M., Yamamoto, T., Michikawa, M., Ikematsu, S., Sakuma, S. and Muramatsu, T.** (2003). Receptor-type protein tyrosine phosphatase zeta as a component of the signaling receptor complex for midkine-dependent survival of embryonic neurons. *Neurosci Res* **45**, 219-24.
- Sambrook, J., Fritsch, E. F. and Maniatis, T.** (1989). Molecular Cloning: A Laboratory Manual. NY: Cold Spring Harbor Laboratory Press.
- Sato, T., Sasai, N. and Sasai, Y.** (2005). Neural crest determination by co-activation of Pax3 and Zic1 genes in Xenopus ectoderm. *Development* **132**, 2355-63.

- Sawada, A., Fritz, A., Jiang, Y. J., Yamamoto, A., Yamasu, K., Kuroiwa, A., Saga, Y. and Takeda, H. (2000). Zebrafish Mesp family genes, *mesp-a* and *mesp-b* are segmentally expressed in the presomitic mesoderm, and *Mesp-b* confers the anterior identity to the developing somites. *Development* **127**, 1691-702.
- Sawada, A., Shinya, M., Jiang, Y. J., Kawakami, A., Kuroiwa, A. and Takeda, H. (2001). Fgf/MAPK signalling is a crucial positional cue in somite boundary formation. *Development* **128**, 4873-80.
- Schafer, M., Rembold, M., Wittbrodt, J., Schartl, M. and Winkler, C. (2005). Medial floor plate formation in zebrafish consists of two phases and requires trunk-derived *Midkine-a*. *Genes Dev* **19**, 897-902.
- Schier, A. F., Neuhauss, S. C., Helde, K. A., Talbot, W. S. and Driever, W. (1997). The one-eyed pinhead gene functions in mesoderm and endoderm formation in zebrafish and interacts with *no tail*. *Development* **124**, 327-42.
- Schilling, T. F. and Knight, R. D. (2001). Origins of anteroposterior patterning and Hox gene regulation during chordate evolution. *Philos Trans R Soc Lond B Biol Sci* **356**, 1599-613.
- Schilling, T. F., Piotrowski, T., Grandel, H., Brand, M., Heisenberg, C. P., Jiang, Y. J., Beuchle, D., Hammerschmidt, M., Kane, D. A., Mullins, M. C. et al. (1996). Jaw and branchial arch mutants in zebrafish I: branchial arches. *Development* **123**, 329-44.
- Schilling, T. F., Prince, V. and Ingham, P. W. (2001). Plasticity in zebrafish hox expression in the hindbrain and cranial neural crest. *Dev Biol* **231**, 201-16.
- Scholpp, S. and Brand, M. (2001). Morpholino-induced knockdown of zebrafish engrailed genes *eng2* and *eng3* reveals redundant and unique functions in midbrain-hindbrain boundary development. *Genesis* **30**, 129-33.
- Scholpp, S., Wolf, O., Brand, M. and Lumsden, A. (2006). Hedgehog signalling from the zona limitans intrathalamica orchestrates patterning of the zebrafish diencephalon. *Development* **133**, 855-64.
- Schulte-Merker, S., Ho, R. K., Herrmann, B. G. and Nusslein-Volhard, C. (1992). The protein product of the zebrafish homologue of the mouse *T* gene is expressed in nuclei of the germ ring and the notochord of the early embryo. *Development* **116**, 1021-32.
- Sekiguchi, K., Yokota, C., Asashima, M., Kaname, T., Fan, Q. W., Muramatsu, T. and Kadomatsu, K. (1995). Restricted expression of *Xenopus* *midkine* gene during early development. *J Biochem (Tokyo)* **118**, 94-100.
- Seo, H. C., Saetre, B. O., Havik, B., Ellingsen, S. and Fjose, A. (1998). The zebrafish *Pax3* and *Pax7* homologues are highly conserved, encode multiple isoforms and show dynamic segment-like expression in the developing brain. *Mech Dev* **70**, 49-63.
- Shimeld, S. M. and Holland, P. W. (2000). Vertebrate innovations. *Proc Natl Acad Sci U S A* **97**, 4449-52.
- Simeone, A., Acampora, D., Gulisano, M., Stornaiuolo, A. and Boncinelli, E. (1992). Nested expression domains of four homeobox genes in developing rostral brain. *Nature* **358**, 687-90.
- Sirotkin, H. I., Gates, M. A., Kelly, P. D., Schier, A. F. and Talbot, W. S. (2000). *Fast1* is required for the development of dorsal axial structures in zebrafish. *Curr Biol* **10**, 1051-4.
- Sive, H. L., Hattori, K. and Weintraub, H. (1989). Progressive determination during formation of the anteroposterior axis in *Xenopus laevis*. *Cell* **58**, 171-80.
- Solnica-Krezel, L. (2002). Pattern Formation in Zebrafish. Berlin: Springer Verlag.
- Souttou, B., Juhl, H., Hackenbruck, J., Rockseisen, M., Klomp, H. J., Raulais, D., Vigny, M. and Wellstein, A. (1998). Relationship between serum concentrations of the growth factor pleiotrophin and pleiotrophin-positive tumors. *J Natl Cancer Inst* **90**, 1468-73.
- Spemann, H. M., Hilde. (1924). Über Induktion von Embryonalanlagen durch Implantation artfremder Organisatoren. *Arch. mikr. Anat. und Entw. mech.* **100**, 599-638.
- Stachel, S. E., Grunwald, D. J. and Myers, P. Z. (1993). Lithium perturbation and gooseoid expression identify a dorsal specification pathway in the pregastrula zebrafish. *Development* **117**, 1261-74.
- Stamatakis, D., Ulloa, F., Tsoni, S. V., Mynett, A. and Briscoe, J. (2005). A gradient of Gli activity mediates graded Sonic Hedgehog signaling in the neural tube. *Genes Dev* **19**, 626-41.
- Stemple, D. L. and Anderson, D. J. (1992). Isolation of a stem cell for neurons and glia from the mammalian neural crest. *Cell* **71**, 973-85.
- Stern, C. D. (2001). Initial patterning of the central nervous system: how many organizers? *Nat Rev Neurosci* **2**, 92-8.
- Stern, C. D. (2005). Neural induction: old problem, new findings, yet more questions. *Development* **132**, 2007-21.
- Stern, C. D. (2006). Neural induction: 10 years on since the 'default model'. *Curr Opin Cell Biol* **18**, 692-7.
- Steventon, B., Carmona-Fontaine, C. and Mayor, R. (2005). Genetic network during neural crest induction: from cell specification to cell survival. *Semin Cell Dev Biol* **16**, 647-54.
- Stoica, G. E., Kuo, A., Aigner, A., Sunitha, I., Souttou, B., Malerczyk, C., Caughey, D. J., Wen, D., Karavanov, A., Riegel, A. T. et al. (2001). Identification of anaplastic lymphoma kinase as a receptor for the growth factor pleiotrophin. *J Biol Chem* **276**, 16772-9.
- Stoica, G. E., Kuo, A., Powers, C., Bowden, E. T., Sale, E. B., Riegel, A. T. and Wellstein, A. (2002). *Midkine* binds to anaplastic lymphoma kinase (ALK) and acts as a growth factor for different cell types. *J Biol Chem* **277**, 35990-8.
- Strahle, U., Lam, C. S., Ertzer, R. and Rastegar, S. (2004). Vertebrate floor-plate specification: variations on common themes. *Trends Genet* **20**, 155-62.
- Stuart, G. W., McMurray, J. V. and Westerfield, M. (1988). Replication, integration and stable germ-line transmission of foreign sequences injected into early zebrafish embryos. *Development* **103**, 403-12.
- Taylor, J. S., Braasch, I., Frickey, T., Meyer, A. and Van de Peer, Y. (2003). Genome duplication, a trait shared by 22000 species of ray-finned fish. *Genome Res* **13**, 382-90.
- Taylor, J. S. and Raes, J. (2004). Duplication and divergence: the evolution of new genes and old ideas. *Annu Rev Genet* **38**, 615-43.
- Thisse, C., Thisse, B. and Postlethwait, J. H. (1995). Expression of *snail2*, a second member of the zebrafish *snail* family, in cephalic mesendoderm and presumptive neural crest of wild-type and *spadetail* mutant embryos. *Dev Biol* **172**, 86-99.

- Tian, J., Yam, C., Balasundaram, G., Wang, H., Gore, A. and Sampath, K. (2003). A temperature-sensitive mutation in the nodal-related gene cyclops reveals that the floor plate is induced during gastrulation in zebrafish. *Development* **130**, 3331-42.
- Tribulo, C., Aybar, M. J., Nguyen, V. H., Mullins, M. C. and Mayor, R. (2003). Regulation of Msx genes by a Bmp gradient is essential for neural crest specification. *Development* **130**, 6441-52.
- Unoki, K., Ohba, N., Arimura, H., Muramatsu, H. and Muramatsu, T. (1994). Rescue of photoreceptors from the damaging effects of constant light by midkine, a retinoic acid-responsive gene product. *Invest Ophthalmol Vis Sci* **35**, 4063-8.
- van Eeden, F. J., Granato, M., Schach, U., Brand, M., Furutani-Seiki, M., Haffter, P., Hammerschmidt, M., Heisenberg, C. P., Jiang, Y. J., Kane, D. A. et al. (1996). Mutations affecting somite formation and patterning in the zebrafish, *Danio rerio*. *Development* **123**, 153-64.
- Vandepoele, K., De Vos, W., Taylor, J. S., Meyer, A. and Van de Peer, Y. (2004). Major events in the genome evolution of vertebrates: paraneome age and size differ considerably between ray-finned fishes and land vertebrates. *Proc Natl Acad Sci U S A* **101**, 1638-43.
- Varga, Z. M., Wegner, J. and Westerfield, M. (1999). Anterior movement of ventral diencephalic precursors separates the primordial eye field in the neural plate and requires cyclops. *Development* **126**, 5533-46.
- Vermot, J., Gallego Llamas, J., Fraulob, V., Niederreither, K., Chambon, P. and Dolle, P. (2005). Retinoic acid controls the bilateral symmetry of somite formation in the mouse embryo. *Science* **308**, 563-6.
- Vermot, J. and Pourquie, O. (2005). Retinoic acid coordinates somitogenesis and left-right patterning in vertebrate embryos. *Nature* **435**, 215-20.
- Villanueva, S., Glavic, A., Ruiz, P. and Mayor, R. (2002). Posteriorization by FGF, Wnt, and retinoic acid is required for neural crest induction. *Dev Biol* **241**, 289-301.
- Volff, J. N. and Schartl, M. (2003). Evolution of signal transduction by gene and genome duplication in fish. *J Struct Funct Genomics* **3**, 139-50.
- Walshe, J., Maroon, H., McGonnell, I. M., Dickson, C. and Mason, I. (2002). Establishment of hindbrain segmental identity requires signaling by FGF3 and FGF8. *Curr Biol* **12**, 1117-23.
- Walshe, J. and Mason, I. (2003). Unique and combinatorial functions of Fgf3 and Fgf8 during zebrafish forebrain development. *Development* **130**, 4337-49.
- Westerfield, M. (1995). *The Zebrafish Book*. Eugene, OR: University of Oregon.
- Wienholds, E., van Eeden, F., Kusters, M., Mudde, J., Plasterk, R. H. and Cuppen, E. (2003). Efficient target-selected mutagenesis in zebrafish. *Genome Res* **13**, 2700-7.
- Wilson, L. and Maden, M. (2005). The mechanisms of dorsoventral patterning in the vertebrate neural tube. *Dev Biol* **282**, 1-13.
- Wilson, P. A. and Hemmati-Brivanlou, A. (1997). Vertebrate neural induction: inducers, inhibitors, and a new synthesis. *Neuron* **18**, 699-710.
- Wilson, S. I. and Edlund, T. (2001). Neural induction: toward a unifying mechanism. *Nat Neurosci* **4 Suppl**, 1161-8.
- Wilson, S. W. and Rubenstein, J. L. (2000). Induction and dorsoventral patterning of the telencephalon. *Neuron* **28**, 641-51.
- Winkler, C. and Moon, R. T. (2001). Zebrafish mdk2, a novel secreted midkine, participates in posterior neurogenesis. *Dev Biol* **229**, 102-18.
- Winkler, C., Schafer, M., Duschl, J., Schartl, M. and Wolff, J. N. (2003). Functional divergence of two zebrafish midkine growth factors following fish-specific gene duplication. *Genome Res* **13**, 1067-81.
- Winkler, C., Vielkind, J. R. and Schartl, M. (1991). Transient expression of foreign DNA during embryonic and larval development of the medaka fish (*Oryzias latipes*). *Mol Gen Genet* **226**, 129-40.
- Wittbrodt, J., Meyer, A. and Schartl, M. (1998). More genes in fish? *Bioessays* **20**, 511-515.
- Woda, J. M., Pastagia, J., Mercola, M. and Artinger, K. B. (2003). Dlx proteins position the neural plate border and determine adjacent cell fates. *Development* **130**, 331-42.
- Woo, K. and Fraser, S. E. (1995). Order and coherence in the fate map of the zebrafish nervous system. *Development* **121**, 2595-609.
- Wurst, W. and Bally-Cuif, L. (2001). Neural plate patterning: upstream and downstream of the isthmus organizer. *Nat Rev Neurosci* **2**, 99-108.
- Yamamoto, A., Amacher, S. L., Kim, S. H., Geissert, D., Kimmel, C. B. and De Robertis, E. M. (1998). Zebrafish paraxial protocadherin is a downstream target of spadetail involved in morphogenesis of gastrula mesoderm. *Development* **125**, 3389-97.
- Yan, Y. L., Willoughby, J., Liu, D., Crump, J. G., Wilson, C., Miller, C. T., Singer, A., Kimmel, C., Westerfield, M. and Postlethwait, J. H. (2005). A pair of Sox: distinct and overlapping functions of zebrafish sox9 co-orthologs in craniofacial and pectoral fin development. *Development* **132**, 1069-83.
- Yanfeng, W., Saint-Jeannet, J. P. and Klein, P. S. (2003). Wnt-frizzled signaling in the induction and differentiation of the neural crest. *Bioessays* **25**, 317-25.
- Zhang, J., Talbot, W. S. and Schier, A. F. (1998). Positional cloning identifies zebrafish one-eyed pinhead as a permissive EGF-related ligand required during gastrulation. *Cell* **92**, 241-51.
- Zon, L. I. and Peterson, R. T. (2005). In vivo drug discovery in the zebrafish. *Nat Rev Drug Discov* **4**, 35-44.
- Zou, P., Muramatsu, H., Sone, M., Hayashi, H., Nakashima, T. and Muramatsu, T. (2006). Mice doubly deficient in the midkine and pleiotrophin genes exhibit deficits in the expression of beta-tectorin gene and in auditory response. *Lab Invest* **86**, 645-53.
- Zupanc, G. K., Hinsch, K. and Gage, F. H. (2005). Proliferation, migration, neuronal differentiation, and long-term survival of new cells in the adult zebrafish brain. *J Comp Neurol* **488**, 290-319.

8. Appendix

8.1. Characterization of *ptn* MO

8.1.1. *ptn* ATG and splice Morpholinos show different potencies

To control for the specificity of the MO induced somite fusion defect, I designed a second independent MO directed against the translational start codon of *ptn*. Injection of this MO at doses higher than 15 ng/nl resulted in nearly 100% lethality, while injection of lower doses did not reveal any fusion of somites as analyzed by expression of *myoD* in injected embryos (5 ng/nl: 3% fused somites, n=32; 10 ng/nl: 17% fused somites, n=12; Fig. 42B,C). The same concentrations of *ptn* splice site MOs led to a higher percentage of embryos with fused somites (5ng/nl: 36% fused somites, n=59; 10ng/nl: 66% fused somites, n=85; Fig. 42D,E). This indicates that different *ptn* MOs may have different inhibiting potencies.

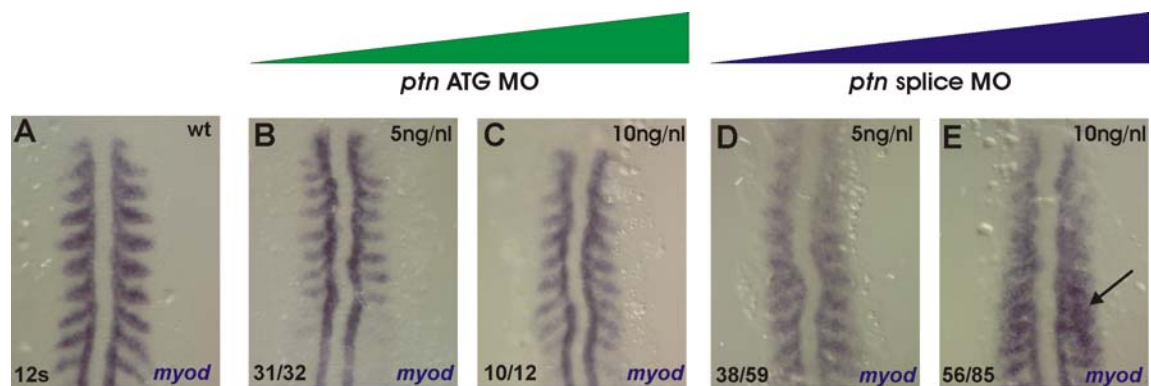


Fig. 42: Different potencies of *ptn* ATG and splice MOs to affect somite formation.

A Dorsal view of *myoD* expression in the somites and adaxial cells of a 12 somite stage embryo. **B,C** Injection of different concentrations of *ptn* ATG MO (5 ng/nl in B and 10 ng/nl in C) had little effect on somite development. **D,E** Injection of different concentrations of *ptn* splice MO (5 ng/nl in B and 10 ng/nl in C) resulted in clear alterations of somite appearance and somite fusion (arrow in E). Numbers indicate occurrence of embryos with displayed phenotype.

Next, I compared the potency of each of the two *ptn* splice MOs when injected separately (splice donor and splice acceptor). In situ hybridization against *myoD* and *papc* (protocadherin 8) mRNA was performed to visualize the adaxial mesoderm, somites and the PSM. Injection of *ptn* MO up (5 ng/nl; MO blocking the splice donor) resulted in a low number of only 23% of embryos showing somite fusion (n=68). However, 66% of these embryos showed irregular and blurred somite borders (arrow Fig. 43B,E). In comparison, 88% of embryos showed somite fusion when *ptn* MO down (5 ng/nl; MO blocking the splice acceptor) was injected (n=50). These embryos showed strong fusion of *myoD* expression domains in the paraxial mesoderm (arrow in Fig. 43C) and a reduction of *papc* expression throughout the complete

PSM (arrows in Fig. 43F). Both groups of MO injected embryos showed a typical shortening of the *papc* expression domain in the PSM when compared to wild-type embryos (n=84). The loss of *papc* expression in *ptn* morphants suggests a possible reduction of cell adhesion in PSM cells (Yamamoto et al., 1998). On the other hand, these results clearly show that both *ptn* splice MOs have different potencies in inducing the somite phenotype when injected individually.

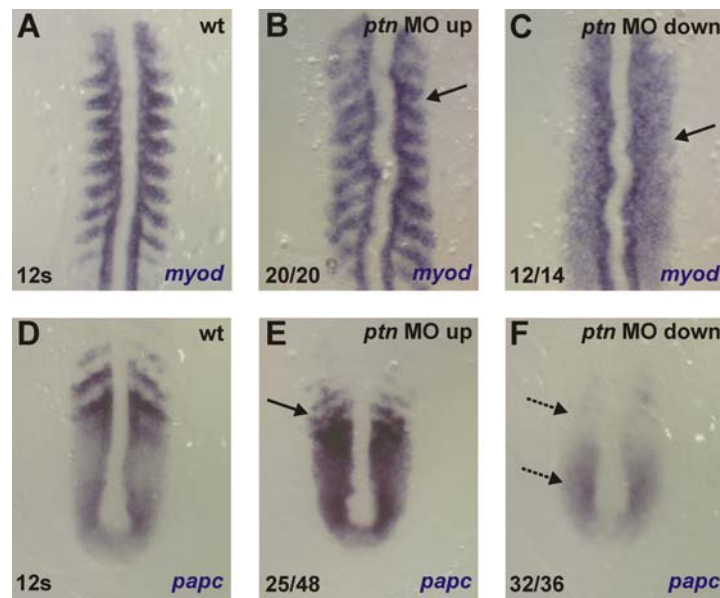


Fig. 43: *ptn* splice MOs have different effects on somite appearance when injected individually.

A-C Dorsal view of *myod* expression in the somites and the adaxial cells of 12 somite stage embryos. Injection of the “splice donor” MO (*ptn* MO up) resulted in moderate alterations of somite appearance (arrow in B), while injection of the same amount of the “splice acceptor” MO (*ptn* MO down) led to pronounced fusion of somitic *myod* expression (arrow in C). **D-F** Dorsal views of *papc* expression in the tail bud of 12 somite stage embryos. Incorrect somite spacing (arrow in E) and compression of the PSM result from injection of *ptn* MO up. Drastic reduction of *papc* expression in the PSM and in somites in *ptn* MO down injected embryos (arrows in F). Numbers indicate occurrence of the displayed phenotype.

To exclude unspecific binding of one of the MO to other related sequences, a whole-genome blast (Basic Local Alignment Search Tool) for highly similar sequences in the zebrafish genome was performed (www.ensembl.org). The sequence of the *ptn* MO up was only identified once in the genome at the expected position of the intron-exon border of *ptn*. Surprisingly, the sequence of the *ptn* MO down was found two times in the genome. One 100% homologous region was positioned at the intron-exon border of *ptn* (chr.6, bp29120986-bp29121010) as expected, but a second sequence was identified upstream of this locus in the first intron of the *ptn* gene (chromosome 6, bp 29118041-bp 29118065; Fig.34). Therefore, a second binding site for the *ptn* MO down was identified in the *ptn* gene locus, which could explain the higher potency of this *ptn* splice MO for inducing the observed somite defects due to enhanced binding capacities (Fig. 44).

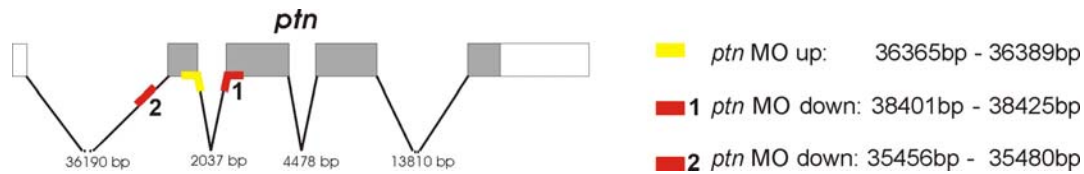


Fig. 44: Multiple binding sites of *ptn* MO

Schematic drawing of the *ptn* locus with different MO binding sites (labeled in red and yellow with bp position).

8.1.2. Combinatorial knockdown reveals no synergistic effects of midkines and pleiotrophin on somite formation

To dissect putative synergistic versus additive effects of *mdka* and *mdkb* in combination with *ptn* on somitogenesis, double knockdown experiments were conducted. To detect a possible synergism, the *ptn* splice MOs (mixture of *ptn* MO up and down in a 1:1 ratio) was used at a dose that is not sufficient to induce a phenotype on its own (0.5 ng/nl). Injection of this low *ptn* MO dose in combination with the same concentration of a standard control MO did not result in somite fusion (n=51; Fig. 45B,F). Neither combination of the same concentration of *mdka* nor the *mdkb* splice MO (mixture of MO up and down in a 1:1 ratio) with the corresponding amount of *ptn* MO resulted in fusion of somites in any case (*mdka*: n=42; Fig. 35C,G; *mdkb*: n=66; Fig. 45D,H). These preliminary results indicate that there is no combinatorial effect of *mdka* or *mdkb* with *ptn* functions during somitogenesis.

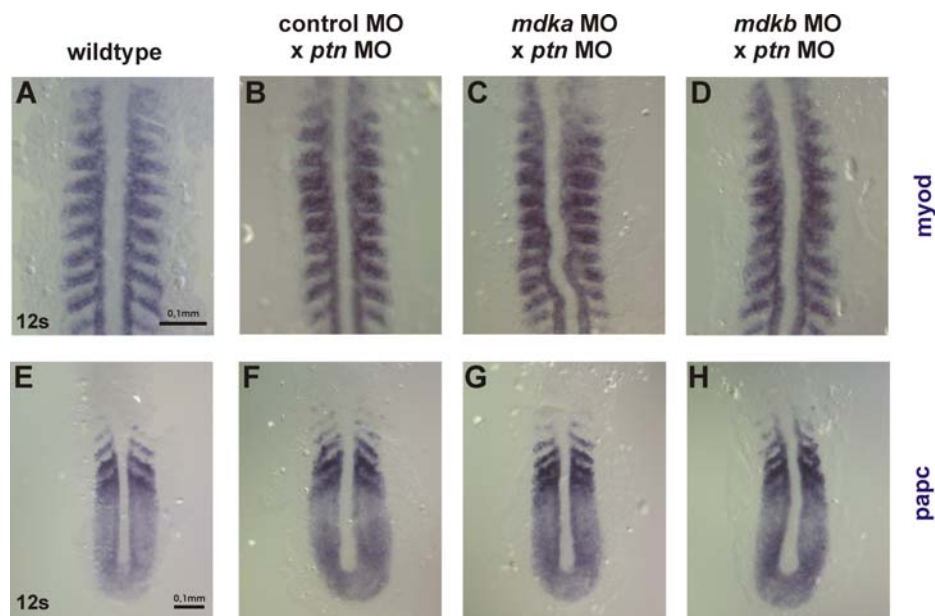


Fig. 45 No obvious effects on somitogenesis after combined knockdown of *midkine* genes.

A-H Expression of *myod* (A-D) and *papc* (E-H) in wild-type (A,E) and double morphants (B,F, control/*ptn* MO; C,G *mdka*/*ptn* MO; D,H *mdkb*/*ptn* MO) at 12-somite stage.

8.2. Table of used primers

Sequences of used oligonucleotide primers:

Name of Primer	Sequence (5'-3')
mk-003	GGG GAT CCC CAC CAT GCG GAG TTT GTT CTC
mk-004	GGC TCG AGC AAG TTA GTT TTC CTT CCC
mkESTup	GTT TCA GTG AGG GAA CTT TCG
mk3-2	GGC TCG AGC CCT TTA GTT CCC TTT CCC
tfptnfl01	ATG CAG CAG CAG TGG GTG TGT
tfptnfl02	CTA GTC TGT AGG GTT TCG CTC
ptnMO01	GAG GAA GCA AAA AGG TGG AA
ptnMO02	GCA TCT TGG TCT TGG GTT TG
RTacta1UP	CCA ACA ACG TCC TTT CTG GT
RTacta1DO	GAG GGA CCT GCC TCA TCA TA
mdkb_intorn3-4_up	GAC TTT GGC GGT AAG CAG TT
mdkb_intron3-4_down	TGC AGT CGG CTA CAA ATA AGA A

8.3. Abriviations

Terms

AP	anterior-posterior
blimp	synonym/ previous name for prdm
Bmp	bone morphogenetic protein
CNS	central nervous system
ddH ₂ O	double distilled water
dig	digoxigenin
dlx	distal-less homeobox gene
DNA	deoxyribonucleic acid
DV	dorso-ventral
eng	engrailed
ENU	N-ethyl-N-nitrosourea (C ₃ H ₆ N ₃ O ₂)
Fgf	fibroblast growth factor
Fig.	figure
flu	fluorescein
foxd	forkhead box gene
gli	GLI-Kruppel family member
HARP	heparin hffin regulatory peptide (=ptn)
HB-GAM	heparin binding growth associated molecule (=ptn)
hox	homeo box gene
hpf	hours past fertilization
ALK	anaplastic lymphoma kinase
LDL	low-density lipoprotein
LRP	LDL receptor-related protein
mafB	v-maf musculoaponeurotic fibrosarcoma oncogene family, protein B (avian)
mdk	midkine
MHB	mid-hindbrain boundary
mRNA	messenger ribonucleic acid
msx	muscle segment homeobox gene
ncc	neural crest cell(s)
NEGF1	neurite growth-promoting factor 1 (=ptn)
olig	oligodendrocyte lineage transcription factor
pax	paired box gene
PBS	phosphate buffered saline
PBST	phosphate buffered saline, 0,1% Tween20
PCR	polymerase chain reaction
PFA	paraformaldehyde
PNS	peripheral nervous system
pou	POU domain transcription factor

prdm	PR domain containing gene
psm	presomitic mesoderm
ptn	pleiotrophin
r	rhombomere
RA	retinoic acid
raldh	aldehyde dehydrogenase 1 family
RBs	Rohon-Beard sensory neurons
RNA	ribonucleic acid
rptp	receptor-type protein tyrosine phosphatase
RT-PCR	reverse transcription polymerase chain reaction
shh	sonic hedgehog
sox	“sex determining region Y”-box containing gene
tfap	transcription factor activating enhancer binding protein
tgf	transforming growth factor
TILLING	targeting induced local lesions in genomes
Wnt	wingless-type mouse mammary tumor virus integration site family gene member

Units

°C	degree Celsius
bp	basepairs
cm	centimeter
d	day
g	gram
h	hours
k	kilo-
kb	kilobases
kD	kilodalton
l	liter
M	molar
μ	micro
m	mili
min	minutes
ml	milliliter
mM	millimolar
nM	nanomolar
rpm	rounds per minute
RT	room temperature
S	seconds
U	unit
V	volt
vol	volume

8.4. Own publications

Elmasri, H., Liedtke, D., Klamt, B., Volf, J.-N., Gessler, M. and Winkler C. (2003).

Evolution and functional diversification of hey bHLH transcriptional factors. *European Journal of Cell Biology* 82, Supplement 53

Elmasri, H., Winkler, C., Liedtke, D., Sasado, T., Morinaga, C., Suwa, H., Niwa, K., Henrich, T., Hirose, Y., Yasuoka, A., Yoda, H., Watanabe, T., Deguchi, T., Iwanami, N., Kunimatsu, S., Osakada, M., Loosli, F., Quiring, R., Carl, M., Grabher, C., Winkler, S., Del Bene, F., Wittbrodt, J., Abe, K., Takahama, Y., Takahashi, K., Katada, T., Nishina, H., Kondoh, H., Furutani-Seiki, M. (2004). Mutations affecting somite formation in the Medaka (*Oryzias latipes*). *Mechanisms of Development* 121, 659-671

Elmasri, H., Liedtke, D., Lücking, G., Gessler, M. and Winkler C. (2004). her7 and hey1, but not lunatic fringe show dynamic expression during somitogenesis in medaka (*Oryzias latipes*). *Gene Expression Patterns* 4 (5), 553-559

Liedtke, D. and Winkler C. (2007). Midkine-b regulates cell specification at the neural plate border in zebrafish. *Developmental Dynamics* (in revision)

Liedtke D., Schäfer M. and Winkler C. (2007). Non-overlapping activities of Midkine growth factors during mid- and hindbrain formation in zebrafish. (in preparation)

8.5. Curriculum vitae

Name: Daniel Dieter Liedtke
Geburtsdatum: 6. August 1976
Geburtsort: Fulda
Nationalität: Deutsch

Schulausbildung:

1983 bis 1987 „Cuno-Raabe-Schule“ Fulda, Grundschule
1987 bis 1993 „Marianum“ Fulda, Realschule
1993 bis 1996 „Marianum“ Fulda, staatl. anerkannte private gymnasiale Oberstufe

Hochschulausbildung:

1997 bis 2003 Studium der Biologie an der Universität Würzburg; Diplomprüfung in den Fächern: Mikrobiologie, Physiologische Chemie und Tierphysiologie (Soziobiologie und Verhaltensphysiologie)
Jan. bis Nov. 2003 Diplomarbeit in der Arbeitsgruppe von Dr. C. Winkler am Lehrstuhl „Physiologische Chemie I“ der Universität Würzburg mit dem Thema: „Untersuchung der *hey1*-Promotorregion im Zebrafisch und Expression von *hey1* in Somitogenese-Mutanten von Medaka“
Dez. 2003 bis Aug. 2007 Doktorarbeit in der Arbeitsgruppe Dr. Winkler am Lehrstuhl „Physiologische Chemie I“ der Universität Würzburg mit dem Thema: “Functional divergence of Midkine growth factors: Non-redundant roles during neural crest induction, brain patterning and somitogenesis”
April 2004 bis Juli 2007 Doktorandenstipendium des DFG-Graduiertenkollegs 1048 „Molecular basis of organ development in vertebrates“

8.6. Teilnahme an wissenschaftlichen Tagungen

Nationale Tagungen

- März 2003 Teilnahme am Kongress „CellBid“ der GfE und DGZ in Bonn, mit Posterpräsentation
- Oktober 2004 Teilnahme am SFB 488 Symposium „From Molecules to Neural Systems“ in Heidelberg
- April 2005 Teilnahme an der Jahrestagung der Gesellschaft für Entwicklungsbiologie (GFE) in Münster, mit Posterpräsentation
- April 2005 Vortrag auf dem „Regional Fish Meeting“ in Burg Landeck
- Juli 2005 Vortrag auf dem „First Würzburg Zebrafish Symposium on Genetics and Development“
- September 2005 Teilnahme und Posterpräsentation an der 5. GfE School „Molecular Control of Organ Development“ auf Schloss Reissensburg bei Günzburg
- Februar 2007 Teilnahme an der Jahrestagung der Gesellschaft für Entwicklungsbiologie (GFE) in Marburg, mit Posterpräsentation

Internationale Tagungen

- August 2004 Teilnahme an der „6th International Conference on Zebrafish Development and Genetics“ an der University of Wisconsin in Madison (WI, USA), mit Posterpräsentation
- Juli 2005 Teilnahme am „4th European Zebrafish Genetics and Development Meeting“ in Dresden, mit Posterpräsentation
- November 2005 Vortrag auf dem „1st International Student Symposium“ in Würzburg
- Juni 2006 Teilnahme an der „7th International Conference on Zebrafish Development and Genetics“ an der University of Wisconsin in Madison (WI, USA), mit Posterpräsentation
- September 2006 Teilnahme am „3rd International PhD Student Symposium - Horizons in Molecular Biology“ in Göttingen
- Posterpräsentation und Preis der Fachzeitschrift „*Nature*“ für das beste Poster
- Juli 2007 Teilnahme am „5th European Zebrafish Genetics and Development Meeting“ in Amsterdam (Holland), mit Posterpräsentation

8.7. Eidesstattliche Erklärung

Hiermit erkläre ich ehrenwörtlich, dass ich die vorliegende Dissertation in allen Teilen selbständig angefertigt und keine anderen als die von mir angegebenen Quellen und Hilfsmittel verwendet habe.

Ich erkläre weiterhin, dass ich diese Dissertation weder in gleicher noch in ähnlicher Form in anderen Prüfungsverfahren vorgelegt habe.

Ich habe außer den mit dem Zulassungsgesuch urkundlich vorgelegten Graden keine weiteren akademischen Grade erworben oder zu erwerben versucht.

Daniel Liedtke

Würzburg, im August 2007

8.8. Danksagung

Zum Gelingen dieser Arbeit haben viele Personen beigetragen, bei denen ich mich an dieser Stelle herzlich bedanken möchte.

Ich bedanke mich bei Prof. Dr. Christoph Winkler vor allem für das in mich gesetzte Vertrauen, die Motivation, die wissenschaftliche Anleitung, sowie für seine fast unendliche Geduld.

PD Dr. med. Ute Felbor gilt mein Dank für das stetige Begleiten der Doktorarbeit und für die Übernahme der Zweitkorrektur.

Den (ehemaligen) Mitgliedern der Arbeitsgruppe Winkler und des Lehrstuhls für Physiologische Chemie I danke ich für die freundliche Arbeitsatmosphäre und Unterstützung, vor allem Cordula, Marieke, Susi, Doris, Matthias, Harun und Jörg.

Ich danke Herrn Prof. Dr. Dr. Manfred Scharl für die Möglichkeit in seinem Lehrstuhl zu arbeiten.

Dem Graduierten Kolleg ‚Molecular Basis of Organ Development in Vertebrates‘ (GK 1048) für die finanzielle Unterstützung und den Stipendiaten für zahlreiche interessante Seminare und Diskussionen. Im Besonderen danke ich Gabi Heilmann für ihre Unterstützung.

Ein spezieller Dank gilt meinen Eltern und meinen guten Freunden Svenja, Toni, Jan, Holger, Kai und Kathleen für Ihre Unterstützung, besonders in schwierigen Phasen der Arbeit und meines Lebens. Bei Sabine bedanke ich mich für ihr Verständnis, ihren Beistand und ihre Liebe.